Functional characterization of the PlGF-2 heparin-binding domain

Inaugural-Dissertation

zur
Erlangung des Doktorgrades
der Mathematisch-Naturwissenschaftlichen Fakultät
der Universität zu Köln

vorgelegt von

Daniel Christopher Hoffmann

aus Düren

Köln, 2011

Berichterstatter:

Prof. Dr. Mats Paulsson
Prof. Dr. Matthias Hammerschmidt

Tag der mündlichen Prüfung: 08. April 2011

Summary

Placenta growth factor (PlGF), a member of the vascular endothelial growth factor (VEGF) protein family, is a critical regulator of vascular growth during processes of tissue remodelling including tissue repair and carcinogenesis. As reported for VEGF-A, the PlGF gene gives raise to different protein isoforms by mRNA splicing, which differ primarily in the presence or absence of a carboxyl-terminal domain, rich in basic amino acids (so called heparin-binding domain). The most abundantly expressed isoforms are PlGF-1 (lacking the heparin-binding domain) and PlGF-2 (expressing the heparin-binding domain). Whereas in recent years the heparin-binding domain of VEGF-A_{165}, the major VEGF-A isoform that shares 46% amino acid sequence identity with PlGF-2, has emerged as essential domain for VEGF-A function, up to date little is known about the functional relevance of this domain present in PlGF-2. The aim of this project was to investigate the functional impact of the heparin-binding domain for PlGF-mediated activities.

rhPlGF-1 and rhPlGF-2 were synthesized in HEK293 cells and used to perform differential structural and functional *in vitro* and *in vivo* bioassays. Analysis of protease sensitivity revealed that rhPlGF-2 is a target of the serine protease plasmin. Western-blot analysis and MALDI-TOF-mass-spectrometry of plasmin-digested rhPlGF-2 fragments identified a specific plasmin cleavage site (Lys_{118}-Met_{119}) resulting in loss of the C-terminal domain comprising the heparin-binding domain encoded by exon 6 and a short stretch of eight amino acids encoded by exon 7. The biological relevance of proteolytic cleavage of rhPlGF was corroborated by identifying a rhPlGF-2 cleavage fragment in non-healing, poorly vascularized human skin wounds, that was consistent with plasmin mediated cleavage. To characterize the functional consequences of plasmin-mediated cleavage of rhPlGF-2, a truncated form of rhPlGF (PlGFStop) was generated, representing the plasmin-resistant N-terminal fragment (Leu_1-Lys_{118}). Chemotaxis and endothelial cell sprouting analysis revealed striking differences among the PlGF isoforms. Whereas rhPlGF-2 induced a robust chemotactic and endothelial cell sprouting response on HUVE and porcine endothelial cells stably transfected with Neuropilin-1 (PAE/Nrp-1), the activity of rhPlGF-1, plasmin processed rhPlGF-2 and the rhPlGFStop mutant was significantly attenuated. Furthermore, the induction of a vascularized granulation tissue in wounds of impaired healing diabetic mice could be significantly stimulated by topical application of rhPlGF-2, whereas application of rhPlGF-1 or rhPlGFStop showed weak effects. These findings indicate that the heparin-binding domain of PlGF-2 stimulates endothelial cell functions *in vitro* and promotes angiogenesis *in vivo*. To unravel the underlying molecular mechanisms for the increased

biological potency of PlGF-2, binding to diverse extracellular matrix components and the VEGFR-1 co-receptor Nrp-1 as well as signalling pathways were investigated.

Surface Plasmon Resonance spectroscopy demonstrated a high affinity of rhPlGF-2, but unexpectedly also of rhPlGF-1 for several glycosaminoglycanes (heparin, heparan sulphate and chondroitin sulphate). These findings indicate that the binding capacity of PlGF to the selected glycosaminoglycanes is dependent on the amino acids encoded by exon 7, which is present in both isoforms. The heparin-binding domain present exclusively in PlGF-2 appears not to be essential for binding of the investigated GAGs. rhPlGF-2 revealed a moderate binding to Nrp-1, which was significantly increased in the presence of heparin. The absence of the entire C-terminal domain encoded by exon 6 and 7 (represented by the rhPlGFStop mutant) resulted in complete loss of any tested binding capacity. Activation of VEGFR-1 appears to be independent of the C-terminal domain, because all isoforms rhPlGF-2 and rhPlGFStop resulted in an activation of VEGFR-1 and its downstream targets Akt and Erk-1/-2. Analysis of signalling pathways in endothelial cells suggested that increased rhPlGF-2-induced cellular responses were in part mediated by increased activation of tyrosine kinases FAK (focal adhesion kinase) and Src family kinases. In addition, activation of both kinases was enhanced by Nrp-1 overexpression and exposure of endothelial cells to collagen I.

Collectively, our findings propose novel functions of the heparin-binding domain of PlGF-2 and of the C-terminal domain of PlGF-1 and indicate that plasmin-mediated proteolysis is a major switch to control PlGF-mediated angiogenesis.

Zusammenfassung

Der plazentale Wachstumsfaktor (PlGF), ein Mitglied der Familie der vaskulären endothelialen Wachstumsfaktoren (VEGF), ist bekannt als wichtiger Mediator für die Regulation des Gefäßwachstums während des Gewebeumbaus. Dies gilt in besonderem Maße für die Hautregeneration und Karzinogenese. Ähnlich wie für VEGF-A gezeigt, wird die Expression von PlGF durch alternatives mRNA Splicing eines *plgf*-Gens reguliert, und führt zur Bildung von verschiedenen Proteinisoformen. Diese unterscheiden sich maßgeblich durch alternative Expression einer stark basischen Domäne am Carboxylende des Proteins (Heparin-bindende Domäne). Bei den am häufigsten exprimierten Isoformen handelt es sich um PlGF-1 (ohne Heparin-bindende Domäne) und PlGF-2 (mit Heparin-bindender Domäne).

Die Funktion der Heparin-bindenden Domäne von VEGF-A_{165} war in den letzten Jahren Forschungsgegenstand zahlreicher Untersuchungen, durch deren Ergebnisse die essentielle Rolle der Heparin-bindenden Domäne für die Aktivität von VEGF-A_{165} gezeigt werden konnte. Die Funktion der Heparin-bindenden Domäne von PlGF-2 hingegen blieb trotz hoher Sequenzhomologie zu VEGF-A_{165} (46%) bis heute weitgehend ungeklärt. Um die strukturellen und funktionellen Unterschiede zwischen rhPlGF-1 und rhPlGF-2 näher zu untersuchen, wurden diese Isoformen in HEK293 Zellen exprimiert und in verschiedenen *in vitro* und *in vivo* Experimenten charakterisiert. Untersuchungen der Proteasesensitivität von rhPlGF-2 ergaben, dass PlGF ein Zielprotein der Serinprotease Plasmin ist. Die daraus resultierende C-terminale Fragmentierung wurde mit Hilfe von Western Blot und MALDI-TOF-Massenspektroskopischer Analyse untersucht. Neben mehreren Schnittstellen innerhalb der Heparin-bindenden Domäne, konnte Lys_{118}-Met_{119} als die am weitesten N-terminal gelegene spezifische Plasminschnittstelle identifiziert werden. Um die funktionellen Konsequenzen dieser proteolytischen Prozessierung von rhPlGF-2 näher zu untersuchen, wurde eine verkürzte Form von rhPlGF (PlGFStop) generiert, welche den plasminresistenten, N-terminalen Bereich von PlGF umfasst (Leu_1-Lys_{118}). Vergleichende Untersuchungen von rhPlGF-1, rhPlGF-2 und rhPlGFStop bezüglich ihrer chemotaktischen Aktivität und ihrer Fähigkeit eine Gefäßaussprossung zu fördern, zeigten signifikante Unterschiede zwischen den einzelnen PlGF Isoformen auf.

Während rhPlGF-2 eine deutliche chemotaktische Antwort in HUVE Zellen und Neurpilin-1-transfizierten Endothelzellen aus der Aorta des Schweins hervorrief und die Ausbildung von gefäßähnlichen Strukturen induzierte, zeigten sowohl rhPlGF-1, Plasmin-prozessiertes rhPlGF-2 als auch die mutierte Form rhPlGFStop eine klar verminderte Aktivität. Weiterhin förderte die topische Applikation von rhPlGF-2 in

Zusammenfassung

Wunden von diabetischen Mäusen mit verzögerter Wundheilung eine signifikante Zunahme an vaskularisiertem Granulationsgewebe. Im Gegensatz dazu, wiesen rhPlGF-1 und rhPlGFStop nur geringe Effekte auf. Zusammenfassend konnten die Ergebnisse eine klare Funktionalität der Heparin-bindenden Domäne von rhPlGF-2 aufzeigen, zum einen durch die Stimulation endothelialer Zellfunktionen *in vitro* und zum anderen durch angiogenesefördernde Effekte *in vivo*.

Um die zugrunde liegenden Mechanismen für die gesteigerte Bioaktivität von PlGF-2 zu identifizieren, wurde sowohl die Bindung der unterschiedlichen PlGF Isoformen an verschiedene Komponenten der extrazellulären Matrix und an den Korezeptor Nrp-1 gemessen, als auch mögliche Signaltransduktionswege untersucht. Mit Hilfe von Surface Plasmon Resonance Spektroskopie wurde gezeigt, dass sowohl rhPlGF-2 als auch – unerwarteter Weise rhPlGF-1 - eine starke Affinität für verschiedene untersuchte Glykosaminoglykane (GAGs) aufweisen (Heparin, Heparansulfat, Chondroitinsulfat). Diese Ergebnisse lassen vermuten, dass die Interaktion zwischen PlGF und den untersuchten GAGs hauptsächlich durch die von Exon 7 codierten Aminosäuren vermittelt wird, welche in beiden Isoformen expremiert werden. Die Heparin-bindenden Domäne in PlGF-2 scheint nicht essentiell für eine Bindung an die untersuchten GAGs zu sein. Zusätzlich konnte eine moderate Bindung von rhPlGF-2 an Nrp-1 gemessen werden, die jedoch in Anwesenheit von Heparin signifikant um den Faktor 100 verstärkt wurde.

Das Fehlen der C-terminalen Domäne (kodiert von Exon 6 und 7) in rhPlGFStop führte zu einem vollständigen Verlust der Bindungskapazität in allen durchgeführten Messungen. Diese C-terminale Verkürzung des Proteins scheint jedoch keinen maßgeblichen Einfluss auf die Bindung an den VEGFR-1 zu haben. Nach Stimulation mit rhPlGFStop oder rhPlGF-2 zeigten sowohl VEGFR-1, als auch die nachgeschalteten Signalproteine Akt und Erk-1/-2 eine vergleichbare Phosphorylierung. Eine weiterführende Analyse möglicher Signaltransduktionswege in Endothelzellen lässt darauf schließen, dass die durch rhPlGF-2 induzierte verstärkte endotheliale Zellaktivität teilweise durch eine Aktivierung der Tyrosinkinasen FAK (focal adhesion kinase) und Src vermittelt sein könnte. Zusätzlich konnte eine verstärkte Phosphorylierung dieser Kinasen bei Nrp-1 Überexpression und Collagen I Exposition beobachtet werden. Zusammenfassend konnten in dieser Arbeit neue Funktionen der Heparin-bindenden Domäne von PlGF-2 und der C-terminalen Domäne von PlGF-1 aufgezeigt werden. Die Ergebnisse legen die Vermutung nahe, dass die durch Plasmin vermittelte, C-terminale Proteolyse eine Schüsselkomponente für die durch PlGF induzierte Angiogenese darstellt.

Table of contents

Table of contents

Table of contents

Table of contents

1 Introduction

1.1 Cellular and molecular mechanisms of vascular growth

1.1.1 Vasculogenesis and angiogenesis

Two distinct processes that partly overlap and complement one another accomplish the formation of a vascular network. Vasculogenesis mainly describes the formation of a primitive vascular network during embryonic development. Arising from mesodermal stem cells, angioblasts migrate to the place of blood vessel formation, differentiate into endothelial cells (Fig 1a), and form lumen-containing vascular network (Drake 2000, Risau 1995). During early development, vessel formation occurs in extra-embryonic as well as in intra-embryonic tissue (Ferguson 2005). Later on, angioblasts migrate to the developing organs, assemble, and form vascular tubes (Coffin 1991, Ash 2000). As cell migration is essential for vessel development, guidance has to be ensured by a highly regulated pattern of growth factors and other regulatory proteins in time and space (Hiratsuka 2005, Shoji 2003, Tomanek 2006).

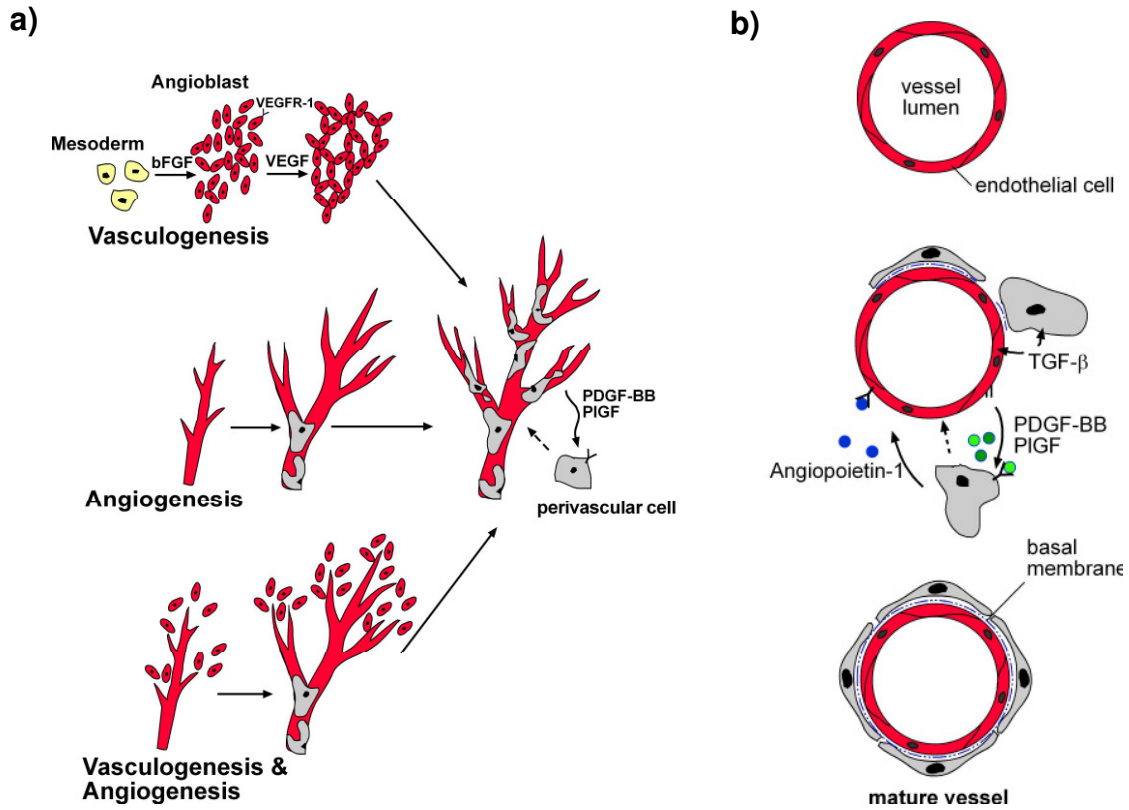

Figure 1: Blood vessel growth in development and disease. (a) Blood vessels are formed by two mechanisms that complement each other: vasculogenesis and angiogenesis. Both processes are critical for the development of the embryonic vasculature. In adult physiology (e.g. wound healing) and under pathological conditions (e.g. tumorigenesis) remodelling of vessels mainly involves angiogenesis but may be supported by vasculogenesis. Vasculogenesis involves the coalescence of endothelial precursors (angioblasts) into loose chords. These cells differentiate into endothelia to form tubes and a primitive network. Angiogenesis involves sprouting and branching of new vessels from pre-existing ones. **(b)** To stabilize vessel structure, pericytes are recruited to newly formed vessels. (Modified: Harvey, *Academic Press*, 1999)

In contrast to vasculogenesis, during angiogenesis new vessels are not formed *de novo* but by sprouting and branching from pre-existing vessels (Fig 1a). Angiogenesis takes place during development to enlarge the primary and primitive network formed by vasculogenesis as well as under physiological and pathological conditions in adult beings. Under physiological conditions, the proliferation rate of endothelial cells is low and angiogenesis is observed only in female reproduction tract and during skin regeneration. As endothelial cells are in a quiescent state under normal conditions, they have to be activated and re-programmed during early stages of angiogenesis (Folkman 2006). Induced by hypoxia and the transcription factors Hypoxia Inducible Factor-1α (HIF-1α), HIF-2α und HIF-3α, endothelial cells and other cell types are activated and start to express a subset of angiogenic growth factors such as Vascular Endothelial Growth Factor-A (VEGF-A), Hepatocyte Growth Factor (HGF), Platelet Derived Growth Factor (PDGF), among others. This release results in endothelial cell proliferation and directed migration, recruitment of endothelial progenitor cells and their interaction with provisional and interstitial extracellular matrices (Cheresh 2008). In addition, these factors recruit pericytes and leukocytes to promote formation and stabilization of mature vessels (Harris 2002, Elson 2001, Vincent 2000) (Fig 1b).
In order to promote directed migration to areas of newly forming vessels, endothelial cells from existing vessels lose their cell-cell contacts resulting in increased migration and an increased vascular permeability (Potter 2005). This permeability further supports recruitment of cells from the circulation, but is also essential to provide a provisional matrix formed by plasma-derived proteins leaking out of the blood to promote migration and invasion. To allow endothelial cell invasion into this provisional matrix, activated endothelial cells express a specific subset of integrins and proteases to recognize substrate molecules and degrade the basal membrane and components of the extracellular matrix, respectively.

During vascular growth, a precise architecture is essential to ensure adequate supply of oxygen and nutrients. The outgrowing vascular sprout is guided by a single specialized endothelial cell, unique by tip structures with potential functions in guidance and migration (Marin-Padilla, 1985). These tip cells are highly polarized and form multiple extensions and dynamic filopodia (Ruhrberg 2002) to sense guiding cues in their surroundings and to migrate to these cues (Fig 2). High levels of VEGFR-2 are localized to tip cell filopodia, and tip cells maintain their active migratory phenotype in respond to VEGF gradients. They are followed by stalk cells, which form vacuoles to generate lumen and exhibit a proliferative state to prolong the newly formed vessel (Gerhardt 2003). Once the new vessel is formed endothelial cells become quiescent, form tight junctions and make

contact to recruited pericytes and therefore stabilize and mature the vessel.

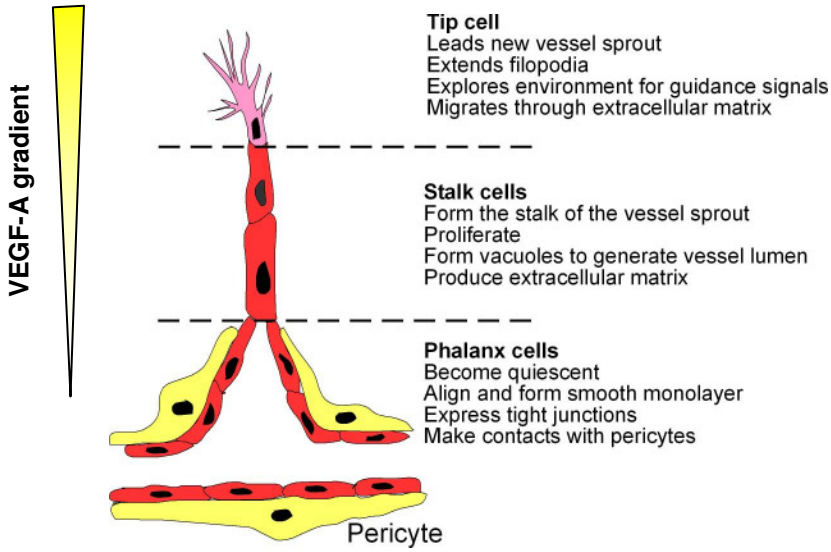

Figure 2: Vascular sprouting. Induced by a VEGF-A gradient, specialized tip cells guide the expanding sprout by exploring the environment for gradients of guiding cues. It is followed by proliferating stalk cells, which form the sprout and generate lumen. Once covered with pericytes, endothelial cells become quiescent and strengthen their cell-cell contacts.

The Delta-like4 (Dll4)-Notch pathway has been identified as regulator to determine tip cell and stalk cell fate. Using different experimental models, several groups were able to demonstrate, that blockage of Dll4 activity by pharmacological inhibitors or heterozygous genetic inactivation resulted in an increase of vascular density due to an increase in tip cell number and vascular sprouts. On the contrary, increased Notch activity led to a decreased vascular density due to a reduced number of tip cells (Hellstrom 2007, Lobov 2007, Siekmann 2007, Suchting 2007). The Dll4-Notch pathway appears to be closely connected to VEGF–VEGFR-2 signalling, which upregulates the expression of Dll4 in tip cells. High levels of Dll4 in the tip cell are able to activate Notch1 in the adjacent stalk cells, causing suppression of the tip cell phenotype. In addition, Notch inactivation through deletion of Dll4 has been shown to result in a reduction of VEGFR-1 levels (Hellstrom 2007, Suchting 2007). Notch signalling may therefore block tip cell formation by regulating the levels of VEGFR-1. Its activity as a decoy receptor therefore may antagonize VEGFR-2 function (Waltenberger 1994). Indeed, disruption of soluble VEGFR-1 (s-Flt1) levels increased sprout bifurcation and filopodia numbers relative to wild type vessels (Cappell 2009).

1.1.2 The role of growth factors in angiogenesis

Due to a high metabolic demand for nutrients and oxygen in skin during tissue repair after injury, angiogenesis is very active and pushed by pro-angiogenic factors secreted by keratinocytes and other skin cell types. In contrast to this, cutaneous vessels are quiescent and obtain their required oxygen from vasculature located in the dermis. The

balance among pro- and anti-angiogenic factors is disturbed in several cutaneous diseases like psoriasis, rosacea, different tumor types, and photo-damage, in which pro-angiogenic factors are upregulated by hypoxia, inflammatory cytokine-derived signals, or mutation, resulting in pathological angiogenesis (Malhotra 1989, Velasco 2002, Streit 2003, Yano 2003).

Among pro-angiogenic factors, angiopoietins, fibroblast growth factor (FGF), transforming growth factor-β (TGF-β), and the members of the VEGF family play key roles in the regulation of angiogenesis as well as lymph-angiogenesis (Folkman 1987, Keck 1989, Yang 1990, Suri 1996).

VEGF-A, the most prominent member of the VEGF family acts as a potent mitogen, chemoattractant and survival factor for endothelial cells and strongly increases vessel permeability (Dvorak 1995, Yuan 1996, Gerber 1998, Asahara 1999, Yamashita 2000). Constitutively expressed at low levels in skin, VEGF expression is upregulated under physiological or pathological conditions connected to angiogenesis by – among other stimuli – hypoxia. VEGF-A gradients have been described as one of the key component for tip cell formation and vascular sprouting (Gerhardt 2003).

Angiopoietins have been identified as endothelial specific growth factors. Especially Angiopoeitin-1 (Ang-1) appears to play an essential role in angiogenesis and has an additive effect on VEGF activity. Involved in the interaction between endothelial cells and pericytes, it maintains vessel stability and protects endothelial cells from apoptosis via binding to its tyrosine kinase receptor Tie-2 (Suri 1996, Wong 1997, Papapetropoulos 2000). As its counterpart, Ang-2 is highly upregulated at sites of active angiogenesis to destabilize existing vessels and thereby allows endothelial cell migration and vascular sprouting (Maisonpierre 1997).

Among the large family of fibroblast growth factors (FGF), FGF-1 and especially FGF-2 (basic FGF) are implicated in angiogenesis (Friesel 1995). During wound healing, both isoforms are synthesized by a variety of cell types, including inflammatory cells, endothelial cells, and dermal fibroblasts (Schweigerer 1987, Kandel 1991, Blotnick 1994). During the early phase of healing, they promote endothelial cell proliferation and differentiation (Kanda 1996) and enable their migration by upregulation of the urokinase-type plasminogen activator (uPA) (Gualandris 1995). At later stages, FGF-2 has been demonstrated to induce $\alpha_V\beta_3$ integrin expression on endothelial cells to further facilitate their migration (Sepp 1994).

Due to its strong and multipotent effects, TGF-β is one of the most important modulators of angiogenesis during wound healing by regulation of cellular proliferation, migration, capillary tubule formation, deposition of extracellular matrix and upregulation of integrin expression (Yang 1990, Enenstein 1992, Kingsley 1994, Collo 1999). As TGF-β is also

involved in granulation tissue formation and was shown to increase growth factor release from dermal fibroblasts (Kim 2001, Trompezinski 2000), the strong response for angiogenesis may be – in part – caused by other factors.

1.1.2.1 The VEGF family and its receptors

VEGF is one of the most prominent factors for the regulation of embryonic vasculogenesis and adult angiogenesis (Ferrara 1997, Neufeld 1999, Ferrara 2003). It was discovered in tumor cells of guinea pigs as a factor to regulate vascular permeability and endothelial cell-specific mitogen (VPF, vascular permeability factor) (Dvorak 1979, Senger 1983, Ferrara 1989). Knockout studies in transgenic mice revealed its essential role for embryonic vasculogenesis. Homozygous as well as heterozygous deletion of the VEGF-A allele resulted in embryonic lethality at embryonic day (E) 9.5-10.5 and E 11-12 respectively, due to severe defects in vascular and cardiovascular development (Ferrara 1996, Carmeliet 1996).

Structurally, the VEGF family members belong to the VEGF/PDGF super-gene family, among which a cysteine knot motive of eight cysteine residues is conserved. Two of these cysteines generate intermolecular cross-linked disulfide bonds and are responsible for dimerization (Muller 1997), whereas the remaining six cysteines form intramolecular disulfide bonds and three loop structures (Wiesmann 1997). Up to date, the VEGF family includes VEGF-A, PlGF (placenta growth factor), VEGF-B, VEGF-C, VEGF-D, VEGF-E and svVEGF (snake venom VEGF). The molecular and biological functions of each ligand have been well characterized.

One of the characteristics of the members of this protein family is, that their expression is regulated by alternative mRNA splicing of a single gene and therefore results in different isoforms with modified binding properties and biological activities due to the presence or absence of a heparin-binding domain (Fig 3).

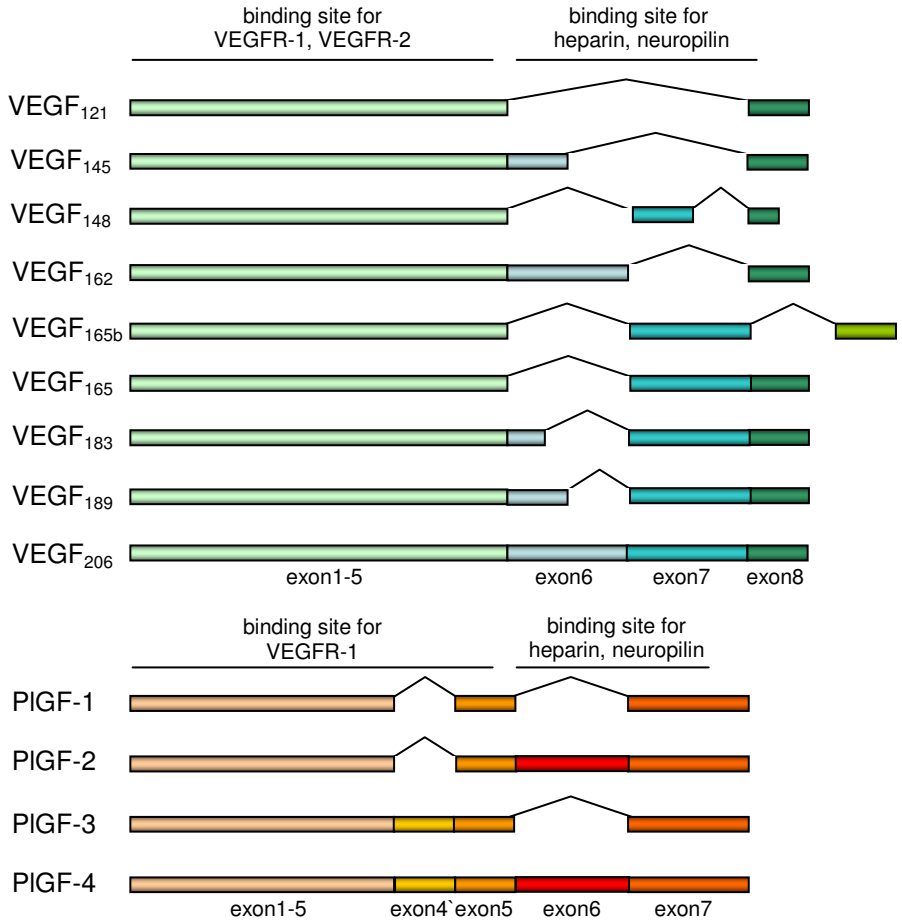

Figure 3: Schematic overview on VEGF-A and PlGF isoforms. Alternative exon splicing results in the generation of several isoforms of VEGF-A and PlGF. Differential expression of a highly basic heparin-binding domain (exon6/7 in blue for VEGF; exon 6 in red for PlGF) regulates matrix binding capacity and co-receptor recruitment. (Modified: Takahashi, *Clinical Science* 2005).

1.1.2.2 The Vascular Endothelial Growth Factor (VEGF-A)

In human, the VEGF-A gene (6p21.3) (Vincenti 1996) is organized into eight exons (Houck 1991, Tischer 1991) and differential splicing results in expression of at least nine secreted isoforms: VEGF-A_{121}, VEGF-A_{145}, VEGF-A_{148}, VEGF-A_{162}, VEGF-A_{165}, VEGF-A_{165b}, VEGF-A_{183}, VEGF-A_{189} and VEGF-A_{206} (Bates 2002, Lange 2003; Fig. 3). VEGF-A is expressed in endothelial cells, macrophages, activated T-cells and a variety of other cell types (Freeman 1995, Ferrara 1997, Melter 2000), but mechanisms that are responsible for the regulation of isoform levels are unknown so far. Predominantly, these cells secrete VEGF-A_{121}, VEGF-A_{165} and VEGF-A_{189}. The isoforms differ in their binding capability to heparin, heparan sulphate and other components of the extracellular matrix due to alternative expression of two highly basic domains coded by exon 6 and 7 (heparin-binding domain) and therefore are regulated in their extracellular localization. VEGF-A_{121} is lacking these domains and freely diffusible, whereas the most prominent isoform VEGF-A_{165} additionally expresses exon 7 and owns an increased binding capacity. This binding strength is further amplified by the expression of exon 6 and 7 in VEGF-A_{189}, which is completely

sequestered in the extracellular matrix upon secretion (Ferrara 1989, Keck 1989, Leung 1989, Ferrara 1997). The heparin-binding domain appears to be essential to provide spatial restricted stimulatory cues by gradient formation to initiate vascular branching. Mice expressing exclusively VEGF-A_{120} (murine VEGF is shorter by one amino acid) die shortly after birth, exhibit a specific decrease in capillary branch formation and suffer from severe defects in retinal vascular outgrowth and pattering. VEGF-A_{164} mice are healthy and normal, and retinal angiogenesis is not affected. Mice expressing exclusively VEGF-A_{188} have a normal venular outgrow but exhibit an impaired arterial development in retinas, dwarfism and other defects (Carmeliet 1999, Maes 2002, Ruhrberg 2002, Stalmans 2002). These results underline the distinct roles of the different VEGF-A isoforms for vascular patterning and arterial development, although VEGF-A_{164} occupies a central role for vascular development.

Besides formation of tissue gradients caused by differential binding strength, anchorage in the extracellular matrix provides a possibility for storage of growth factors. From this depot, they can be released by proteolytic cleavage of the heparin-binding domain. It has been shown for VEGF-A_{165}, that proteases like plasmin, urokinase and matrix metalloproteinases are able to process VEGF-A_{165} resulting in the loss of the heparin-binding domain and release of bioactive VEGF-A core-fragments (Plouet 1997, Lee 2005, Roth 2006). Several publications dealing with this topic have demonstrated that proteolytic processing may result in a decrease of VEGF-A_{165} isoform-specific biological activity (Keyt 1996, Lauer 2000, Lee 2005, Roth 2006). In addition to its capability to bind to matrix molecules, heparin-binding isoforms are able to bind and recruit co-receptors (Soker 1998).

The biological activities of VEGF-A (in special VEGF-A_{165}) are various and mostly mediated by the activation of VEGFR-2 (Waltenberger 1994). As one of the most important players for developmental angiogenesis and haematopoiesis, it ensures survival, proliferation, differentiation and migration/chemotaxis of precursor cells (Gerber 2002, Kubo 2003, Schattenman 2004) and regulates the formation of a proper vessel network by gradient formation and tip cell guidance of sprouting vessels (Ruhrberg 2002, Gerhardt 2003). In adult stages, VEGF-A and its receptors are upregulated in a variety of pathological processes and therefore are targets of several clinical studies. They play a major role in tumor angiogenesis, diabetic retinopathy, and progression of rheumatoid arthritis (Carmeliet 2001, Luttun 2002, Zhao 2004). Furthermore, VEGF-A plays an essential role in physiological and pathological wound healing (Lauer 2000, Roth 2006). VEGF-A induces vascular leakage, vessel vasodilatation and recruitment of myeloid cells to induce inflammation (Senger 1983, Ku 1993, Broxmeyer 1995, Dvorak 1995),

underlining that a balance of VEGF-A, its receptors and regulators are essential under physiological and pathological conditions, postnatally.

Expressed at low levels during skin homeostasis, the expression of the VEGF-A gene is increased in areas of hypoxia that are characterized by active angiogenesis. Hypoxia induces VEGF-A expression by stabilization of HIF-1α, which in turn is able to form a transcriptional complex with the nuclear HIF-1β subunit and to bind to specific VEGF-A enhancer elements to increase VEGF-A expression (Ikeda 1995, Stein 1995, Pugh 2003). Additionally, VEGF-mRNA stability is increased under hypoxic conditions. This is achieved by several proteins binding to the 3`untranslated region of the VEGF mRNA and thus protects it from degradation (Levy 1998, Onesto 2004). Beside hypoxia, several growth factors such as PDGF-BB (Finkenzeller 1997), KGF (Keratinocyte Growth Factor), EGF (Epidermal Growth Factor), (Frank 1995), FGF-4 (Deroanne 1997), TGF-β (Pertovaara 1995), IGF-1 (Insulin Growth Factor; Goad 1996), interleukin-1β and interleukin-6 (Li 1995; Cohen 1996) might be involved in VEGF-A expression.

Immunohistological and *in situ* hybridization analysis identified epidermal keratinocytes and infiltrating macrophages as the principal VEGF-A source during skin repair, but *in vitro* analysis revealed that also platelets, neutrophils, fibroblasts and mast cells might provide additional VEGF-A sources during wound angiogenesis (Brown 1992, Fukumura 1998; Kishimoto 2000). During skin repair VEGF-A activity is involved in a variety of processes, including vascular permeability, recruitment of inflammatory cells to the site of injury, migration and proliferation of resident endothelial cells as well as recruitment of bone marrow derived endothelial precursor cells (Brown 1992; Nissen 1998; Galiano 2004; Weis and Cheresh, 2005). Its role during tissue repair was first demonstrated in diabetic mice that are characterized by an impaired angiogenesis and healing response. These mice exhibited a significant decrease in VEGF-A mRNA and intracellular VEGF-A protein level during the repair process (Frank 1995). These data therefore provided a causative link between decreased VEGF-A activity, impaired wound angiogenesis and delayed healing. In addition, VEGF neutralizing antibodies caused a striking reduction in wound angiogenesis, fluid accumulation, and granulation tissue formation in the pig (Howdieshell 2001). Recently, cell-specific ablation of VEGF-A expression in the epidermis supported an important role of epidermal-derived VEGF-A for wound closure (Rossiter 2004). Together, these data provide substantial evidence that VEGF-A activity is a crucial regulator of wound repair in skin.

1.1.2.3 The Placenta Growth Factor (PlGF)

Placenta growth factor (PlGF) was discovered in early 1990 by Maglione *et al.* in human placental tissue where the PlGF gene (14q24.3) is highly expressed (Maglione 1991), but expression can also be detected in a variety of other tissues (Persico 1999). As VEGF-A, PlGF is secreted as an N-glycosylated, anti-parallel homodimer but it also forms heterodimers with other family members to change or fine-tune angiogenic signals (DiSalvo 1995; Cao 1996a). VEGF-A/PlGF heterodimers bind to the VEGFR-2 or to the VEGFR-1/VEGFR-2 heterodimer receptor complex (Autiero 2003).

Although PlGF only shares 46% sequence identity to VEGF-A, both proteins exhibit a related structure (Iyer 2001). Similar to VEGF-A, the expression of the human PlGF gene gives rise to different secreted isoforms by alternative mRNA splicing which differ in their binding properties and biological activities due to the presence or absence of a basic heparin-binding domain. Up to the present, four isoforms have been identified: PlGF-1 ($PlGF_{131}$), PlGF-2 ($PlGF_{152}$), PlGF-3 ($PlGF_{203}$), and PlGF-4 ($PlGF_{224}$) (Maglione 1993, Cao 1997, Yang 2003; Fig 3). PlGF-2, the most abundant isoform expressed in human and the only isoform expressed in the mouse, is able to bind to heparin and other molecules of the extracellular matrix (Hauser 1993, Mamluk 2002) as well as to the co-receptors Neuropilin-1 and -2. This binding is predicted to be highly dependent on the expression of a basic heparin-binding domain coded by exon 6 (Migdal 1998, Gluzman-Poltorak 2000, Mamluk 2002). This idea was supported as PlGF-1, in which this exon is spliced, failed to bind to heparin-sepharose and only slightly competed with PlGF-2 for the binding to Nrp-1. Interestingly, the same authors demonstrated that synthetic peptides of the heparin-binding domain (exon 6) as well as of the sequence of exon 7 are able to compete with PlGF-2 for its binding to Nrp-1 (Migdal 1998). The exact role of the heparin-binding domain for the interaction between PlGF and Nrp-1 therefore remains to be elucidated. PlGF-3 is identical to PlGF-1, but additionally exhibit a 72 amino acids sequence inserted between exon 4 and 5. The sequence of PlGF-4 reflects that of PlGF-3, but it accessorily expresses the heparin-binding domain coded by exon 6 and therefore might have similar extracellular matrix binding properties as PlGF-2 (Cao 1997, Yang 2003). The function and biological activity of PlGF-3 and -4 remain to be investigated.

The biological relevance of PlGF for angiogenesis was demonstrated by classical loss or gain of function studies. Carmeliet *et al*. demonstrated in a complete knock-out mouse ($PlGF^{-/-}$), that loss of PlGF resulted in impaired postnatal plasma extravasion, angiogenesis and collateral growth during wound healing, ischemia, inflammation and cancer, whereas embryonic angiogenesis was not affected (Carmeliet 2001). Furthermore, this group demonstrated that the absence of PlGF reduced vascular leakage induced by

skin wounding, allergens, and neurogenic inflammation. These findings suggest that inhibition of PlGF might be an attractive tool to reduce vascular leakage in various diseases (Luttun 2002). In contrast, overexpression of PlGF in skin under the control of the keratin-14 promoter (K14-PlGF) led to enhanced branched and enlarged vessels in skin (Odorisio 2002). Moreover, ear microvasculature of transgenic mice was characterized by neo-angiogenesis-associated phenomena, such as collateral vessel emission, intussusceptions and numerous varicosities resembling the glomeruloid bodies as described in VEGF-A-induced and tumor-associated angiogenesis (Sundberg 2001).

As seen for VEGF-A, PlGF expression is low during skin homeostasis and strongly upregulated in the angiogenic phase of wound healing, temporally overlapping with VEGF-A expression. It is induced by EGF, TGF-α, TGF-β and interleukin-6 and is expressed in both migrating keratinocytes and the endothelial cells of small blood vessels within the wound bed (Failla 2000). PlGF was found to strongly induce directed migration of VEGFR-1 expressing cells, particularly endothelial cells and monocytes/macrophages, and to potentiate VEGF-A activity, *in vitro* and *in vivo* (Park 1994; Clauss 1996). In addition to local effects on pre-existing endothelial cells, PlGF is capable to recruit and mobilize VEGFR-1$^+$ haematopoietic precursor cells from the bone marrow (Hattori 2002) to promote healing progression during wound healing. In later phases of healing, PlGF promotes vessel maturation by recruitment of smooth muscle cells/pericytes (Ishida 2001, Luttun 2002) and acts as a survival factor for endothelial cells and macrophages (Adini 2002).
With respect to pathological angiogenesis, PlGF is expressed by melanoma cells and in tissue specimen of both primary and metastatic tumors in culture (Graeven 2000, Lacal 2000). VEGFR-1, Neuropilin-1 and Neuropilin-2 are also transcribed by cultured melanoma cells and treatment with PlGF induces tumor cell proliferation, indicating that PlGF might contribute to melanoma growth through an autocrine mechanism (Lacal 2000). Expression of PlGF and VEGFR-1 appears to be essential for tumor angiogenesis and tumorgrowth. In α_2-integrin knock out mice, VEGFR-1 expression is significantly upregulated on microvascular endothelial cells in the tumor microenvironment when challenged with B16F12 melanoma cells, resulting in a significant increase in tumor angiogenesis and growth compared to wild type mice. Interestingly, B16F12 cells exhibit a strong expression of PlGF, but low levels of VEGF-A. Contrary, when challenged with Lewis lung carcinoma cells (LLC; low levels of PlGF, high levels of VEGF-A), no $\alpha_2\beta_1$ integrin dependent differences were observed. Transfection of LLC with PlGF restored these differences and increases tumor angiogenesis and growth (Zhang 2008).
In addition, PlGF is upregulated in acute cutaneous inflammation. Overexpression of PlGF in the skin of transgenic mice is able to elicit an increased and prolonged inflammatory

reaction when treated with a sensitizing agent. This reaction is less intense and shorter in PlGF-deficient mice compared to wild-type mice (Oura 2003). These findings indicate that PlGF plays a role in inducing the inflammation-associated vascular response.

Although being dispensable for the formation of a primary vascular network and fetal angiogenesis (Carmeliet 2001), PlGF has a strong impact on physiological and pathological angiogenesis in adult. Different mechanisms may be involved: PlGF may induce signal transduction on its own by activation of VEGFR-1, resulting in a variety of cellular responses (as described above) as well as in the expression of a large set proteins including growth factors, receptors and proteases (Autiero 2003). These signals may be even enhanced by recruitment of co-receptors. Another possibility is that PlGF may increase VEGF-A mediated activities by displacing VEGF from VEGFR-1, making it available to activate VEGFR-2 (Hiratsuka 1998, Fong 1999). Recent reports also indicate, that activation of VEGFR-1 by PlGF binding is able to trans-phosphorylate the VEGFR-2 receptor, resulting in an amplified VEGF-A activity (Autiero 2003). Besides its homodimeric activities, several publications report on VEGF-A/PlGF heterodimer biological activity (DiSalvo 1995; Cao 1996a). *In vivo* evidence indicated that VEGF-A/PlGF heterodimers induce vascularization in a corneal micro pocket assay and stimulate myocardial angiogenesis to an extent comparable to that of VEGF-A (Cao 1996b, Autiero 2003). By the formation of VEGFR-1/VEGFR-2 heterodimeric receptors (Autiero 2003) and/or differential recruitment of co-receptors depending on the isoform configuration in the heterodimer, the VEGF-A-mediated activity may be further driven.

1.1.2.4 VEGF receptors and Neuropilin

To promote angiogenesis and/or lymph-angiogenesis, the members of the expanding VEGF family act through one or more VEGF-tyrosine kinase transmembrane receptors (VEGFR; Ferrara 2003). These RTKs (receptor tyrosine kinase) belong to the same subclass of receptors as receptors for PDGFs and fibroblast growth factors (FGFs). Up to date, three VEGF receptors have been identified (named VEGFR-1, VEGFR-2, VEGFR-3), which share sequence homology and structural features (Shibuya 1990, Alitalo 2002). Approximately 750 amino acids form an extracellular domain, which is organized into seven immunoglobulin (Ig)-like folds. It is followed by a single membrane spanning helix, a juxtamembrane domain, a split tyrosine-kinase domain interrupted by a 70-amino-acid kinase insert and a C-terminal tail. The isoforms of VEGF-A are able to bind VEGFR-1 and VEGFR-2 to mediate their angiogenic activities, whereas PlGF-1 and PlGF-2 bind to VEGFR-1, exclusively.

In addition to the VEGFRs, heparin-binding domain-expressing family members are able to recruit co-receptors of the Neuropilin family (Nrp) (Fig 4).

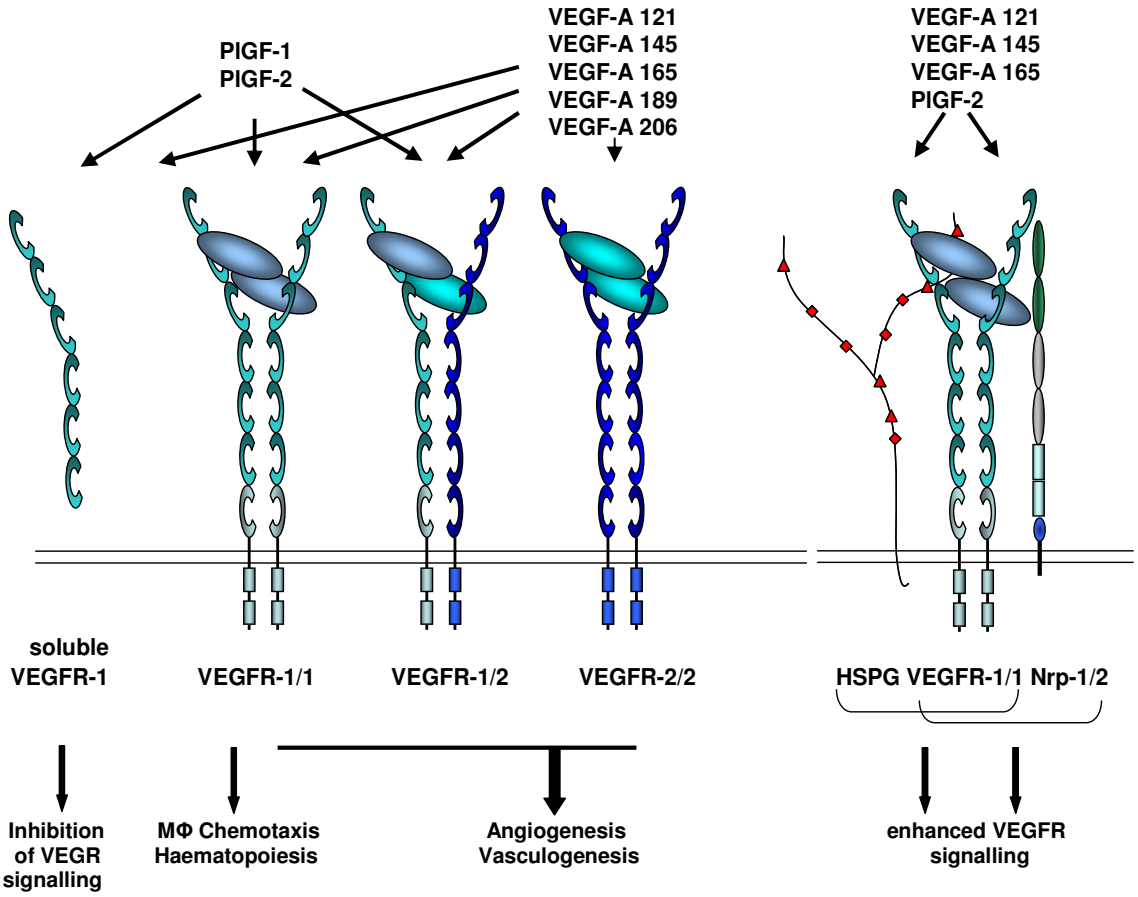

Figure 4: Schematic representation of interactions between VEGF family members and their receptors. Complex network of interactions of VEGF family members with transmembrane and soluble VEGFR-1, VEGFR-2, and Nrp. Interaction between receptor and ligand may be enhanced by heparan sulphate-proteoglycans (HSPG). (Modified: Olsson, *Nature Reviews* 2006).

1.1.2.4.1 VEGFR-1

The VEGFR-1 (Flt-1; Fms-like-tyrosine-kinase-receptor-1) functions as receptor for VEGF-A, -B, and PlGF. Its role has been discussed controversially for a long time. The affinity of VEGF-A to VERGR-1 is approximately one magnitude higher than its affinity to VEGFR-2 (de Vries 1992, Terman 1992, Sawano 1996), but VEGFR-1 auto-phosphorylation is barely detectable in response to VEGF-A (de Vries 1992). Its essential role for embryonic angiogenesis has been demonstrated by formation of unorganized vasculature and endothelial overgrowth in VEGFR-1 deficient mice, resulting in embryonic lethality (Fong 1999). Interestingly, its tyrosine kinase activity appears to be uninvolved in these defects as mice lacking the tyrosine kinase domain (VEGFR-1 $TK^{-/-}$) were healthy and developed almost normal vessels (Hiratsuka 1998). This raised the theory, that VEGFR-1 may act as a “decoy”-receptor. By trapping VEGF-A and therefore preventing binding to VEGFR-2, it may weaken VEGF-A mediated angiogenic signals (Hiratsuka 1998, Fong 1999). Nevertheless, macrophages in these mice exhibit a defective migratory responsiveness for

VEGF-A.

VEGF-A and PlGF exhibit overlapping binding-interfaces to immunoglobulin (Ig)-like domain 2 of VEGFR-1 (Christinger 2004, Errico 2004) but in contrast to VEGF-A, PlGF-glycosylation (Asn_{84}) participates in PlGF binding to VEGFR-1. Interestingly, not all amino acids located in the ligand interface of VEGFR-1 are identical for PlGF and VEGF-A (Wiesmann 1997, Iyer 2001). The affinity of VEGFR-1 for VEGF-A (K_D, 1–20 pM) is higher than that for PlGF-1 and -2 (K_D, about 200 pM) (de Vries 1992, Terman 1992, Waltenberger 1994, Sawano 1996, Yamazaki 2006). Similar to VEGFR-2, immunoglobulin (Ig)-like domains 4-7 are involved in receptor dimerization and activation (Shinkai 1997, Tanaka 1997).

Activation of VEGFR-1 by either PlGF or VEGF-A induces tyrosine phosphorylation in the tyrosine kinase domain of VEGFR-1. Even though VEGF-A_{165} increases VEGFR-1 phosphorylation, it appears not to alter gene expression in cells. In contrast, PlGF induced phosphorylation results in up- or downregulation of the expression of more than 50 target genes. These genes include receptors, protease inhibitors, and transcription factors involved in proliferation (*Ets2*, *Map4k4*, *Fst*, *Jak2*, *Egr1*), apoptosis (*Birc2*) or angiogenesis (*Nrp2*, *Angptl4*, *Dcn*, *Flt1*) (Autiero 2003). Furthermore, it appears to mediate vascular permeability, cell survival, and migration in response to VEGF-A and PlGF (For review see Shibuja 2006)

The downstream signalling of VEGFR-1 to mediate biological activities and distinct gene expression is not completely understood, mainly due to the mild biological activity of this receptor in culture. Several auto-phosphorylation sites in VEGFR-1 have been identified at Tyr_{1169}, Tyr_{1213}, Tyr_{1242}, Tyr_{1309} $Tyr_{1327,}$ and Tyr_{1333} by analysis of point mutations (Cunningham 1995; Sawano 1997, Ito 2001). Tyr_{1213} exhibits the highest degree of auto-phosphorylation in response to VEGF-A, and appears to be involved in a variety of signalling pathways (Fig 5). In addition, Tyr_{1309} is activated exclusively by PlGF. Its role and induced signal transduction remains to be elucidated (Autiero 2003). These phosphorylation sites serve as binding sites for SH2 domain-binding proteins (identified by two-hybrid analysis) and have been shown to activate the downstream targets PLC-γ (phospholipase C-γ), SHP-2 (Src-homology-2-domain-containing PTP2), Grb-2 (growth-factor-receptor-bound-2), PI3K (Phosphatidyl-inositol-3-kinase, p85 subunit), Nck and Crk in response to VEGF-A (Cunningham 1997, Igarashi 1998, Ito 1998, Ito 2001; Fig 5).

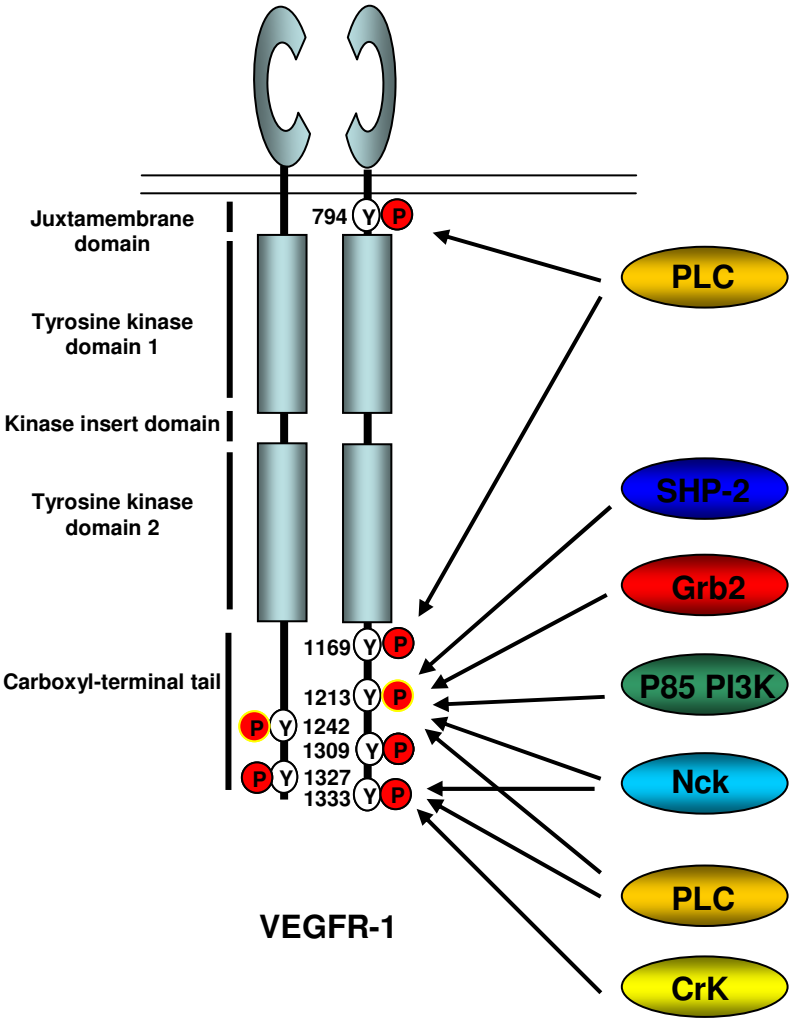

Figure 5: Schematic overview of phosphorylation sites of VEGFR-1 and intracellular mediators Binding of SH2 domain containing signal transduction molecules to different phosphorylated tyrosine residues in intracellular domains of homodimeric VEGFR-1. Positions of the tyrosine residues are indicated by amino acid numbers and by an encircled Y. Auto-phosphorylation sites are indicated by an encircled P. Ps in yellow circles represent major phosphorylation sites. (Modified: Matsumoto, *Science,* 2001).

Activation of VEGFR-1 by PlGF was demonstrated to induce a variety of signal transduction pathways to promote angiogenesis and wound healing. In monocytes, the activation of PI3K and its downstream targets Akt and Erk-1/-2 has been demonstrated to be involved in PlGF mediated chemotaxis. This activation was clearly reduced by corresponding inhibitors as well as function blocking antibodies against VEGFR-1 (Tchaikovski 2008). Furthermore, VEGFR-1 was demonstrated to be directly linked to FAK signalling. Lesslie and colleagues identified the family of Src-kinases as linker between VEGF-A mediated VEGFR-1 signalling and integrin signalling, resulting in specific activation of FAK and $p130^{Cas}$ (Lesslie 2004).

During collateral growth, VEGF-A and PlGF have been demonstrated to activate vascular smooth muscle cell (VSMC) proliferation by activation of VEGFR-1 and induction of the MAPK-cascade (Parenti 2002). In addition, VEGFR-1 mediates tube formation and

survival of endothelial cells when activated by PlGF (Cai 2003). These cellular activities appear to be - at least in part – dependent on a prolonged activation of PI3K signalling und an increase in Bcl-2 expression.

1.1.2.4.2 Neuropilin

To modulate the activities transduced via either VEGFR-1 or -2, the heparin-binding isoforms of the VEGF family are able to recruit co-receptors. Originally identified as a co-receptor for class 3 semaphorines to promote axonal guidance in *Xenopus laevis* (Fujisawa 1995), the members of the Neuropilin (Nrp) family have been demonstrated to increase angiogenic signalling induced by VEGF and its family members by enhancing VEGFR mediated activities (Klagsbrun 2002). Nrp-1 and -2 are transmembrane glycoproteins of 923 and 926 amino acids (130-140 kDa) respectively, and share a similar domain structure as well as an overall amino acid homology of 44% (Chen H 1997). Its large extracellular domain contains two CUB [complement binding factors C1s/C1r, Uegf, BMP1 (bone morphogenetic protein 1)] (a1/a2) domains, two factor V/VIII homology (b1/b2) domains (Takagi S 1991) and a MAM (meprin, A5 antigen, receptor tyrosine phosphatase μ) domain responsible for receptor dimerization. It crosses membrane with a single transmembrane domain and owns a short cytoplasmic tail without any enzymatic activity.

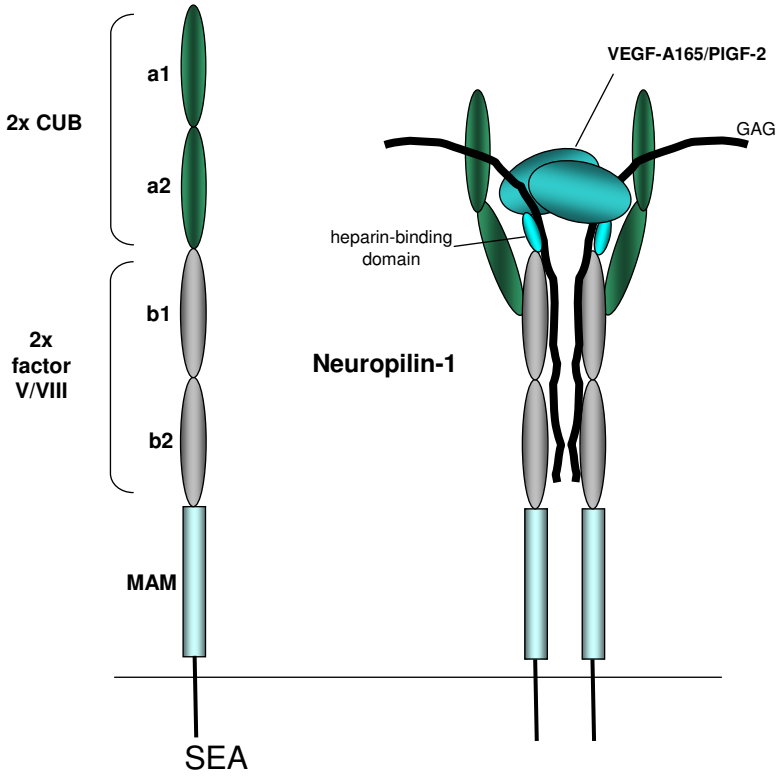

Figure 6: Structural model of Nrp interaction to VEGF-A_{165} or PlGF-2. Model represents the interactions at the core of the ligand-binding interface (b1/b2). The heparin-binding domain of VEGF-A_{165} and PlGF-2 directly interacts with the b1 domain via the terminal residues, encoded by exon 8/7, and also couples heparin and Nrp binding. (Modified: Vander Kooi, *PNAS*, 2007)

The three amino acids closest to the C-terminus constitute the SEA domain (Ser-Glu-Ala), a PDZ domain-binding motif to mediate association with NIP1 (neuropilin interacting protein-1) (Cai 1999).

The binding of VEGF family members to Nrp-1 was predicted to be highly dependent on the expression of the heparin-binding domain as seen for VEGF-A_{165} and PlGF-2, and to be enhanced by heparin (Soker 1995, Migdal 1998). Surprisingly, recent publication identified VEGF-A_{121} as a binding partner for Nrp-1 (Pan 2007a). Among others, the authors identified the amino acids coded by exon 8 (DKPRR) of VEGF-A as the critical determinant for a direct binding to Nrp-1 and confirmed an interaction independent of the heparin-binding domain. This interaction of VEGF-A_{121} and Nrp-1 revealed an affinity, which was comparable to that of VEGF-A_{165} (K_D values of 120 and 220 nM for VEGF-A_{165} and VEGF-A_{121}, respectively) (Pan 2007a). Interestingly, the sequence coded by exon 7 of PlGF (GDAVPRR), which is common to all isoforms, reveals striking similarities to exon 8 in VEGF-A. Although this peptide was found to compete with the binding of PlGF-2 to Nrp-1 in cross-linking experiments (Migdal 1998), a function for exon 7 of PlGF for the binding to Nrp-1 was rarely discussed in the last years. These findings raise the possibility that all PlGF isoforms might bind to Nrp-1. Nevertheless, critical determinants for interaction between PlGF and Nrp-1 remain to be elucidated.

The direct binding site of VEGF-A and PlGF is located in the b1/b2 domain of Nrp-1, as revealed by domain specific binding experiments (Mamluk 2002). This binding of either VEGF-A_{165} or PlGF-2 has been demonstrated to be further enhanced in the presence of heparin. As heparin is bound directly via the b1/b2 domain, it was concluded that heparin is a critical component for the regulation of VEGF-A_{165} and PlGF-2 interaction with Nrp1. The presence of a heparin-binding domain seems to be involved in Nrp-1 binding and – of more importance – appears to be crucial for its activity as co-receptor (Vander Kooi 2007). To promote optimal interaction of VEGF-A_{165} or PlGF-2 with Nrp-1, a 22- saccharide fragment or a 24 monosaccharide is required, respectively (Mamluk 2002, Robinson 2006). The ligand bound heparin-induced dimer of b1/b2 domain likely works in concert with the MAM domain in orienting Nrp to activate VEGF receptors (Vander Kooi 2007). In conclusion, these data strongly argue for a general binding capacity for Nrp-1 binding among VEGF-A and PlGF isoforms. Nevertheless, Nrp-1 recruitment to the VEGFRs appears to be highly dependent on the presence of the heparin-binding domain and binding of heparin or other GAGs. According to this model, the recent finding that Nrp-1 itself can be heparan sulphate or chondroitin sulphate modified on a serine between the b2 and the MAM domains suggests a self-organized active Nrp subform (Shintani 2006).

Several experimental settings have confirmed the role of Nrp-1 as an enhancer of VEGF-A_{165} or PlGF-2 induced activities by co-activation of either VEGFR-1 or -2 to promote

cellular responses (Murga 2005, Becker 2005), but exact mechanisms remain to be elucidated. Recent publications demonstrated a direct role of Nrp-1 in VEGF-A induced phosphorylation of $p130^{Cas}$ and endothelial cell migration (Evans 2011). Furthermore, Nrp-1 was shown to interact directly with integrins to promote its internalization and rapid recycling and therefore migration (Valdembri 2009).

Its essential role for vessel formation during development was demonstrated by overexpression of Nrp-1 in mice. Beside abnormalities of the nervous system, these mice exhibited an excessive capillary outgrowth, haemorrhages, and malformed hearts (Kitsuwaka T 1995). On the contrary, homozygous deletion of Nrp-1 ($Nrp\text{-}1^{-/-}$) resulted in embryonic lethality between E 10 and E 13.5 due to a defective vascular development (Kawasaki 1999, Takashima 2002). Furthermore, Nrp-1 contributes to tumor growth, as induction of Nrp-1 expression in tumor cells *in vivo* resulted in larger and more vascularized tumors (Miao 2000). Strong evidence point to a role of Nrp-1 in cell migration, adhesion and morphogenesis in response to VEGF-A, as neutralizing antibodies that specifically prevent VEGF-A binding to Nrp-1 blocked endothelial cell sprouting and neo-vascularization *in vitro* (Pan 2007b). Interestingly this treatment also prevented pericyte recruitment, suggesting a role of Nrp-1 in maturation and stabilization of new vessels. In addition, Nrp-1 appears to be involved in tip cell guidance in newly sprouting vessels. Analysis of vascularization in the developing hindbrain of $Nrp\text{-}1^{-/-}$ mice revealed, that tip cell filopodia remain associated with radial glia in the subventricular zone of the hindbrain and fail to move laterally across this region, forming characteristic tufts (Gerhard 2004). These findings indicate that Nrp-1 may not be essential for endothelial cell migration, or for elaboration of the cellular migratory apparatus, but rather for determining the trajectories of migrating cells, similar to its path-finding and homing role in neuronal patterning.

1.1.3 The role of the extracellular matrix for angiogenesis

The extracellular matrix is critical for all aspects of vascular biology. It includes the interstitial matrix and the basement membrane, and has to be adjusted to cellular requirements as it regulates intracellular communication as well as cell's motile behaviour. Although gradients of cytokines or other agonists are essential to drive chemotactic migration, such directed motility is dependent on endothelial cell adhesion to extracellular matrix. Furthermore, it appears that some extracellular matrix molecules involved in sprouting angiogenesis are capable to support haptotactic migration by themselves (Dejana 1985, Senger 2002). In this context, interstitial collagen has been demonstrated to be highly effective in promoting haptotactic migration in vitro. Thus, sprouting endothelial cells may migrate in response to both chemotactic gradients of angiogenic cytokines and haptotactic gradients of extracellular matrix molecules (Senger 1996, Senger 2002).

Beside migration, extracellular matrix molecules support endothelial cell proliferation and survival, which is highly dependent on adhesion through integrins (Meredith 1997, Giancotti 1999).

During wound healing, fibroblasts deposit a complex provisional wound matrix consisting of glycosaminoglycans, proteoglycans, collagen III, thrombospondin, fibronectin, and vitronectin, which promote migration, endothelial tube formation and vessel growth (Eming 2007). The cellular response to these molecules is mediated by a specific set of cellular adhesion molecules (integrins), resulting in cytoskeleton re-organization and outside-in signalling (Midwood 2004). During vascular morphogenesis, endothelial cells have to organize themselves into multi-cellular structures. In this context, the extracellular matrix serves as an elastic 3D scaffold in which individual endothelial cells and clusters of endothelial cells can transduce mechanical forces to other endothelial cells at a considerable distance. Thus, by generating mechanical, contractile forces within the extracellular matrix, endothelial cells are able to establish tension-based guidance pathways that allow them to form interconnected cords. These guidance pathways provide a mechanism for endothelial cells to organize into cords at a distance without the initial requirement of cell-cell contact (Vernon 1995, Davis 1996). In addition to mechanical force, components of the extracellular matrix have an important signalling function on cellular shape and contractility: *in vitro* experiments on endothelial cells revealed a drastic effect of collagen I on its morphogenesis. Added to confluent monolayer, cells started to form solid cords and matured into tubes with hollow lumens (Montesano 1983, Davis 1996).

Blood vessel endothelial cells are anchored to the basement membrane, a dense polymeric sheet that is crucial for the proper function of blood vessels. It is known that removal of some of the major components of the basement membrane results in leakiness of the vessels (Poschl 2004). The major constituents of this polymer structure are laminins, nidogens, collagen IV, the heparan sulphate proteoglycan perlecan, and other macromolecules. In addition, basement membranes often contain collagen XV/XVIII and fibronectin. The main collagens expressed in small vessels are collagen IV, XV, and XVIII. Additional collagens are localized in smooth muscle layer around larger vessel, e.g. collagen VIII, XII, and XIV. Networks consisting of polymerized laminins and collagen IV act as a primary scaffold around which the rest of the basement membrane constitutes. Linker proteins such as nidogens interconnect both networks (for review see Yurchenco 2004).

The major laminin isoforms in vascular endothelial basement membranes are laminin 411 and laminin 551 (for review see Hallmann 2005). Loss the of laminin α4 chain in knockout

mice revealed a general delay in basement membrane formation and a weakening of the capillary basement membrane, resulting in haemorrhages (Thyboll 2002). Due to embryonic lethality of laminin α5 knockout mice, its role for angiogenesis remains open. Beside their structural role, laminins are involved in processes as cell migration, differentiation, and proliferation (Colognato 2000, Li 2006).

Perlecan is a multi-domain proteoglycan that interacts with almost all of the other components in the basement membrane and therefore stabilizes its structure. Interaction is predominantly mediated by heparan sulphate side chains that are attached to domains I and V (for review see Knox 2006). This GAG chains are also important to sequester and store growth factor such as FGF-2.

During neo-angiogenesis, new vessels sprout out of existing vessels and grow along a growth factor gradient. To mediate this outgrowth, endothelial cells have to degrade the basement membrane and the surrounding extracellular matrix by expression of proteases, mainly metalloproteases, serine- and cysteine-proteases (for review see Roy 2006). Since endothelial cells are in continuous contact with the matrix, it is not surprising that the interaction with different molecules either supports or inhibits the cells (i.e. in cell migration or cell proliferation). This can be viewed as a balanced system that both forms new blood vessels and prevents overgrowth.

1.1.3.1 The role of integrins

Beside on growth factor stimulation, angiogenesis is highly dependent on outside-in signalling mediated by integrins. These heterodimeric transmembrane cell-surface receptors specifically bind to components of the extracellular matrix and therefore link it to the intracellular cytoskeleton. Composed of one α and one β subunit, subunit assembly is responsible for substrate specificity and resulting cellular behaviour. Integrins have a major impact on cellular functions such as survival, cell-cycle progression, substrate adhesion and cell migration. As angiogenesis is strongly dependent on components of the extracellular matrix, involvement of integrins during vascular remodelling and development is not surprising. On quiescent endothelial cells, integrins $\alpha_1\beta_1$, $\alpha_2\beta_1$, $\alpha_3\beta_1$, $\alpha_5\beta_1$, $\alpha_6\beta_1$, $\alpha_6\beta_4$, and $\alpha_v\beta_5$ are expressed (Stupack 2002) and mediate the attachment to laminins, collagens, fibronectin or vitronectin. This expression profile changes with induction of angiogenesis, and integrin expression is adapted to interact with proteins of the provisional matrix by upregulation of $\alpha_1\beta_1$, $\alpha_1\beta_2$, $\alpha_6\beta_1$ and $\alpha_v\beta_3$ (Stupack 2002; Lee 2006) to promote endothelial cell migration. In addition, binding of collagen I to $\alpha_1\beta_1$ and $\alpha_2\beta_1$ provokes endothelial cell morphogenesis and formation of cord-like structures (Senger 1997, Whelan 2003). Upregulation of $\alpha_1\beta_1$ and $\alpha_2\beta_1$ in part appears to be dependent on VEGF-A. Furthermore, these integrins have been shown to be directly involved in VEGF-A induced

angiogenic activity, as antibodies that block α_1 and α_2 substantially inhibited VEGF-A induced angiogenesis without affecting the pre-existing vasculature (Senger 1997). Overlapping with a change of integrin expression pattern, activated endothelial cells secrete a set of proteases to degrade the basement membrane and components of the extracellular matrix to promote vascular sprouting (for review see Roy 2006). Caused by the degradation of the basement membrane, endothelial cells are exposed to underlying interstitial collagens. This exposure results in $\alpha_1\beta_1$ and $\alpha_2\beta_1$ integrin activation and the cells start to invade the extracellular matrix. Integrin activation results in a marked induction of actin polymerization, this process contributes to the formation of prominent stress fibres, endothelial cell contractility, and initiation of capillary morphogenesis. The degradation of extracellular matrix molecules also results in the exposure of matricryptic sites to endothelial cell adhesion receptors (Davis 2000). One of the critical matricryptic sites present in e.g. fibronectin, collagens and vitronectin is Arg-Gly-Asp (RGD) (Ruoslahti 1996, Newby 2008, Astrof S 2009). The RGD motive can bind to $\alpha_5\beta_1$ and $\alpha_v\beta_3/\alpha_v\beta_5$ integrins and thus has an impact on endothelial cell adhesion, migration, proliferation, survival and cell–cell interactions during angiogenesis (Ramjaun 2009). Requirement of $\alpha_v\beta_3$ for angiogenesis was demonstrated by its inhibition by either function blocking antibodies or cyclic RGD-peptides. This inhibition selectively induced apoptosis of activated endothelial cells (Brooks 1994a; Brooks 1994b).

1.1.3.2 Growth factor-matrix interactions

The role of interaction between growth factors and molecules of the extracellular matrix has a strong impact on inflammation, vascular morphogenesis and remodelling during wound healing. For VEGF and many other growth factors, matrix-binding properties are regulated by alternative splicing and generation of isoforms with distinct affinities for specific extracellular matrix molecules and an altered diffusability. Expression of a varied isoform subset allows a spatially regulated activity. Beside regulation of isoform expression, matrix bound isoforms can be released by proteases expressed by inflammatory cells and subsequent proteolytic processing. Taking VEGF-A as an example, plasmin and a subset of MMPs can cleave the C-terminal region of the protein to release a bioactive growth factor from its anchorage site in the extracellular matrix (Lee 2005). By this release, levels of soluble and matrix bound VEGF-A are modulated, which has been demonstrated to have an impact on either increased vessel size or sprouting angiogenesis. This was confirmed by experiments using engineered VEGF-A forms. VEGF-A_{113}, mimicking the soluble, processed VEGF-A induced a vascular network with low density and poor branching, whereas a mutant VEGF-A, resistant to plasmin or MMP cleavage resulted in thin and highly branched vessels (Lee 2005). Although the exact

mechanisms remain to be elucidated, differential activity among soluble and bound VEGF-A on endothelial cell response appear to involve VEGFR-2 clustering, increased receptor internalization and alteration of downstream phosphorylation kinetics (Chen 2010).
Beside storage, release and regulation of bioavailability, binding to matrix molecules has been demonstrated to be essential for the activation or inhibition of certain growth factors. The association of TGF-β to thrombospondin-1 (TSP-1) is pivotal for its physiological relevant activation (Young 2004). On the contrary, binding of VEGF-A to TSP-1 inhibits its activity (Greenway 2007).

1.1.4 The role of cell-cell communication

To induce angiogenesis and restore skin homeostasis after injury, a variety of structures have to be re-organized to promote processes such as cellular re-programming and differentiation or migration and proliferation. In this context, cell-cell contacts are essential, as they trigger intracellular responses either to maintain homeostasis or – by disturbance of interaction or alteration of surface receptor expression – to induce specific cellular activities.
During blood vessel homeostasis, two types of specialized endothelial junctional complexes maintain the barrier function of endothelial cells. Tight junctions are organized by claudins, occludins, and junctional adhesion molecules, whereas adherens junctions are organized by catenins and cadherins, mainly VE-cadherin (Dejana 2009). Together, the extracellular associations of these complexes and their intracellular linkage to the cytoskeleton maintain and actively regulate the vascular barrier (Dejana E 2008). Induced by inflammatory stimuli, an enhanced vascular permeability by untightening junctional complexes enables an increased deposition of provisional matrix by leakage from the blood and infiltration of leukocytes into the tissue. Disruption of barrier function was shown to be induced by VEGF-A mediated clatrin-dependent internalization of VE-cadherin (Gavard 2006). Besides an increasing permeability, loosening of cell-cell junctions is a prerequisite for cells to migrate (Potter 2005). Furthermore, VEGF-A signalling drives the turnover of focal adhesions and re-organization of the cytoskeleton resulting in a loss of cell polarity and induction of proliferation. Changed in their cellular features and molecular expression pattern, these activated endothelial cells are enabled to infiltrate into the tissue to form new vascular sprouts.

To stabilize the newly formed sprout, its maturation by direct interaction between endothelial cells and pericytes is essential. Pericytes are recruited to the vessel by PDGF-B (Hoch 2003), which in binding to the PDGFR-β induces the proliferation of pericytes and their migration along the nascent vessel (Hellstrom 1999). PDGF-B in turn is secreted by

tip cells (Gerhardt 2003) and localized to the growing vessel's wall by binding to heparan sulphate proteoglycans (Abramsson 2007). Between the two cell types, cell-cell contacts are established, which allow communication between the cells (Armulik 2005). As single pericytes often interact with several endothelial cells through these contacts, they may integrate and coordinate adjacent endothelial cell responses (Armulik 2005).

1.2 Tissue repair and regeneration

Tissue repair and/or regeneration following injury ensure the survival of a variety of organisms. The optimal process to handle tissue defects is regeneration, as it represents a replacement of lost or damaged tissue with an exact copy, such that both morphology and functionality are completely restored. Although it can be found in all organisms, the capability for regeneration decreases with the grade of evolutionary development of organisms. In mammals, the capability for regeneration is restricted to a few tissues like liver, bones, and nerve cells. A variety of stem cells can be found in adult that can differentiate in various cell types, and are under intense investigation as they may help to develop therapies and regenerate injured or lost tissue.

In contrast to regeneration, repair is the more common mechanism to correct tissue defects. Although it restores the direct defects and in part the main function of the injured tissue, a complete restoration of function and shape is not achieved (an example is scar formation in skin in mammals). Interestingly, injured embryos heal scar less, which in turn means that wound healing of mammals in embryonic stages reflects regeneration rather than repair.

1.2.1 Skin morphology

The functions of skin are various but it mainly protects the inner organs from the surrounding environment. Beside protection from mechanical, chemical and UV-damage, and its role in thermoregulation, it mainly acts as a barrier to regulate water loss and to protect from microorganisms. Besides passively protecting from pathogens, it hosts components of the humoral, cellular and complement immune response. Furthermore, it also acts as a sense organ and mediates mechanical, thermal, chemical and pain impulses.

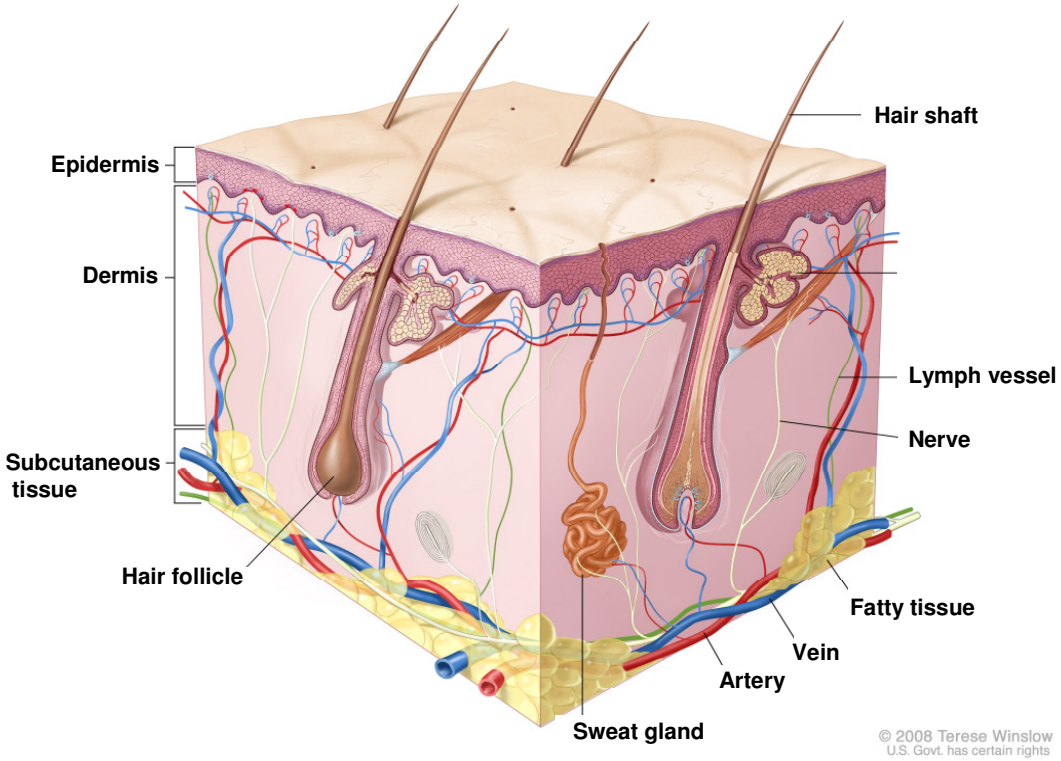

Figure 7: Schematic composition of human skin (©Terese Winslow, 2008)

Adult skin consists of two tissue layers, a keratinized stratified epidermis, and an underlying thick layer of collagen-rich dermal connective tissue providing support and nourishment, both separated by a basal membrane (Fig 7). The dermis ensures reversible flexibility and tensile strength by a dense network of collagen fibers and other components of the extracellular matrix. In addition, these molecules prevent water loss due to their negative charge (Rook`s Textbook of Dermatology, 2008). Although derived from the epidermis, appendages like hairs and glands project deep into the dermal layer. Besides a dense network of capillaries and lymph vessels to ensure supply of both layers with nutrients, nerve endings, several cell types like fibroblasts and cells of the immune system (lymphocytes, macrophages, and mast cells) are located in the dermis.

The epidermis functions as the actual barrier of the organism to the environment and undergoes a constant flow of proliferation, differentiation, and desquamation. To ensure constant renewal and turnover of the epidermis (Koster 2008), the keratinocytes of the epidermis are affected by an intense regeneration activity in which epidermal stem cell division mainly takes place in the stratum basal, located above the basal membrane. Mitosis results in two daughter cells from which one keeps its stem cell characteristics and stays resident, whereas the other migrates through the layers of the epidermis to reach final differentiation. Entering the stratum spinosum, keratinocytes increase volume of

cytoplasm and amount of organelles (rough endoplasmatic reticulum, ribosomes and mitochondria) suggesting an intensive synthesis activity. These cells produce keratin, an intermediate filament, which polymerizes and aggregates into bundles (Smack 1994). In the stratum granulosum, keratinocytes show keratohyalin granulae embodying e.g. filaggrin and loricrin (Fuchs 1990, 1993) and nuclei and organelles start to regress. Reaching the stratum corneum keratinocytes obtain terminal differentiation and become apoptotic. Due to dehydration, secretion of lipids into the extracellular space and formation of a keratin filled cornified envelope, the flattened and dead keratinocytes form a barrier to prevent water loss (Smack 1994, Proksch 2008). As in skin a homeostatic flow of proliferation, differentiation, and desquamation of dead cells takes place, epidermis is renewed constantly within around 30 days. In addition to keratinocytes, sensory Merkel cells, melanocytes and Langerhans cells, a subset of dendritic cells are present in the epidermis whereas vasculature is absent.

1.3.2 Phases of cutaneous tissue repair

Restoration of tissue integrity and homeostasis following injury is a fundamental property of all organisms. Although wound healing processes take place in many human tissues, only epithelia have the potency for a complete regeneration.

Wound healing is a highly dynamic process and involves a complex interaction among extracellular matrix molecules, soluble mediators and various resident or recruited cell types. The involved processes follow defined, partially overlapping phases: haemostasis, inflammation, tissue formation and tissue maturation (Fig 8) (Martin 1997, Singer 1999, Gurtner 2008). All these phases exert specific contributions on blood vessel growth and remodelling, and a well-defined chronology of wound phases is crucial for optimal repair and restoration of a functional vasculature (Eming 2007).

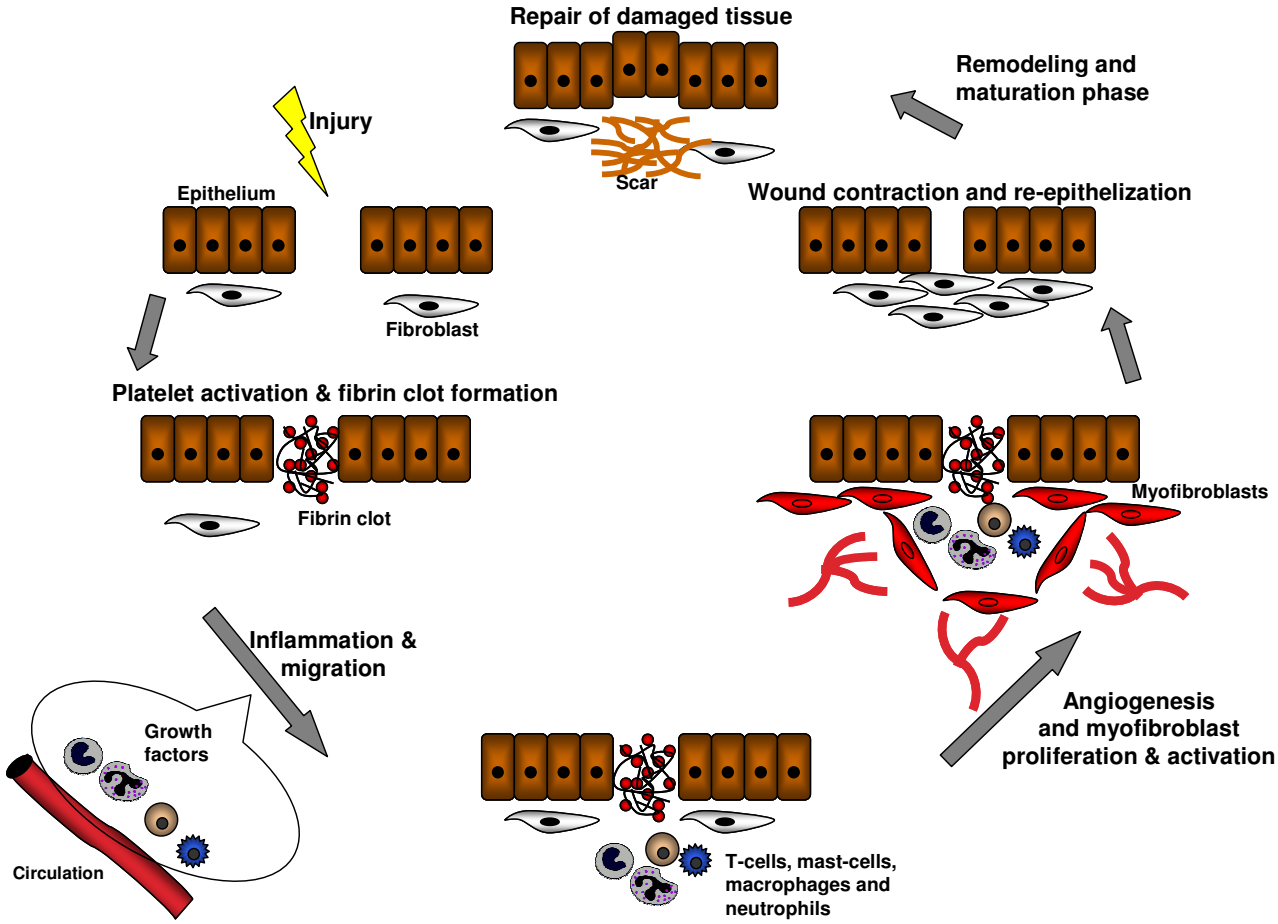

Figure 8: Phases of cutaneous wound healing. Following tissue injury, epithelial and/or endothelial cells release inflammatory mediators that initiate the coagulation cascade, which triggers blood clot formation. This is followed by an inflammatory and proliferative phase, during which leukocytes are recruited, activated, and induced to proliferate by chemokines and growth factors. The activated leukocytes secrete pro-inflammatory cytokines. Stimulated epithelial cells, endothelial cells, and myofibroblasts produce MMPs, which disrupt the basement membrane, and additional cytokines and chemokines that recruit and activate neutrophils, macrophages, T-cells, B-cells, and eosinophils. The activated macrophages and neutrophils phagocyte tissue debris, dead cells and invading organisms. Shortly after the initial inflammatory phase, myofibroblasts produce extracellular matrix components, and endothelial cells form new blood vessels. In the subsequent remodelling and maturation phase, the activated myofibroblasts stimulate wound contraction. Collagen fibers also become more organized, blood vessels are restored to normal levels, and scar tissue is eliminated (Modified: Wynn, *Clin Invest*, 2007).

1.3.2.1 Haemostasis

As a primary response to injury of epidermis, dermis, and blood vessels, the clotting cascade is initiated to stop bleeding. Vasoconstriction of the injured blood vessels is induced by pro-inflammatory factors such as prostaglandins released from ruptured cell membranes to minimize bleeding. Platelets that got in contact with collagen start to form aggregates and release further pro-inflammatory factors, resulting in vessel vasodilatation and increased permeability to promote the re-location of plasma cells and growth factors into the wound site. By cross-linkage of fibrin and fibronectin, a fibrin clot is formed that serves as a structural support and provides a matrix for cell migration (Midwood 2004,

Nguyen 2009; Fig 8).

1.3.2.2 Inflammation

Attracted by chemokines, polymorphonuclear neutrophils (PMNs) enter the wound site by transmigration across the endothelial cell wall of blood capillaries, activated by pro-inflammatory cytokines such as interleukin-1β, TGF-α and interferon-γ in the early phase of inflammation within 1 hour (de la Torre 2008, Eming 2007). The primary function of recruited neutrophils is to kill bacteria by the release of free radicals (respiratory burst) (Greenhalgh 1998, Muller 2003). They clear the wound site by phagocytosis of debris and bacteria, and break down damaged tissue by release of proteases (Martin 2005). In addition, neutrophils have been identified as an important source for pro-angiogenic factors, including VEGF-A and interleukin-8 (Li 2003a/b, Ancelin 2004, Ohki 2005; Schruefer 2006). Mouse models for ischemia and wound healing identified PMNs as an important source of these factors crucial for wound angiogenesis (Ancelin 2004; Ohki 2005). The number of PMNs is further increased by vasoactive mediators released by tissue resident mast cells (Weller 2006, Eming 2007) Once activated, neutrophils release chemokines and cytokines that in turn activate tissue resident immune cells (Dearman 2000), keratinocytes and fibroblasts (Hubner 1996). In addition, other leukocytes such as T-helper cells enter the wound area and secrete cytokines to induce T-cell proliferation. This cytokine release further increases the inflammation and enhances macrophage activity (Dealey 1999, Santorro 2005). Monocytes from the blood are attracted to the wound site by highly regulated gradients of growth factors secreted by platelets 1-1.5 days post wounding and mature into macrophages (Eming 2007). Besides their immunological function as antigen presenting cells and phagocytosis during wound repair, macrophages are thought to play an integral role in a successful outcome of the healing response. They synthesize numerous potent growth factors such as TGF-β, TGF-α, bFGF, PDGF and VEGF-A, which promote angiogenesis, cell proliferation and the synthesis of extracellular matrix molecules by resident skin cells (Deodhar 1997, Mercandetti 2005, Moklovan 2005, Santorro 2005, Swirski 2009).

As inflammation declines, macrophages and neutrophils are removed by lymph vessels or undergo apoptosis and the amount of inflammatory factors decreases, indicating a change from the inflammation phase to the proliferation phase. Although essential for a proper healing response, a prolongation of inflammation may lead to tissue damage and chronic non-healing wounds (Midwood 2004, de la Torre 2006).

1.3.2.3 Proliferative phase

Concomitantly with late inflammation, the proliferative phase starts between day 2 and 3 post wounding by infiltration of fibroblasts and endothelial cells. As a first step of the proliferation phase (2-5 days after wounding), fibroblasts migrate from the uninjured cutaneous tissue into the wound site using the fibrin cross-linking fibers as a substrate and start to proliferate. (Stadelmann 1998, Romo 2005, de la Torre 2006). By deposition of extracellular matrix components they provide a provisional matrix consisting of fibronectin, collagen, glycosaminoglycans, elastin, glycoproteins and proteoglycans, which facilitates cell migration and serves as a depot for growth factors (Lorenz 2003, Romo 2005).

Simultaneously with fibroblasts, endothelial cells from uninjured blood vessels and endothelial stem cells infiltrate the wound area, attracted by fibronectin and chemotactic growth factors released by macrophages and others, to form new blood vessels (angiogenesis) and to supply nutrients and oxygen to the healing tissue. Migration, proliferation, and angiogenesis are ensured by secretion of proteases such as collagenases, plasminogen activator and MMPs by endothelial cells. As new vessels are established and oxygenation rate is normalized, macrophages stop producing angiogenic factors and endothelial cell proliferation decreases. (Greenhalgh 1998, Stadelmann 1998, Lansdown 2001, Romo 2005, de la Torre 2006).

By infiltration of a variety of cell types into the wound site, matrix deposition and formation of new blood vessels a rudimentary and provisional tissue is formed, and grows until the wound bed is covered. This granulation tissue varies from uninjured tissue by its high cell number and extracellular matrix composition and it is replaced in the late phases of healing.

With begin of granulation tissue formation the basis for re-epithelialization is created, and epithelial cells migrate into the wound area in order to re-establish a barrier between wound and environment (Romo 2005). The main cells responsible for re- epithelialization are basal keratinocytes and cells from dermal appendages such as hair follicles, sweat glands and sebaceous glands (DiPietro 2003). Migration of keratinocytes is stimulated by lack of contact inhibition and chemicals such as nitric oxide released in the wound site (Witte 2002). As migration is induced, cells dissolve their desmosomes and hemidesmosomes, and integrins are re-located from the intermediate filaments to the actin filaments to allow migration. Interaction of integrins with the extracellular matrix further stimulates keratinocytes to proliferate. Keratinocytes migrate as a sheet and new epithelial cells must proliferate at the wound edges to provide sufficient cells for the advancing epithelial tip (Deodhar 1997). Once the wound is covered, proliferation and migration are stopped by contact inhibition. Cells start to secrete components of the basement membrane and re-establish desmosomes and hemidesmosomes (Lorenz 2003, Santoro

2005).

Re-epithelialization is supported by contraction of the wound and is pushed by myofibroblasts (Eichler 2005). They migrate to the wound edges, form connections to the extracellular matrix and attach to each other by desmosomes. Wound edges are pulled together by actin contraction (Deodhar 1997, Mirastschijski 2004). As wound healing proceeds and the provisional matrix is exchanged, myofibroblasts stop contraction and commit apoptosis. These events trigger the onset of the maturation stage of wound healing.

1.3.2.4 Tissue maturation

Tissue maturation starts, when homeostasis between collagen production and break down by secreted proteases is achieved, and may last more than a year (Greenhalgh 1998). During maturation, collagen type III, which is laid down predominantly during the proliferation phase, is degraded and replaced by collagen type I (Dealey 1999), which is re-arranged, cross-linked and aligned along tension lines (Lorenz 2003) to increase tensile strength. As cell activity and metabolism decrease, the need for nutrients and oxygen declines, and blood vessels partly regress (Greenhalgh 1998). There are several hypotheses for mechanisms, that might contribute to vascular regression at the wound site: first by a decrease in the expression of growth factors crucial for endothelial cell survival; second by the increased expression of angiogenic inhibitors (Polverini 1995; Streit 2000) or third by the transition from a provisional extracellular matrix consisting of highly pro-angiogenic molecules such as vitronectin, fibronectin and fibrin to a permanent collagenous extracellular matrix. The latter assumption is supported by recent studies in mice deficient for the collagen receptor $\alpha_2\beta_1$-integrin, which showed a prolonged and increased angiogenic response during cutaneous repair (Eming 2007, Zweers 2007, Grenache 2007). Remaining vessels mature by recruitment of pericytes and the network re-organizes by pruning. (Braiman-Wiksman 2007). Both endothelial cells and pericytes assemble the novel basement membrane, containing laminins, fibronectin, nidogen-1, and perlecan (Stratman 2009). Basement membrane synthesis is accompanied by a change of integrin expression profile in both cell types and contributes to the regulation of the vessel's diameter. In addition, the release of protease inhibitors by vascular cells stabilizes the basement membrane: endothelial cells secrete the soluble tissue inhibitor of metalloproteinase-2 (TIMP-2) while pericytes secrete TIMP-3, which becomes sequestered in the basal membrane due to heparin-binding motifs (Saunders 2006).

1.3.3 Conditions of disturbed wound healing

During wound healing, all involved processes are transient and highly synchronized and a tight control of all mediators is essential to orchestrate the behaviour of the various cell types for a normal healing. Disturbance of this normal progression may result in chronic, non-healing wounds. These chronic wounds are rather frequent with 3-4% of people older than 60 years concerned (Tredget 2009), and case numbers are expected to increase due to a progressive demographic development. To date, no efficient treatment for disturbed wound healing is available, thus therapy and care cause immense costs to the health care system (Walmsley 2002).

Reasons for impaired wound healing are various, but mainly are based on tissue ischemia, venous insufficiency, diabetes or pressure (Nwomeh 1998). Resulting hypoxia promotes apoptosis of affected tissue and recruitment of macrophages, which in turn secrete neutrophil chemoattractants and pro-inflammatory substances (Eming 2007). Extensive amounts of proteases such as MMPs, neutrophil-derived elastase and plasmin are released by neutrophils and other inflammatory cells located at the wound site (Nwomeh 1998, Lauer 2000). During normal wound healing, these proteases are highly regulated by inhibitors and restricted in their activity in time and space. Dysregulated proteases damage tissue resident cells, degrade extracellular matrix components or process growth factors essential for healing and therefore disturb normal healing progression and further increase the inflammatory response (Menke 2007).

1.3.4 The db/db-mouse as a model for disturbed wound healing

In order to analyse the role of PlGF for angiogenesis during cutaneous wound healing, the diabetic mouse C57BLKS/J-m+/+ $Lepr^{db}$ (db/db mouse) was used as a model for disturbed wound healing. In these mice, the leptin receptor expression is disrupted by deletion of a single base in the db gene locus (coding for the leptin receptor), resulting in a truncated receptor partially lacking the intracellular domain. Upon ligand binding, signal transduction is inhibited. Carrying this mutation homozygously, mice develop diabetes and suffer from an adipose, hyperglycaemic and hyperinsulinemic phenotype beginning at 4 weeks of age (Coleman 1982).

Interestingly, these diabetic mice exhibit an impaired healing response upon wounding, characterized by attenuated inflammatory and proliferative response, and decreased in granulation tissue formation, re-epithelialization, and vascularization (Frank 2000, Goova 2001). The reasons for a disturbance in wound healing are not completely understood, but it appears that direct effects caused by the defective leptin receptor, as well as indirect effects caused by pathomechanisms due to hyperglycaemia are responsible. As a direct effect of missing leptin-induced signal transduction, promotion of angiogenesis is disturbed

and endothelial cells, keratinocytes, T-lymphocytes and haematopoietic precursor cells lack its proliferative stimulus (Sierra-Honigmann 1998, Fantuzzi 2000, Frank 2000). Furthermore, fibroblasts are less migrative in these mice (Lerman 2003) which may contribute the decrease in granulation tissue formation and maturation.

Caused by hyperglycaemia, the expression of several growth factors such as KGF, VEGF-A, Ang-2, MIP-2, and MCP-1 essential for normal healing is misregulated, resulting in for example prolonged persistence of neutrophils and macrophages (Werner 1994, Frank 1995, Wetzler 2000, Benjamin 2001, Kämpfer 2001, Ozawa 2001).

A variety of these alterations, directly or indirectly involve VEGF-A-mediated effects on angiogenesis during wound healing. The overall level of VEGF-A mRNA and protein is markedly decreased in db/db mice. As KGF is one of the inducers of VEGF-A expression, VEGF-A downregulation appears to be, at least in part, reasonable. Furthermore it has been shown, that a disturbed intracellular vesicle trafficking decreases VEGF-A levels (Werner 1994, Frank 1995, Ozawa 2001). VEGF`s bioactivity is further diminished by enhanced expression of several proteases, demonstrated to proteolytically process the heparin-binding domain of VEGF-A. This degradation results in a reduced activity and disturbed anchorage to the extracellular matrix (Lauer 2000, Goova 2001, Lee 2005, Chen 2010).

Similar to VEGF-A, PlGF has been reported to be dysregulated in diabetes as demonstrated in streptozotocin-induced diabetes, a model of type 1 diabetes. Normally expressed at high levels during cutaneous wound healing, PlGF expression is markedly reduced by five fold (mRNA level: 2.82 ± 0.43 in diabetics versus 14.85 ± 0.33 in healthy mice) at day 3 in these mice (Cianfarani 2006). In contrast, diabetic mice overexpressing PlGF in the skin displayed an accelerated healing process compared with diabetic wild-type littermates. Moreover, diabetic wound treatment with an adenoviral vector expressing the human PlGF gene significantly accelerated the healing process, as compared to wounds treated with a control vector. PlGF gene transfer improved granulation tissue formation, maturation and vascularization, as well as the local recruitment of monocytes/macrophages. As PlGF markedly increases the expression of other growth factors such as PDGF, FGF-2 and VEGF-A, the positive effects of PlGF may be further enhanced. In addition, PlGF treatment induced migration of cultured dermal fibroblasts underlining a direct role in acceleration granulation tissue maturation (Cianfarani 2006). As during wound healing the upregulation of PlGF temporarily coincides with that of VEGF-A (Brown 1992, Failla 2000) and as PlGF is able to potentiate VEGF-A mediated pro-angiogenic activities (Carmeliet P 2001), these two factors may have a synergistic activity during the repair process. Therefore, both growth factors are interesting therapeutic targets. VEGF-A treatment results in an improved re-epithelialization of diabetic wounds

associated with enhanced vessel formation (Deodato 2002, Romano Di Peppe 2002, Galiano 2004). However, exogenous administration of VEGF-A induces sustained vascular leakage and promotes the formation of disorganized blood vessels, as well as malformed and poorly functional lymphatic vessels (Carmeliet 2000, Nagy 2002). In contrast, PlGF treatment resulted in a normal and homogenous vessel distribution, and promotes vessel stabilization and maturation by recruitment of pericytes and may therefore be favourable for therapeutic use. Furthermore, it has a strong impact on granulation tissue formation and maturation and therefore promotes an increase of quality of wound healing. Whether these effects are direct or indirect by increased expression of pro-angiogenic growth factors and/or pushing VEGF-A activity has to be further investigated

.

Objectives

PlGF has been demonstrated to have a major impact on physiological as well as on pathological angiogenesis. As a member of the VEGF family, PlGF shares a variety of structural attributes and pro-angiogenic activities with VEGF-A. Similarly to VEGF-A, PlGF is regulated by mRNA splicing resulting in the expression of alternative protein isoforms that mainly differ in the presence or absence of a C-terminal heparin-binding domain. The exact role of this domain for the regulation of PlGF-mediated activities is unknown. Functional analysis of the heparin-binding domain in VEGF-A have clearly underlined its essential role to mediate pro-angiogenic activities. These observations raised the hypothesis, whether the presence of the heparin-binding domain (either regulated by alternative mRNA splicing or proteolytic processing) provides a principle mechanism to regulate the activity of VEGF-family members. The specific function of the heparin-binding domain of PlGF remains to be elucidated and is the objective of the present study.

The specific aims of this study are:

1) To analyse the role of proteolytic processing for the regulation of PlGF mediated activities. In this context, the protease sensitivity of PlGF-1 and PlGF-2 will be analysed, and involved proteases have to be identified. Assuming a regulation by C-terminal cleavage, the identification of cleavage sites provides the possibility to generate truncated PlGF isoform and to analyse the functional consequence of this degradation.

2) Determine the functional relevance of the heparin-binding domain of PlGF. For this purpose PlGF-1 and PlGF-2, as well as a truncated form of PlGF (lacking the C-terminus) will be expressed in HEK293 cells. A direct comparison of the diverse isoforms will help to identify functional differences as well as altered biological activities due to the presence/absence of the heparin-binding domain.

a) The binding capacity of the PlGF-isoforms to GAGs and Nrp-1 will be tested using Surface Plasmon Resonance spectroscopy.

b) The functional relevance of the C-terminal domain will be assessed by analysis of the *in vitro* chemotactic activity and endothelial cell sprouting capability of PlGF-isoforms on endothelial cells

c) The functional impact of the PlGF C-terminal domain *in vivo* will be determined by studying the angiogenic effect of PlGF-isoforms in a diabetic mouse model of impaired wound healing

2 Results

2.1 PlGF is proteolytically processed by plasmin

Expressed in the liver as a pro-enzyme, plasmin is locally activated during normal wound healing to promote cellular infiltration into the provisional extracellular matrix and therefore facilitates processes as angiogenesis. Under non-healing conditions plasmin and other proteases are misregulated, resulting in its increased activation. Under these conditions, VEGF-A_{165} has been demonstrated to be proteolytically processed resulting in the loss of its heparin-binding domain and a marked reduction of its pro-angiogenic activity (Lauer 2000, Roth 2006). Due to high structural and sequential homology among VEGF-A and PlGF, this form of regulation might be a general mechanism of regulation in the VEGF-family. To analyse the sensitivity of rhPlGF-1 and -2 for plasmin-mediated proteolytic processing, both isoforms were incubated with the serine protease plasmin and samples were subjected to SDS-PAGE and silver-staining. Incubation of rhPlGF-2 (46 kDa as dimer) in presence of plasmin resulted in its degradation and formation of a cleavage product of approximately 32 kDa under non-reducing conditions (Fig 9a). Consistent with this data, the rhPlGF-2 monomer exhibited an electrophoretic mobility shift from 23 kDa to approximately 16 kDa under reducing conditions (Fig 9b). Due to this consistence, retention of cleavage fragments bound by disulfide bonds is excluded. This 16 kDa core-fragment was not subjected to further degradation and retained its stability over 4 hours of incubation. No small cleavage products were detectable, arguing for more than one cleavage sites. Fragmentation of rhPlGF-2 was prevented by the specific plasmin-inhibitor α2-antiplasmin (Fig 9c). This excluded weak protein stability as a reason for degradation, and confirmed plasmin specific digestion.

Interestingly, incubation of rhPlGF-1, which has a molecular weight of 17 kDa under reducing conditions with plasmin, resulted in a mobility shift of approximately 1-2 kDa (Fig 9d) and formation of a core-fragment identical in size to plasmin processed PlGF-2 under reducing conditions. rhPlGF-1 and rhPlGF-2 are identical in sequence except the C-terminal heparin-binding domain. The formation of plasmin-resistant core-fragments with identical molecular weight, therefore strongly argued for a degradation of the C-terminus of the protein, N-terminal of the heparin-binding domain.

To further support the idea that proteolytic processing of rhPlGF-2 by plasmin results in a C-terminal cleavage and loss of the heparin-binding domain, an antibody detecting the N-terminus was used to analyse the concentration-dependent degradation of rhPlGF-2.

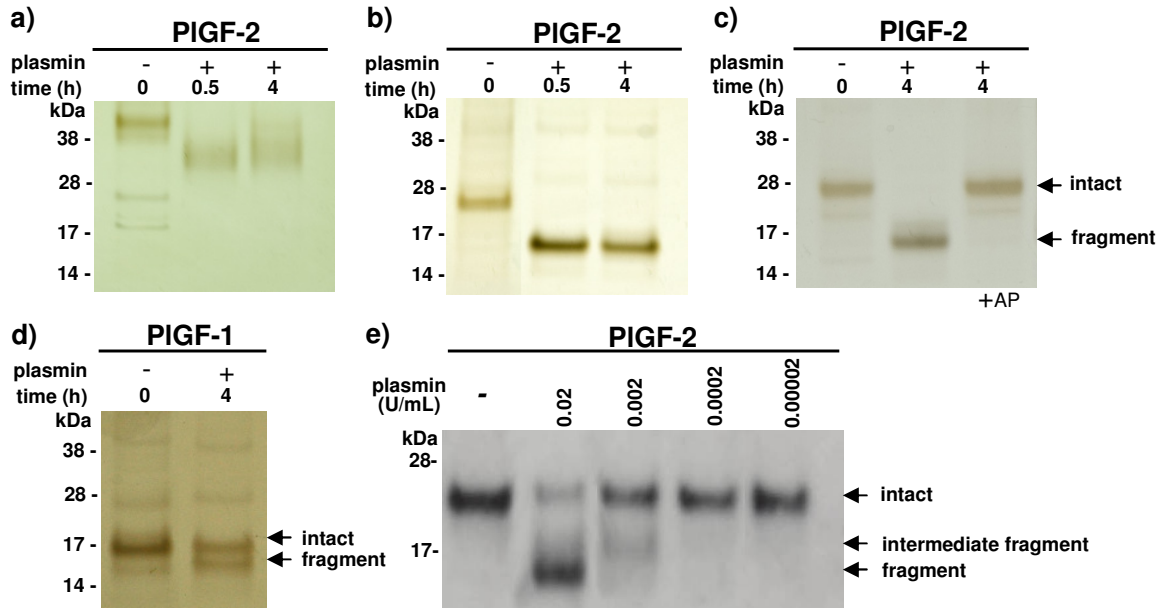

Figure 9: PlGF is proteolytically processed by plasmin. (a-d) silver-stain: rhPlGF-1 and rhPlGF-2 (expressed in Sf9 cells; 500 ng/lane) were incubated with plasmin (0.02 U/mL) and α_2-antiplasmin (AP; 0.4 U/mL) for different periods of time, as indicated. **(e) Western blot:** rhPlGF-2 (200 ng/lane) was incubated with decreasing concentrations of plasmin (as indicated) for 30 minutes and was detected by a PlGF-specific antibody (raised against the N-terminus of the protein). SDS-Page was performed under **(a)** non-reducing and **(b-e)** reducing conditions.

Western blot analysis confirmed C-terminal cleavage and N-terminal core-fragment formation (Fig 9e), which strongly indicated a processing of the heparin-binding domain. Furthermore, a decrease in plasmin concentration resulted in the generation of an intermediate fragment with an electrophoretic mobility of approximately 19 kDa, arguing for at least one additional cleavage site within the heparin-binding domain. Due to the formation of intermediate products, this successive C-terminal processing appeared to start at the C-terminus or at least within the heparin-binding domain.

2.2 Expression and purification of rhPlGF isoforms in HEK293 cells

For the synthesis of rhPlGF isoforms, the cDNA of human PlGF-1 and PlGF-2 from placenta, was cloned into the eukaryotic expression vector pCEP V149 and expressed in HEK293 cells. Both isoforms are flanked by an N-terminal 6x his-tag and a C-terminal 2x strep-tag, which were necessary for the purification and the identification of the plasmin cleavage sites (Fig 10a). To enable cleavage of the C-terminal strep-tag in the PlGF protein, the vector sequence carries the recognition site for FactorXa cleavage, which permits specific removal of the tag after purification. In addition, the same sequence was inserted at the 5`-end of the DNA-sequence of PlGF by primer design, prior to cloning into the vector. Unexpectedly, FactorXa cleavage revealed, that PlGF is sensitive for FactorXa processing within its protein sequence. As the step-tag is well established and

known to lack an unspecific reactivity, functionality of rhPlGF-1 and PlGF-2 was further analysed without cleavage of the tags. Besides the wild type forms of rhPlGF-1 and -2, a truncated PlGF isoform which mimics the plasmin processed PlGF was generated by insertion of a stop-codon C-terminal of Lys_{118}, which corresponds to the plasmin cleavage site closest to the N-terminus identified by LC/MSMS analysis (see 2.3). To avoid cleavage with FactorXa, the expression vector V19 was used. This vector is identical to pCEP V143 but lacks the C-terminal 2x strep-tag (Fig 10a). As sensitivity of wild type isoforms for FactorXa was unexpected during cloning of PlGFStop, rhPlGF-1 and rhPlGF-2 differ by expression of the strep-tag.

Analysis of eluted protein fractions by SDS-PAGE and coomassie stain revealed high purity (Fig 10b). Due to expression in a eukaryotic cell line and differential glycosylation as compared to expression in insect cells, all expressed rhPlGF isoforms shifted to a higher molecular weight.

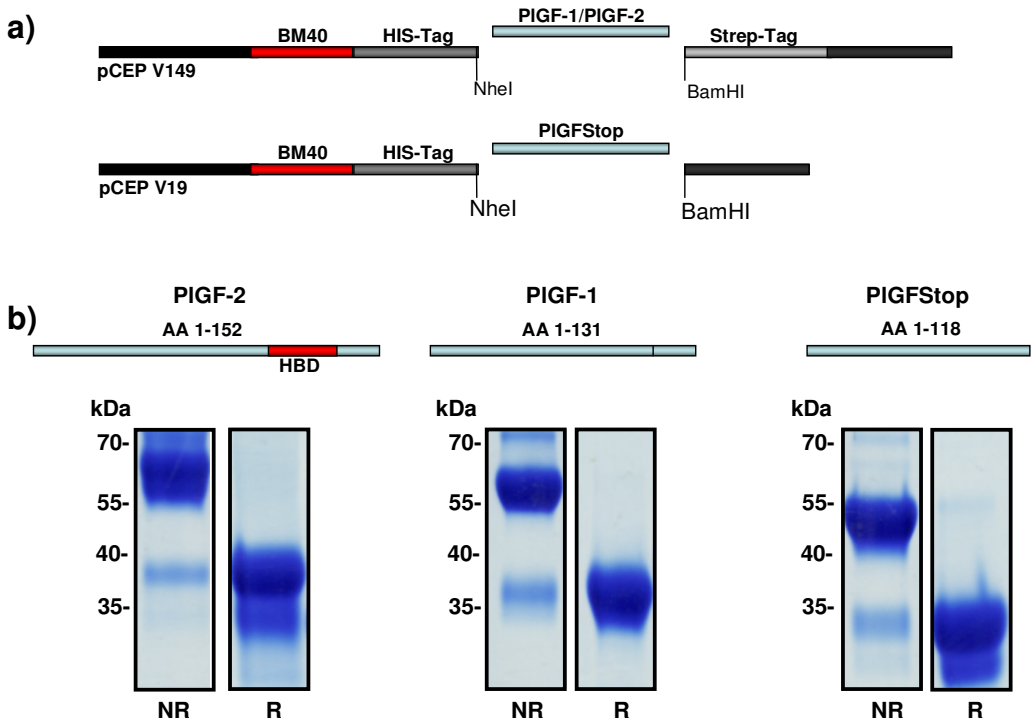

Figure 10: Expression and purification of rhPlGF isoforms. (a) hPlGF-1, hPlGF-2 and mutant PlGFStop cDNA was cloned into the eukaryotic expression vectors pCEP V143 (rhPlGF-1 and -2; N-terminal his-tag, C-terminal strep-tag) and pCEP V19 (rhPlGFStop; N-terminal his-Tag). Recombinant proteins were purified from supernatant via streptavidin- (rhPlGF-1 and -2) and Ni-NTA-sepharose columns (rhPlGFStop). **(b)** Samples were subjected to SDS-PAGE under reducing (R) and non-reducing (NR) conditions, and stained with coomassie.

Reducing conditions revealed a monomeric electrophoretic mobility of approximately 39 kDa for rhPlGF-2, 35 kDa for rhPlGF-1 and 34 kDa for rhPlGFStop. All PlGF isoforms were dimerized properly as demonstrated under non-reducing conditions (Fig 10b) and only a minimal portion of protein was secreted in its monomeric form. Identity of protein

bands was confirmed by mass spectroscopy. Purification resulted in a high yield of at least several hundred micrograms per litre of conditioned medium (Fig 10b).

2.3 Identification of plasmin cleavage sites in PlGF

To identify the plasmin cleavage sites in PlGF, his-tagged rhPlGF-2 expressed in HEK293 cells was incubated with low concentrations of plasmin for 5 (0.04 U/ml) and 30 minutes (0.008 U/ml, specificity control) and subsequently bound to Ni-NTA-sepharose beats. The supernatant containing the C-terminal cleavage fragments was subjected to LC-MS/MS analysis.

Five different cleavage sites were identified within rhPlGF-2, located exclusively in the C-terminal region of the protein (Fig 11; Table 1). The cleavage site closest to the N-terminus was located between amino acids Lys_{118} and Met_{119}, which proves the hypothesis that the heparin-binding domain is cleaved of the core-fragment. It does not affect major structural properties as inter- or intramolecular disulfide-bonds and no glycosylation site was affected. Besides, the heparin-binding domain appears to be a target of intense proteolytic processing and to be degraded completely.

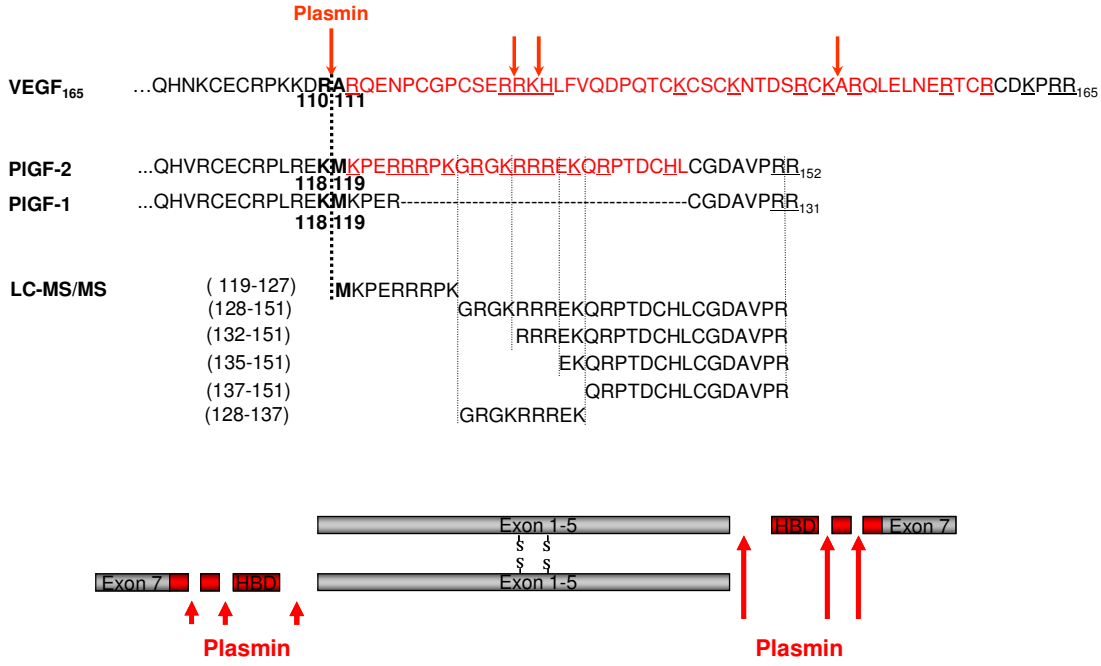

Figure 11: Identification of plasmin cleavage sites in rhPlGF-2 by LC-MS/MS. 25 µg of rhPlGF-2 were incubated with plasmin (0.04 U/mL, 5 minutes and 0.0008 U/mL 30 minutes). LC-MS/MS analysis identified Lys_{118}/Met_{119} as cleavage site closest to the N-terminus. Additionally, the heparin-binding domain is cleaved at position Lys_{127}/Gly_{128}, Lys_{131}/Arg_{132}, Arg_{134}/Glu_{135} and Lys_{136}/Gln_{137}. The heparin-binding site in PlGF-2 is illustrated in red, basic amino acids are underlined. The plasmin cleavage site of $VEGF\text{-}A_{165}$ is aligned with the plasmin cleavage site within the PlGF proteins.

In addition to formation of a stable N-terminal core-fragment (visualized by western blot in 2.1) bearing the cysteine-knot motive and VEGFR-1 binding sites, degradation resulted in the release of six fragments, which were identified in both samples with high

confidence and incidence. They reflect plasmin cleavage between amino acids Lys_{127}/Gly_{128}, Lys_{131}/Arg_{132}, Arg_{134}/Glu_{135} and Lys_{136}/Gln_{137}. All cleavage sites are in line with the consensus cleavage site of plasmin, and cleaved C-terminally of basic amino acids. The relative frequency of identified fragments was equal, only one fragment was rarely detected (135-151: EKQRPTDCHLCGDAVPR). Therefore, one might conclude that cleavage at Arg_{134}/Glu_{135} is not preferred by plasmin. In addition, the fragment Gly_{128}-Lys_{136} was detected solely in the sample incubated in 0.008 U/mL for 30 minutes.
Furthermore, all fragments which comprise the sequence of exon 7 (CGDAVPRR) are shortened by the last C-terminal amino acid (Arg_{152}). For all fragments the absolute deviation between the expected and identified molecular weight was less than 0.09 Da (Table 1).
Interestingly, alignment of the amino acid sequence of rPlGF-2 with the sequence of hVEGF-A_{165} revealed high similarities in amino acid composition around the plasmin cleavage site closest to the N-terminus with respect to their chemical properties. Besides the structural similarities of PlGF and VEGF-A in general, this underlines the possibility for a general mechanism of regulation by proteolytic processing by plasmin in this family.

Table 1: Absolute deviation between expected and found molecular weight of identified peptide fragments after PlGF-2 digestion with plasmin.

Fragment	Relative frequency	Measured m/z (Th)	Found MW (Da)	Expected MW (Da)	Absolute deviation (Da)	Fragment sequence
119-127	+++	599.38	1196.75	1196.69	0.06	MKPERRRPK
128-151	+++	698.14	2788.53	2788.45	0.09	GRGKRRREKQRPTDCHLCGDAVPR
128-136	+++	571.87	1141.73	1141.69	0.04	GRGKRRREK *
132-151	+++	797.77	2390.3	2390.21	0.09	RRREKQRPTDCHLCGDAVPR
135-151	+	641.66	1921.96	1921.9	0.06	EKQRPTDCHLCGDAVPR
137-151	+++	833.43	1664.84	1664.77	0.07	QRPTDCHLCGDAVPR

* Fragment detected in sample incubated in 0.008 U/mL for 30 minutes

2.4 PlGF-2 is degraded in exudates obtained from non-healing human wounds

To investigate the physiological relevance of the observed proteolytic sensitivity of rhPlGF in the context of wound healing, the concentration of PlGF in exudates obtained from normal healing or non-healing human wounds was measured and the integrity of rhPlGF-2 in these exudates was analysed. Wound exudate is the interstitial fluid of wounded tissue and contains numerous soluble mediators, extracellular matrix molecules, proteases and their inhibitors. Therefore, wound exudate is a liquid biopsy that reflects the metabolic condition of the wound and has been proven to be useful for identification of factors involved in skin physiology and pathology (Lauer 2000, Stechmiller 2006, Eming 2007). The level of endogenous PlGF during wound healing was measured by ELISA (Fig 12a). In all exudates analysed, the concentration of PlGF was significantly increased (at least 30-fold) as compared to the mean concentration of plasma serum levels of 26.43 pg/mL, arguing for local expression in the wound area. During all phases of normal wound healing high levels of PlGF were detected without significant differences during healing progression. Average concentrations determined were 734.6 pg/mL on day 2, 1046 pg/mL on day 7 and 1130 pg/mL on day 14. Under non-healing conditions, the expression of PlGF appears to be upregulated. In exudates obtained from non-healing wounds, the PlGF concentration was clearly increased with an average concentration of 1776 pg/mL (Fig 12a), but did not reach significance. As PlGF concentrations are too low to be detected by immuno-blotting and ELISA detects total human PlGF protein, neither isoform expression nor potential proteolytic processing of PlGF can be analysed directly with these methods.

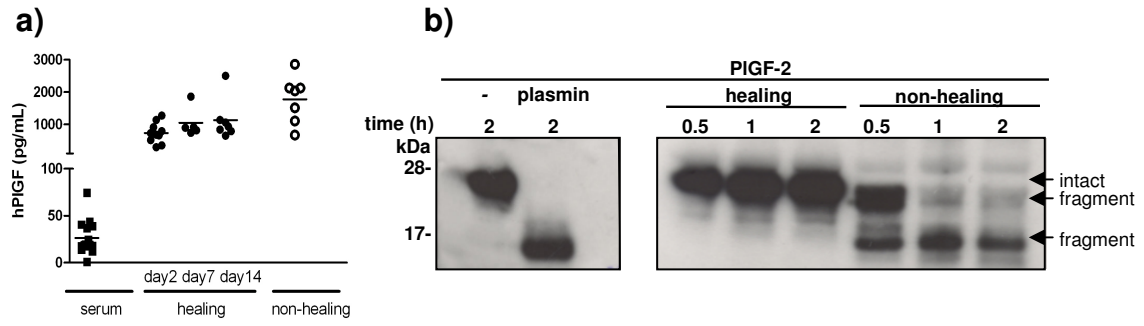

Figure 12: Locally synthesized PlGF in non-healing human wounds is a target of proteolytic degradation. (a) Protein levels of PlGF in exudates obtained from normal healing and non-healing human wounds were quantified by ELISA and compared to serum levels (serum n=15, normal healing day 2 n=10, day 7 n=5, day 14 n=7, non-healing n=7). **(b)** rhPlGF-2 (200 ng/lane; expressed in Sf9 cells) was incubated with or without plasmin (0.02U/mL) or wound exudates obtained from healing or non-healing human wounds as indicated. Samples were subjected to SDS-PAGE under reducing conditions, and detected by a PlGF-specific antibody (raised against the N-terminus of the protein).

To analyse the integrity of rhPlGF in wound environment, rhPlGF-2 was incubated in wound exudates obtained from normal healing or non-healing human wounds (Fig 12b). As revealed by western blot analysis, rhPlGF-2 maintained its stability when incubated in exudates obtained from normal healing wounds. The protein migrated with an approximate molecular weight of 23 kDa without formation of cleavage products. By contrast, when incubated in exudates obtained from non-healing wounds, rhPlGF-2 underwent a gradual degradation resulting in the formation of a core-fragment of an approximate molecular weight of 16 kDa. This fragment appeared to be resistant to further degradation. At early time points, two intermediate cleavage products with an electrophoretic motility of 21 and 18 kDa became visible, reflecting a cleavage within the heparin-binding domain. With increasing time, these intermediate cleavage products disappeared and rhPlGF-2 was degraded to the protease-resistant core-fragment. These data strongly underline the results from the LC-MS/MS analysis (Fig 11) and plasmin specific western blot analysis (Fig 9e). The cleavage site at position Lys_{118}/Met_{119} may be consistent with formation protease resistant core-fragment of 16 kDa identified (Fig 12b). These experiments confirm that a regulation by proteolytic processing by plasmin in this protein family might be possible *in vivo*. Nevertheless, proteolytic sensitivity of PlGF for other proteases upregulated under non-healing conditions (MMPs, neutrophil elastase, etc.) cannot be excluded.

2.5 Site directed mutagenesis at $Lysine_{118}$ does not improve stability of rhPlGF in response to plasmin

In the proteolytic milieu of non-healing wounds, protease-resistant VEGF-A_{165} has been demonstrated to improve the angiogenic response and to promote healing progression. Based on the finding, that mutation of one plasmin cleavage site in VEGF-A_{165} ($Arg_{110}\rightarrow Pro_{110}$) markedly prevented plasmin-mediated degradation of its heparin-binding domain, although four plasmin cleavage sites were identified in this domain (Lauer 2000), we generated two mutant forms of rhPlGF-2 and analysed its stability by western blot. Targeting the plasmin cleavage site located closest to the N-terminus, we used site directed mutagenesis to exchange lysine at position 118 to either alanine or proline. Alanine was chosen as it lacks a large or charged side chain that may interfere with structure and folding of the heparin-binding domain. In addition, lysine was exchange by proline as this mutation resulted in an overall stabilization of VEGF-A_{165} and completely prevented not only cleavage at Arg_{110}/Ala_{111} but also cleavage of further sites located C-terminal of the mutated cleavage site.

Mutated proteins expressed in HEK293 cells were purified via their C-terminal strep-tag. Whereas rhPlGF-$2^{lys\text{-}pro}$ was expressed at a high level, which was comparable to rhPlGF-1, rhPlGF-2 and rhPlGF-Stop, the yield for rhPlGF-$2^{lys\text{-}ala}$ was quite low (Fig 13a). To

analyse protein integrity upon incubation with plasmin, rhPlGF-2$^{lys\text{-}pro}$ and rhPlGF-2$^{lys\text{-}ala}$ were incubated with decreasing protease concentrations and results were compared to rhPlGF-2 wild type protein. As depicted in Figure 13b, mutation of the plasmin cleavage site closest to the N-terminus did not prevent degradation by plasmin. When incubated with 0.02 U/mL plasmin, both mutant proteins were degraded to a core-fragment with a comparable electrophoretic mobility as observed for PlGF-2.

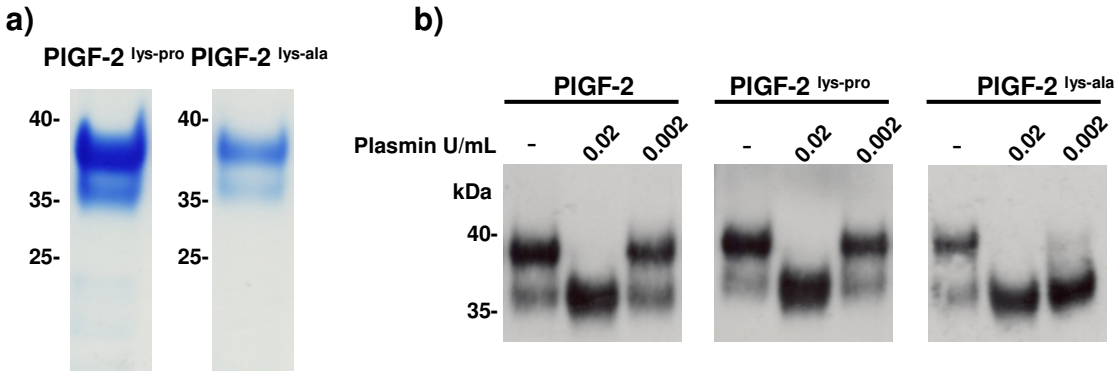

Figure 13: Site-directed mutagenesis of Lysine$_{118}$ does not rescue PlGF degradation by plasmin. Using site-directed mutagenesis, the cleavage site closest to the N-terminus of rhPlGF-2 was mutated by exchange of Lys$_{118}$ to either proline or alanine. **(a)** Mutated proteins rhPlGF-2$^{lys\text{-}pro}$ and rhPlGF-2$^{lys\text{-}ala}$ were expressed in HEK293 cells and purified via its strep-tag. **(b)** To analyse protein integrity in response to plasmin, rhPlGF-2, rhPlGF-2$^{lys\text{-}pro}$ and rhPlGF-2$^{lys\text{-}ala}$ (300 ng/lane) were incubated with decreasing concentrations of plasmin (as indicated, 30 minutes). Samples were subjected to SDS-PAGE under reducing conditions and detected by **(a)** coomassie stain or **(b)** western blotting using a PlGF-specific antibody.

No degradation products of rhPlGF-2$^{lys\text{-}pro}$ were detectable by a further decrease of the plasmin concentration, which is in line with results obtained from rhPlGF-2. Interestingly, rhPlGF-2$^{lys\text{-}ala}$ is completely degraded to the core-fragment at both concentrations of plasmin (Fig 13b). Therefore, exchange of Lys$_{118}$ to Ala$_{118}$ appears to enhance sensitivity for plasmin within the heparin-binding domain. Nevertheless, site directed mutagenesis at Lys$_{118}$ did not improve integrity of rhPlGF-2 with respect to proteolytic processing by plasmin. Therefore, mutant proteins were not further analysed.

2.6 Binding properties of PlGF

To determine the role of the heparin-binding domain for the interaction between PlGF and glycosaminoglycans (GAGs), Surface Plasmon Resonance-analysis (SPR) was performed in collaboration with Manuel Koch (Medical faculty, Institute of Biochemistry II, University of Cologne). The kinetics of this interaction were analysed by determination of the association rate constant k_a and the dissociation constant k_d to determine the K_D-value mathematically.

Different concentrations of either rhPlGF-1, -2 and rhPlGFStop were used as soluble analyte (10, 30, 100 and 300 nM in Fig 14a,b, 300nM in Fig 14c) and were monitored by

measurement of the variation in the plasmon resonance angle as function of time, and described as response units (RU).

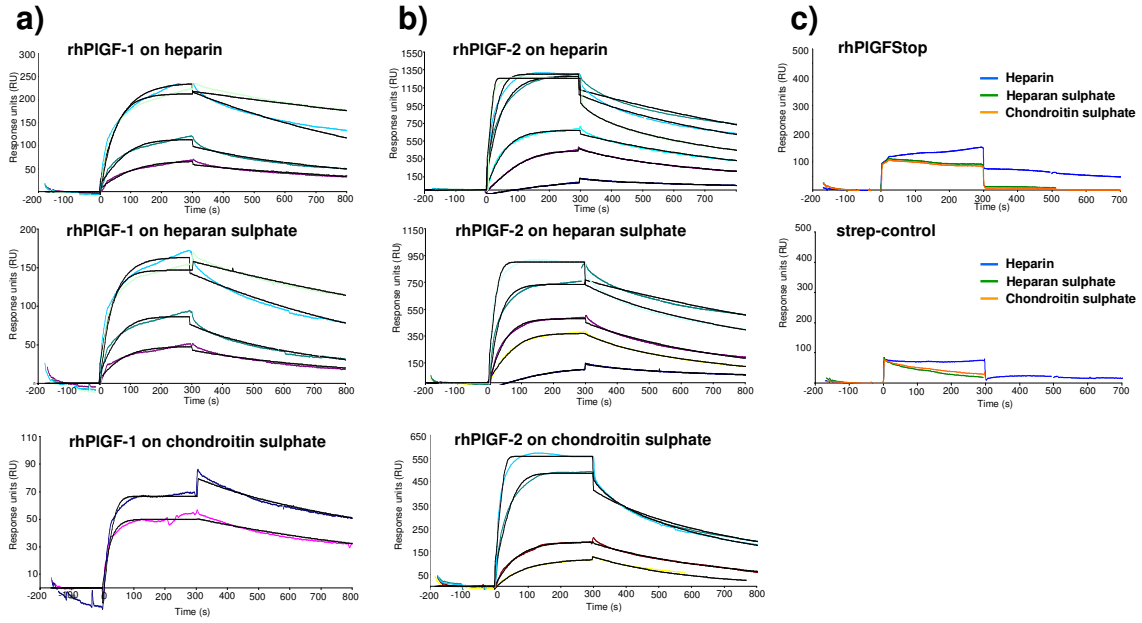

GAG	KD [M]
Heparin (unfractionated)	$5.4*10^{-9}$
Heparan sulphate	$3.9*10^{-9}$
Chondroitin sulphate	$3.3*10^{-9}$

GAG	KD [M]
Heparin (unfractionated)	$1.5*10^{-9}$
Heparan sulphate	$1.5*10^{-9}$
Chondroitin sulphate	$2.1*10^{-9}$

Figure 14: Binding of rhPlGF-1, rhPlGF-2, and rhPlGF-Stop to heparin, heparan sulphate and chondroitin sulphate measured by Surface Plasmon Resonance spectroscopy. Glycosaminoglycans (as indicated) were immobilized on BIAcore SA-chips, and binding sensorgrams were recorded for **(a)** rhPlGF-1, **(b)** rhPlGF-2 and **(c)** rhPlGF-Stop as soluble analyte. Different concentrations of **(a,b)** rhPlGF-1 or rhPlGF-2 (10, 30, 100 and 300 nM) or **(c)** rhPlGFStop (300 nM) were monitored by measuring the variation in the plasmon resonance angle as function of time and described as response units (RU). The background signal was subtracted from each curve (strep-control); the curves are shown in ascending order depending on their analyte's concentration. Fittings and overlay plots were done with the BIAevaluation software 4.1. The black lines represent the fitted curves. The average of K_D-values determined at different analyte concentrations is presented in tables below the curves.

The GAGs heparin, heparan sulphate, and chondroitin sulphate were immobilized on SA-chips, and the binding to rhPlGF-1, rhPlGF-2, and rhPlGFStop were analysed by calculation of the K_D-value. Unexpectedly, rhPlGF-1 and rhPlGF-2 both exhibited a strong and comparable, specific binding capacity to all GAGs tested.

K_D-values for binding to heparin revealed a strong binding to rhPlGF-1 and rhPlGF-2 with $K_D = 5.4 * 10^{-9}$ M, and $K_D = 1.5 * 10^{-9}$ M, respectively (Fig 14a,b). Although the interaction of rhPlGF-2 to heparin was approximately 3.5 fold increased, as compared to the binding strength of rhPlGF-1 to heparin, the difference among the two isoforms was expected to be more pronounced, due to the expression of the heparin-binding domain. Similarly, the binding of rhPlGF-2 to heparan sulphate with a $K_D = 1.5 * 10^{-9}$ M was only two fold increased as compared to rhPlGF-1 binding to heparan sulphate with a K_D-value of $K_D = 3.9 * 10^{-9}$ M (Fig 14a,b). In contrast to this results it was published, that rhPlGF-1

was unable to bind heparin on a heparin-sepharose column, which was interpreted to be dependent on a lack of the highly basic heparin-binding domain (Hauser 1993, Park 1994).

The binding of both isoforms to chondroitin sulphate was almost equal. K_D-values of K_D = 3.3 * 10^{-9} M and K_D = 2.1 *10^{-9} M for rhPlGF-1 and rhPlGF-2, respectively revealed a negligible 1.5 fold increase in binding strength with regard to the presence of the heparin-binding domain (Fig 14a,b). As in strep-control no unspecific interaction to any of the tested GAGs was measured, the expression of the C-terminal strep-tag of rhPlGF-1 and -2 may not be responsible for the comparable binding strength among isoforms. Interestingly, rhPlGFStop as soluble analyte did not interact with the tested GAGs (Fig 14c). As it is shortened by only 13 amino acids (MKPERCGDAVPRR) as compared to rhPlGF-1, the interaction appeared to be highly dependent on this sequence. Experiments performed clearly confirmed specific binding of both rhPlGF-1 and rhPlGF-2 to heparin, heparan sulphate, and chondroitin sulphate. Although the binding strength to the analysed GAGs was slightly increased for rhPlGF-2, the presence of the heparin-binding domain appeared not to be crucial for binding, but to enhance interaction. To analyse kinetics of the interaction in detail, additional experiments would be necessary.

The heparin-binding domain was predicted to be a crucial characteristic of PlGF-2 and VEGF-A_{165} to bind to heparin as well as for their interaction to Nrp-1, but detailed analysis is missing for PlGF isoforms so far. The recruitment of Nrp-1 to VEGFR-1 to enhance signalling, displays one mechanism that may be differently regulated by expression of the heparin-binding domain. The binding of rhPlGF-1, rhPlGF-2 and rhPlGFStop to Nrp-1 therefore was analysed, without or in presence of unfractionated heparin. The different PlGF isoforms were immobilized on a CM5-chip, and binding to rhNrp-1 as soluble analyte was measured at different concentrations of rhNrp-1.

In the absence of heparin, rhPlGF-2 revealed a relatively weak binding to Nrp-1, with an average K_D-value of K_D = 1.25 * 10^{-6} M (Fig 15a). As it was reported, that the binding of PlGF-2 to Nrp-1 was clearly enhanced in the presence of heparin (Migdal 1998), 100 nM of rhNrp-1 was pre-incubated with increasing concentrations of unfractionated heparin prior to measurement of binding to rhPlGF-2. Analysis revealed a strongly enhanced binding strength between rhPlGF-2 and rhNrp-1 in presence of heparin. Overlapping with an increase of the heparin concentration, a successive increase of the binding strength between rhPlGF-2 was observed, which was reflected by K_D-values K_D = 1.1 * 10^{-8} M and K_D = 9.0 * 10^{-9} M at concentration of 0.1 µg /mL and 100 µg/mL heparin, respectively, as compared to K_D = 1.14 * 10^{-6} M without heparin (Fig 15b).

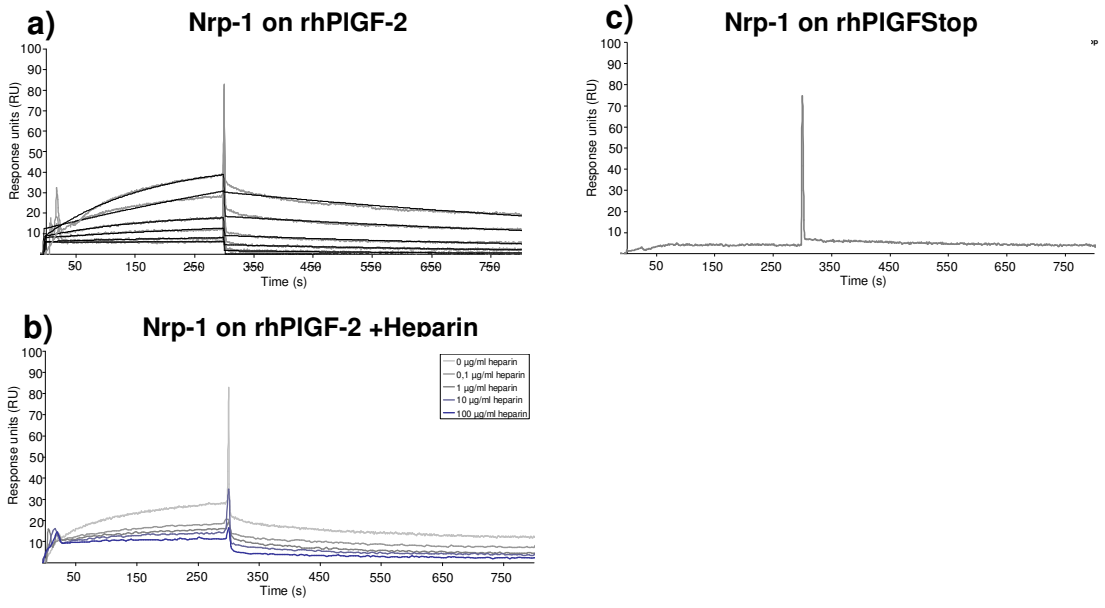

	KD [M]
Nrp-1 on rhPlGF-2	**$1.25*10^{-6}$**
+Heparin (unfractionated) 0 µg/mL	$1.14*10^{-6}$
0.1 µg/mL	$1.10*10^{-8}$
1 µg/mL	$1.47*10^{-8}$
100 µg/mL	$9.00*10^{-9}$

Figure 15: Binding of rhPlGF-2 or rhPlGFStop to rhNrp-1 measured by Surface Plasmon Resonance spectroscopy. The PlGF isoforms **(a,b)** rhPlGF-2 or **(c)** rhPlGF-Stop were immobilized on BIAcore CM5-chips and binding sensorgrams were recorded for soluble rhNrp-1 as soluble analyte. Different concentrations of **(a,c)** soluble rhNrp-1 (1, 3, 10, 30, 100, 300 nM on rhPlGF-2, 300 nM on rhPlGFStop) or **(b)** 100 nM rhNrp-1, pre-incubated with different concentrations of unfractionated heparin (as indicated) and monitored by measuring the variation in the plasmon resonance angle as function of time and described as response units (RU). The background signal was subtracted from each curve; the curves are shown in ascending order depending on their analyte's concentration. Fittings and overlay plots were performed using the BIAevaluation software 4.1. The black lines represent the fitted curves. Average of K_D-values is presented in tables below the curves.

In conclusion, concentrations higher than 1 µg/mL heparin did not significantly increase the binding strength. Nevertheless, even low concentrations of 0.1 µg/mL heparin strongly enhanced the interaction between ligand and receptor by approximately 100 fold, as compared to conditions in which heparin is absent. This enhancing effect of heparin for the interaction between PlGF-2 and Nrp-1 was described by Migdal and co-workers, using a different method. Analysed by cross-linking experiments, heparin largely increased complex-formation of ^{125}I-PlGF-2 with Nrp-1 (Migdal 1998). Interestingly, measurements for the interaction between PlGFStop and Nrp-1 revealed no detectable interaction, in neither presence nor absence of heparin (Fig 15c). These data strongly supported the hypothesis, that the C-terminus of PlGF may be pivotal for its general binding capacity. Unfortunately, results for rhPlGF-1 are lacking so far, and

the measurement for the interaction between rhPlGF-1 and Nrp-1 has to be repeated.
To understand the mechanisms that may be promote binding of PlGF to GAGs, 3D structure of dimeric hPlGF (amino acid 1-117) and hVEGF-A (amino acid 9-109), obtained from NCBI structure data base were analysed. As depicted in Figure 16a, several charged amino acids are exposed to the surface of the PlGF core-fragment dimer. As displayed in blue, basic amino acids form a highly basic pattern on the surface of the dimer, which might contribute to GAG-binding.

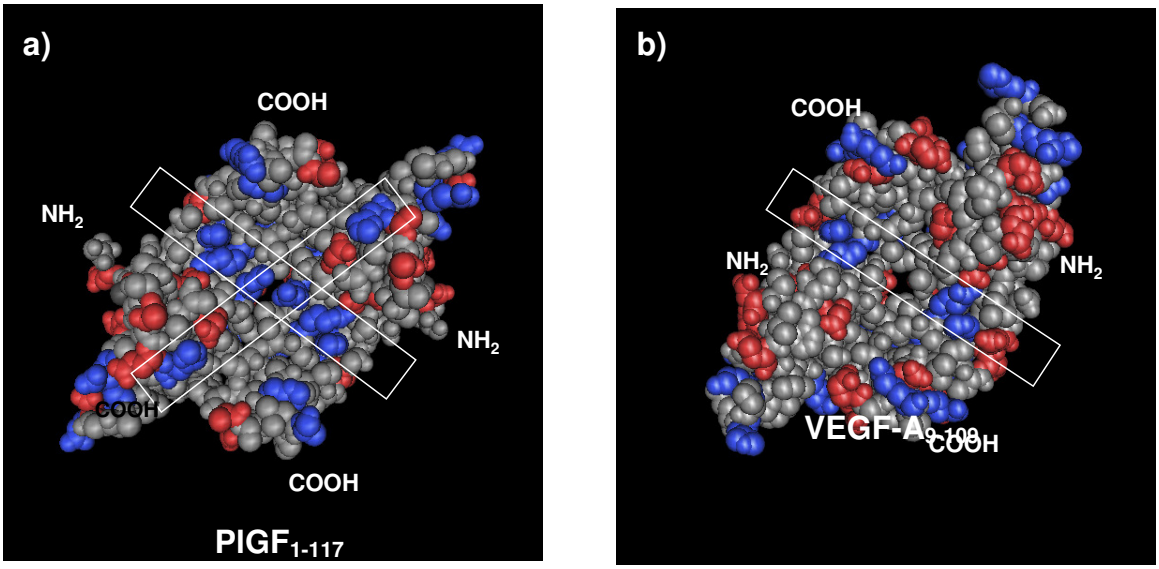

Figure 16: 3D-model of homodimeric hPlGF and hVEGF-A. 3D-calotte-model of hPlGF (amino acids 1-117; PDB ID 1FZV) and hVEGF-A (amino acids 9-109; PDB ID 1VPF), colour-coded for potential GAG binding sites. Blue and red indicate negative and positive charged patches on the surface of growth factor, respectively

As 3D structure of full-length hPlGF-1 and hPlGF-2 were not available, this model shows the PlGF sequence of the core-protein coded by exon 1-5. It is therefore identical to rhPlGFStop and lacks the heparin- binding domain as well as the sequence coded by exon 7. As the C-terminal domain of PlGF, which has been demonstrated to be crucial for GAG and Nrp-1 interaction is not displayed, the basic amino acids of the core-fragment may support GAG or Nrp-1 binding, but solely are not sufficient to promote binding, as demonstrated in Figure 14c.
The comparison of the surface pattern of charged amino acids in core-fragment of hPlGF and VEGF-A revealed high similarities (Fig 16a,b). This may explain overlapping receptor- and GAG-binding interfaces among PlGF and VEGF-A. In the central portion of hPlGF, the density of clustered basic amino acids is clearly increased as compared to hVEGF-A (boxed in Fig 16a,b), which may contribute to an altered binding profile. A detailed biochemical analysis to determine amino acids within hPlGF, that participate in either GAG binding or interaction to Nrp-1 would be an interesting topic and would help to understand regulatory mechanisms in PlGF-mediated activities.

2.7 Chemotactic activity of PlGF on endothelial cells

To analyse the functional role of the heparin-binding domain for PlGF-mediated activities, the chemotactic activity of rhPlGF on endothelial cells was analysed in the Boyden chamber assay. The co-receptor Neuropilin-1 is known to be involved in the chemotactic or chemorepellant response of different cell types. As recruitment of Nrp-1 to the VEGFRs by VEGF-A or PlGF to enhance its signals is predicted to be dependent on the heparin-binding domain, an increased expression of this co-receptor may be supportive to analyse the heparin-binding domain for PlGF mediated activity. Therefore, porcine aortic endothelial cells (PAE), stable transfected with the neuropilin-1 receptor (PAE/Nrp-1) or untransfected cells (PAE) were analysed (Fig 17a).

Nrp-1 transfected PAE cells treated with rhPlGF-2 expressed in insect cells exhibited an about 3-4 fold higher chemotactic response as compared to cells treated with rhPlGF-1 or vehicle treated control cells (Fig 17a). Pre-incubation of rhPlGF-2 with plasmin resulted in a dramatic loss of its chemotactic activity. This loss of activity was partly rescued by α_2-antiplasmin – which is a specific inhibitor for plasmin. Both, rhPlGF-1 and rhPlGF-2 were not able to significantly induce chemotaxis in untransfected cells lacking Nrp-1 expression (Fig 17a,d), underlining the essential of Nrp-1 for chemotaxis in endothelial cells.

To test, if the different rhPlGF wild type variants and the rhPlGFStop mutant expressed in HEK293 cells are functional, the chemotaxis assay was repeated in PAE/Nrp-1 cells (Fig 17b). About 2-3 times more of the rhPlGF-2 stimulated cells were able to migrate towards the stimulus as observed for vehicle treated control or rhPlGF-1 treated cells. Additionally, the rhPlGFStop mutant mimicked the results of plasmin-processed rhPlGF-2, resulting in a dramatic loss of its chemotactic activity, underlining the role of the heparin-binding domain for chemotaxis.

To analyse the chemotactic activity of PlGF on physiological relevant cells, the Boyden chamber assay was repeated using HUVE cells. Again, rhPlGF-2 revealed a strong activity comparable to the results obtained from the PAE/Nrp-1 cells, whereas rhPlGFStop had no chemotactic activity on HUVE cells (Fig 17c).

Altogether, this data strongly indicates that the heparin-binding domain regulates the activity of PlGF through binding to Nrp-1 and that its activity is regulated by plasmin-mediated proteolytic cleavage.

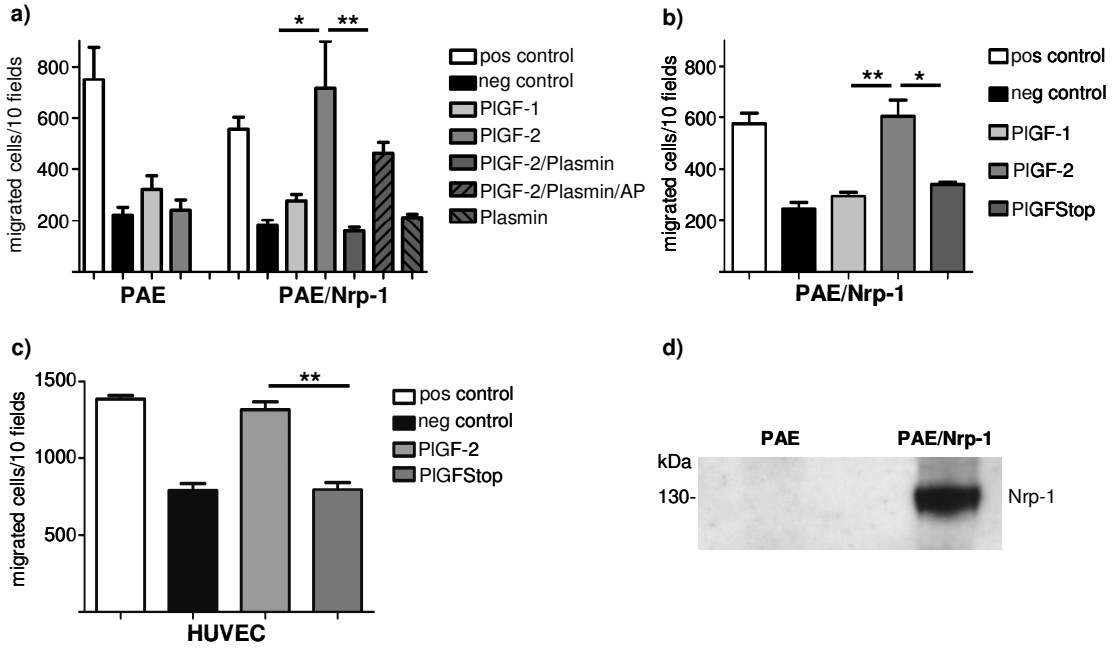

Figure 17: Chemotactic activity of rhPlGF-2 on endothelial cells is increased by the heparin-binding domain. (a) PAE and PAE/Nrp-1 were seeded on a collagen I coated (10 µg/mL) polycarbonate filter (8 µm pore size) and incubated for 4.5 h. Stimulation conditions: positive control (Ham`s F12 + 10% FCS), vehicle treated control (negative control: Ham`s F12 + 0.1% FCS), rhPlGF-1 and rhPlGF-2 (100 ng/mL, expressed Sf9), rhPlGF-2 pre-incubated with 0.02 U/mL plasmin and rhPlGF-2 pre-incubated with plasmin and/or antiplasmin (AP)**. (b)** PAE/Nrp1 or **(c)** HUVE cells seeded onto collagen I coated polycarbonate filter and stimulated with different PlGF isoforms (100ng/mL, expressed in HEK293 cells). 100 ng/mL rhVEGF$_{165}$ was used as positive control. **(d)** Cell lysate of Nrp-1-transfected and untransfected PAE cells were subjected to SDS-Page. Expression of Nrp-1 was detected by western blotting and a specific antibody directed against Nrp-1. Experiments were performed in triplicates and repeated in at least three independent experiments. Significance: * ≤ 0.05; ** ≤ 0.01.

2.8 The heparin-binding domain of PlGF-2 promotes vascular sprouting *in vitro*

PlGF is known to promote vascular sprouting if overexpressed in murine skin (Odorisio 2002), but the role of the PlGF heparin-binding domain in tip cell formation and vessel sprouting remains open.

To investigate the impact of the heparin-binding domain of PlGF on angiogenic sprouting, a 3D spheroid assay was performed using rhPlGF-1, rhPlGF-2, and rhPlGFStop for stimulation (Fig 18a). Spheroids treated with medium only were markedly reduced in their competence to sprout, as revealed by analysis of the cumulative sprouting length as well as in the number of sprouts per spheroid (Fig 18b,c). Furthermore, these spheroids appeared to be less stable.

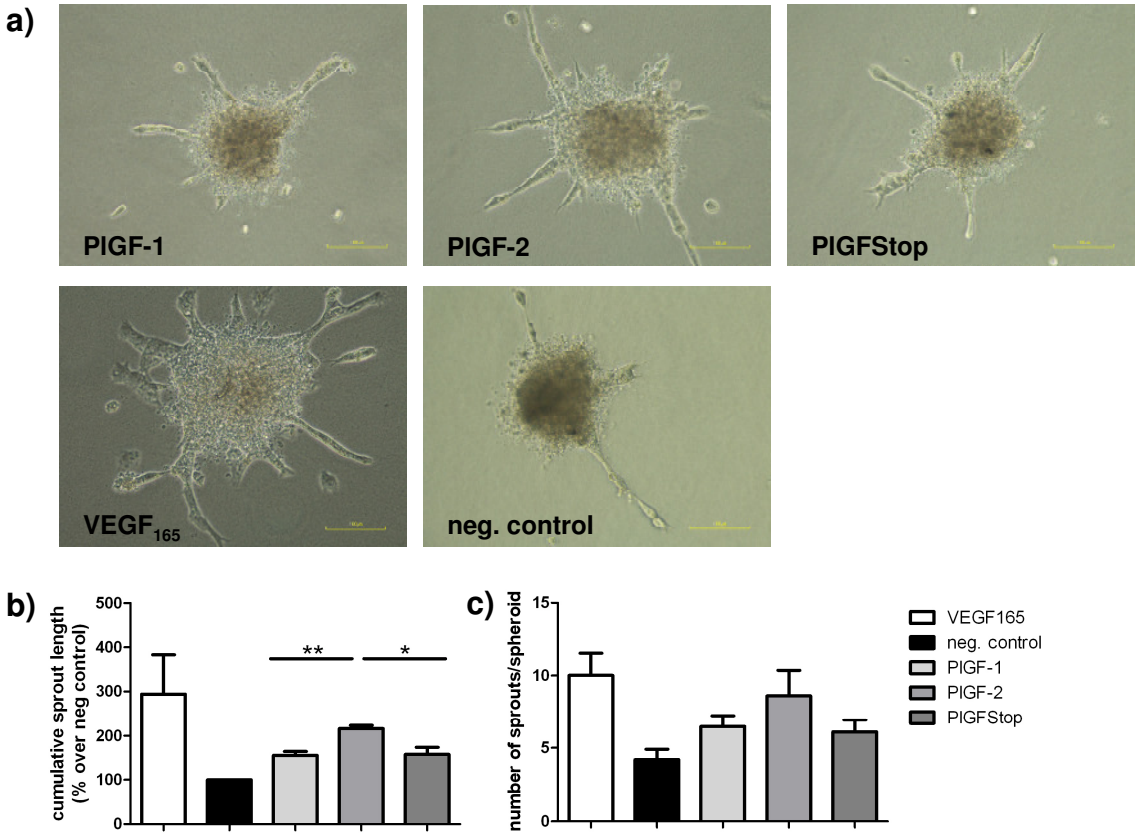

Figure 18: PlGF isoforms induce sprouting in a 3D-spheroid assay. (a) HUVE cells were allowed to develop spheroids and seeded into 500 µL collagen type I solution per well (24-well plate, 50 spheroids/well; 2 mg/mL collagen I). After gel polymerisation, 200 µL EGM-2 (without supplements; 40 ng/mL of various PlGF isoforms, 5 ng/mL VEGF-A_{165} as positive control, or basal EGM-2 as negative control) were added onto the gel and incubated for 24h. **(b)** Cumulative sprout length and **(c)** number of sprouts/spheroid were analysed (10 spheroids/condition; 20x magnification; ImageJ software). Significance was calculated out of three independent experiments; * ≤ 0.05, ** ≤ 0.01.

In contrast, all rhPlGF isoforms increased the cumulative sprouting length as well as the number of sprouts per spheroid over control levels. The heparin-binding isoform rhPlGF-2 significantly increased the cumulative sprouting length compared to rhPlGF-1 and rhPlGFStop (Fig 18b). Thus, sprout induction and outgrowth appeared to be largely enhanced by the heparin-binding domain. Nevertheless, the PlGF core-protein alone (rhPlGFStop) clearly promotes sprouting as compared to untreated control.

Interestingly, the number of sprouts per spheroid induced by rhPlGF-2 was clearly increased compared to heparin-binding domain-lacking isoforms, although this increase was not significant. Spheroids treated with rhPlGF-2 reached sprout numbers comparable to rhVEGF-A_{165} treated ones, which is known to induce vascular sprouting. In conclusion, these results argue for an increased sprout induction in dependence of the heparin-binding domain. As all PlGF-treated spheroids were more stable compared to untreated control, PlGF might act as a survival factor for endothelial cells, independently of the heparin-binding domain.

2.9 The heparin-binding domain of rhPlGF-2 promotes deposition of granulation tissue in wounds of diabetic mice

To analyse the role of the heparin-binding domain of PlGF during tissue repair with focus on angiogenesis, we evaluated the wound healing response in diabetic mice locally treated with repetitive application of the different rhPlGF isoforms. These mice suffer from an impaired healing response due to the lack of a functional leptin receptor. Because of a delay in wound healing processes, this mouse model allows a more detailed analysis of treatment response on single phases of healing as e.g. granulation tissue formation or angiogenesis.

Mice were wounded on the back skin and treated with either PBS (vehicle control), rhPlGF-1, rhPlGF-2 or rhPlGFStop with 1 µg/day for up to seven days. Wounds were harvested at day 10 or 14 post wounding. Sections were stained with haematoxylin/eosin (H&E) or were analysed immunohistologically (for detailed information on the parameters for analysis of morphometric parameters see 4.5.4.1).

The most obvious difference in PlGF isoform mediated activities was observed by analysis of the area of granulation tissue (Fig 19a,b). H&E stained sections demonstrated a robust and significant increase in granulation tissue formation in day 10 and day 14 wounds treated with rhPlGF-2, as compared to the heparin-binding domain lacking PlGF isoforms (Fig 19b). Treatment with either rhPlGF-1 or rhPlGFStop resulted in the formation of granulation tissue that occupied an area that was slightly increased as compared to vehicle treated control wounds. All day 10 wounds (either treated with vehicle control or rhPlGF isoforms) were completely re- epithelialized and closed, as reflected by analysis of the length of epithelial tongue (Fig 19a,c). Being complement to the width of the wound set by biopsy punch (6 mm) at day 10, length of epithelial tongue decreases at day 14 due to wound contraction (Fig 19c).

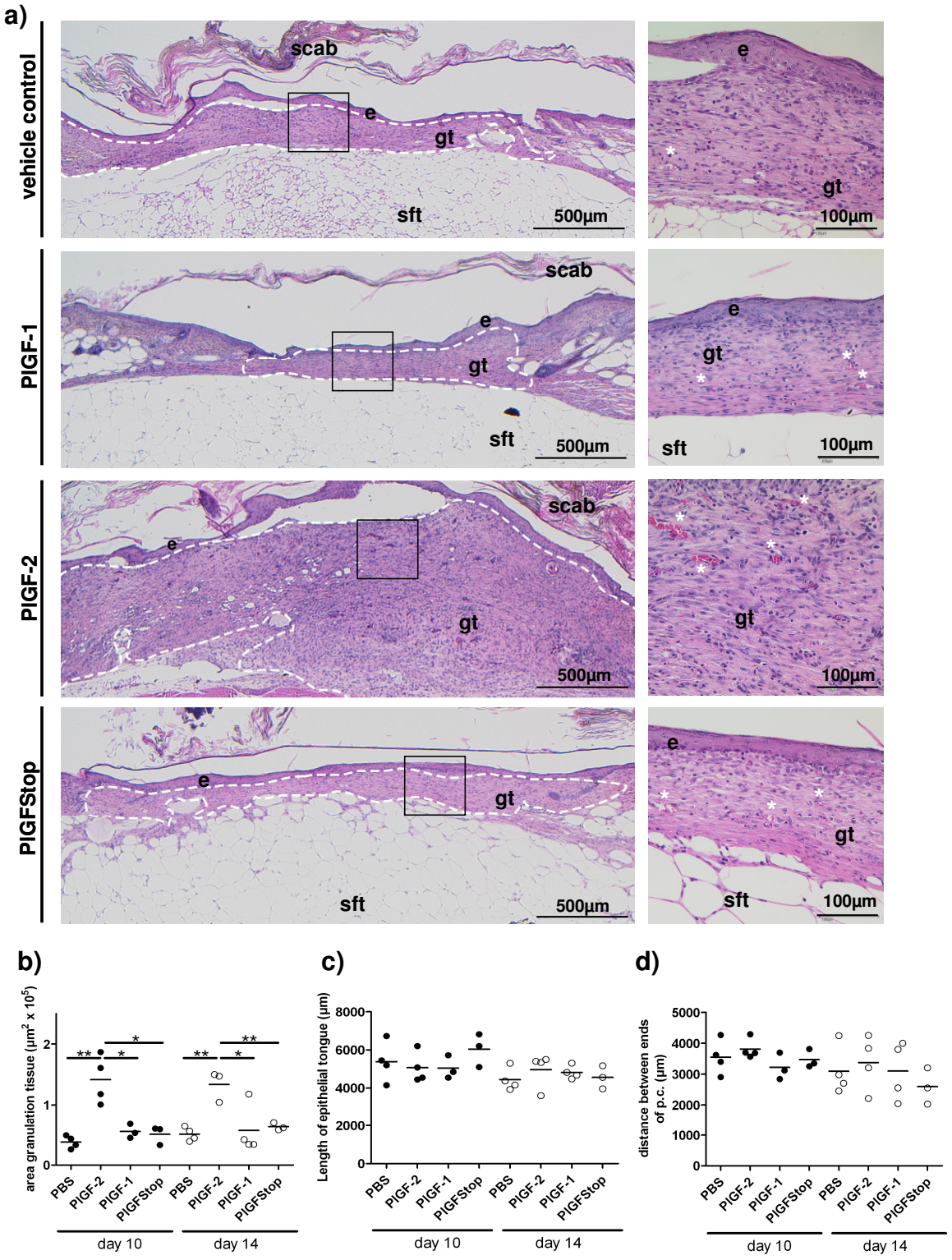

Figure 19: Topical application of rhPlGF-2 accelerates granulation tissue formation in diabetic mice. (a) Representative H&E staining of wound tissues day 14 post injury. Repetitive application of rhPlGF-2 significantly accelerated granulation tissue formation in diabetic mice compared to rhPlGF-1, rhPlGFStop (1 µg per day for a period of 7 days) or vehicle treated control. All wounds were covered by a hyper-proliferative and closed epithelium. **(b-d)** Morphometric analysis of wound tissue at day 10 and day 14 post injury. **(b)** Area of granulation tissue **(c)** length of epithelial tongue **(d)** distance between ends of panniculus carnosus. At each time point and for each condition four wounds from four different mice were analysed; Boxed area in the left panel represents photograph at higher magnification in the right panel; dashed line indicates granulation tissue; e epidermis, gt granulation tissue, sft subcutaneous fat tissue, white asterix indicate blood vessel; scale bar as indicated.

As analysis was not performed at earlier time points, a statement for an accelerated wound closure rate in response to the heparin-binding domain bearing PlGF isoform cannot be made. Measurement of the distance between the ends of *panniculus carnosus* revealed no significant differences among PlGF isoforms or vehicle treated control (Fig 19a,d).

2.10 The heparin-binding domain of rhPlGF-2 increases wound angiogenesis

As one phenotype of db/db mice is a decreased formation of granulation tissue, rhPlGF-2 appears to improve the wound healing response in diabetic mice. Granulation tissue is known to be essential for wound angiogenesis and quality of wound healing, therefore we analysed, if rhPlGF treatment – in dependence of the presence of a heparin-binding domain - may improve angiogenesis under conditions of disturbed wound healing.

To analyse the angiogenic response upon differential PlGF isoform treatment qualitatively and quantitatively, cryo-sections from day 10 and day 14 wounds were stained immunohistologically. Double staining for CD31, a marker for vascular structures and endothelial cells and desmin, a marker for perivascular cells, was performed and quantified in a semi-quantitative manner. Representative images of wound tissue of day 10 and 14 post wounding are shown in Figure 20a whereas quantification is summarized in Figure 20b-g.

As depicted in Figure 20a, the vascular response during granulation tissue formation was less intense in vehicle treated control wounds as compared to wounds treated with the PlGF-isoforms at day 10 post wounding, although not significant. Among the isoforms, treatment with rhPlGF-2 appeared to increase vessel number and to improve an equal vessel distribution as compared to rhPlGF-1 and rhPlGFStop. Although rhPlGFStop treated wounds revealed a comparable degree of CD31-positive structures, vessels appeared to be unorganized and distribution seems to be disturbed (Fig 20a). In addition, the desmin-positive area within the granulation tissue is increased upon PlGF treatment. Whereas the desmin-positive area is only slightly increased in wounds treated with the short PlGF isoforms as compared to vehicle control, PlGF-2 clearly promoted the recruitment of desmin-positive cells. With progression of wound healing, the differences in the vascular response to the PlGF isoforms became more obvious in day 14 wounds (Fig 20a). Most of the vascular structures observed in rhPlGF-2 treated wounds were covered with pericytes, which might contribute to vessel stabilization. In contrast, vessels appeared to regress in day 14 wounds, when treated with either rhPlGF-1, rhPlGFStop or vehicle treated control. These vessels revealed a poor coverage with pericytes, which may be reasonable for regression (Fig 20a)

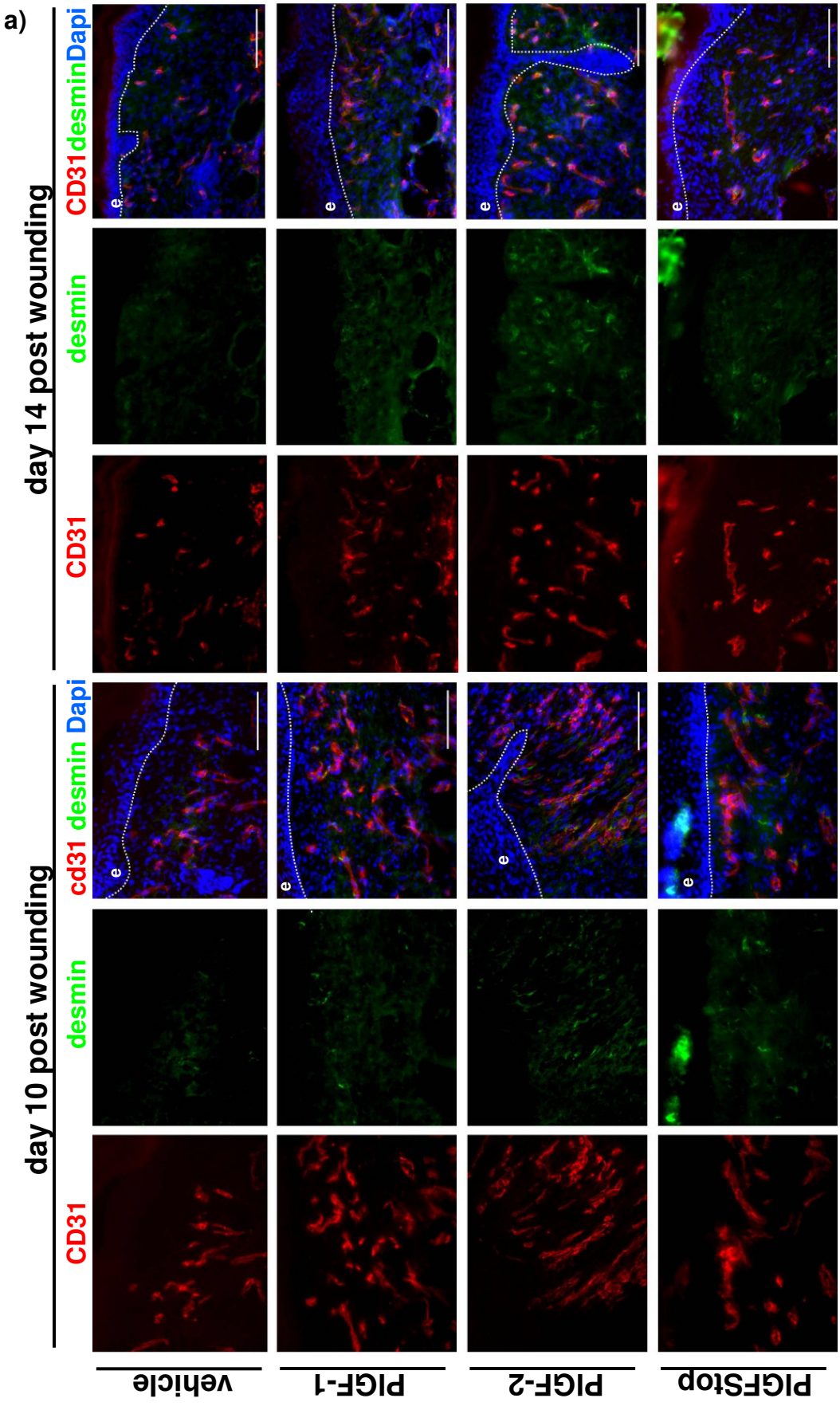
a)
day 14 post wounding
day 10 post wounding
CD31 desmin Dapi
desmin
CD31
cd31 desmin Dapi
desmin
CD31
e
vehicle
PlGF-1
PlGF-2
PlGFStop

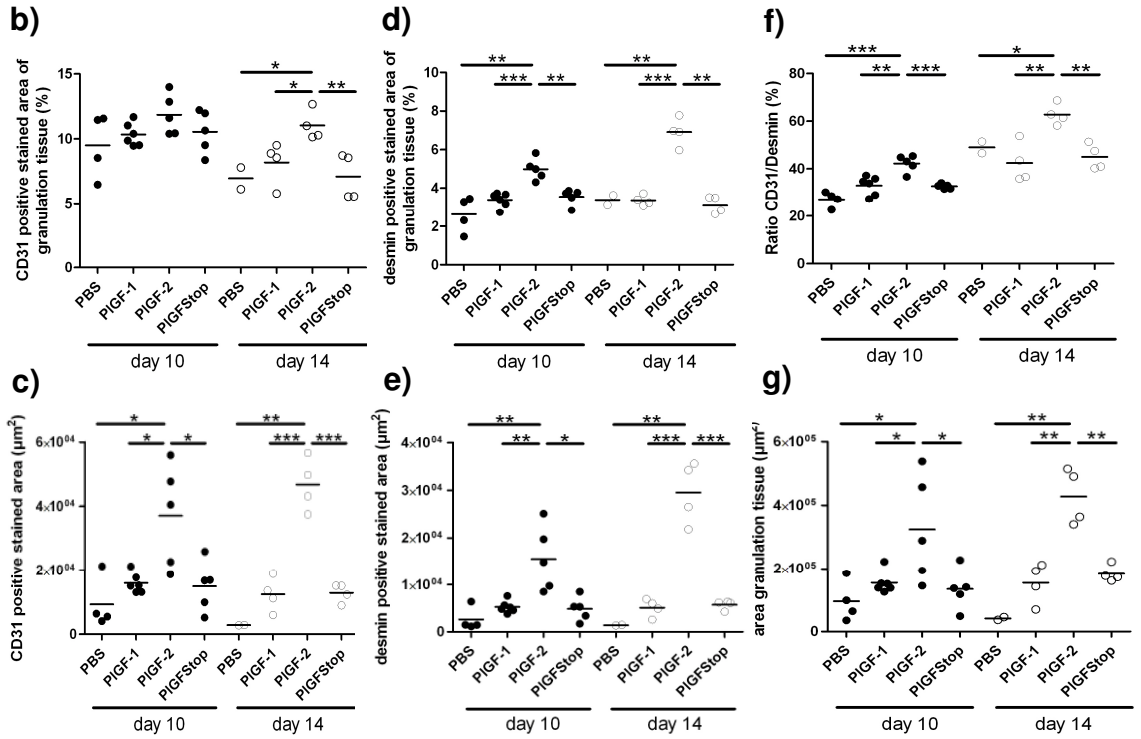

Figure 20: The heparin-binding domain of PlGF promotes vessel coverage by recruitment of perivascular cells. (a) Immunohistochemical staining of cryo-sections from day 14 wounds treated with rhPlGF-1, rhPlGF-2, rhPlGFStop (1µg/mL per day for up to 7 days), or vesicle treated controls, as indicated. **(b)** Morphometric quantification of the **(b,d)** CD31 or desmin positive stained area as percentage of the area of granulation tissue, day 10 and day 14 post injury. **(c,e)** CD31 or desmin positive stained area as total values within granulation tissue, day 10 and day 14 post injury. **(f)** Coverage of vessels with pericytes analysed as percentage of CD31/desmin double stained area. **(g)** Area of granulation tissue. For each condition and time point, at least four wounds from four different mice were analysed. Dotted line indicates epidermal-dermal junction; e, epidermis; scale bar 100 µm.

Quantitative analysis of vessel infiltration into the wound site and its coverage with pericytes, was performed as measurement of CD31- and desmin-positive area in relation to the area of granulation tissue (Fig 20b,d) and as total values within the granulation tissue (Fig 20c,e).

Interestingly, in day 10 wounds all of the PlGF isoforms increased the angiogenic response with respect to vehicle treated control, when analysing the CD31-positive stained area in relation to the area of granulation tissue, although not reaching significance (Fig 20b,c). PlGF in general therefore appeared to promote vessel infiltration, independently of the heparin-binding domain.

By contrast, analysis of angiogenesis in day 14 wounds revealed significant differences in the percentage of CD31-positive area for the various treatments. Whereas vessels appeared to regress in wounds treated with rhPlGF-1, rhPlGFStop and vehicle control, the percentage of CD31 positive staining remained elevated in rhPlGF-2 treated wounds. rhPlGF-2 treated wounds were significantly more vascularized than wound receiving other treatment options (Fig 20b,c). Analysis of the desmin-positive stained area revealed a significantly enhanced recruitment of pericytes by rhPlGF-2 in

comparison to the two short PlGF forms or vehicle control at day 10, which therefore might be a heparin-binding domain dependent effect (Fig 20d,e). This difference was even more pronounced at day 14 post wounding. A possible explanation for the rhPlGF-2 induced vessel persistence might be a function as survival factor or the observed recruitment of pericytes, but this has to be analysed in detail.

Vessel stabilisation and/or maturation by recruitment of pericytes therefore might be reasonable for the persistent detection of CD31 positive structures in wounds treated with rhPlGF-2, whereas vessels induced by rhPlGF-1 or rhPlGFStop seemed to regress in later phase of wound healing, as reflected by day 14 wounds. This hypothesis was underlined by analysis of CD31/desmin double positive stained areas (Fig 20f). The percentage of structures positive for both CD31 and desmin was clearly increased by rhPlGF-2 at day 10 post wounding, and reached an even higher level by day 14. In contrast, rhPlGF-1 and rhPlGFStop failed to increase this percentage and pericyte covered structures only reached levels of vehicle treated controls.

2.11 Heparin-binding domain dependent signalling involved in PlGF mediated migration/chemotaxis

As the PlGF isoforms were active and revealed functional differences in their bioactivity *in vitro* (Boyden chamber assay, spheroid assay), *in vivo* (granulation tissue formation/angiogenesis during wound healing) and in their binding properties (Surface Plasmon Resonance spectroscopy), the next step was to analyse the heparin-binding domain mediated signalling pathways.

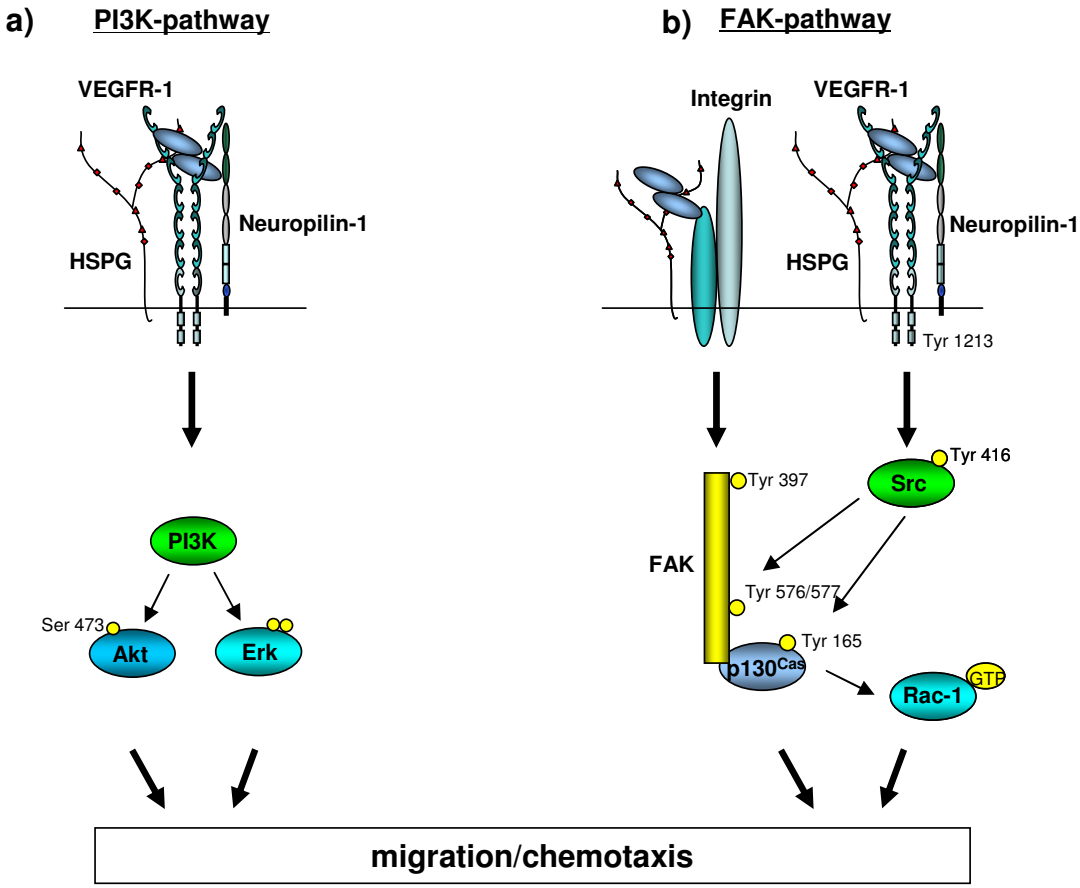

Figure 21: Model for PlGF mediated migration and chemotaxis. (a) Phosphoinositid-3-Kinase (PI3K) activation as well as **(b)** focal adhesion kinase (FAK) activation might be attractive processes to analyse the function of PlGF and its heparin-binding domain for migration and chemotaxis. Both are known to be important for the re-organization of the cytoskeleton and focal-adhesion turnover. **(a)** In monocytes, the activation of PI3K and its downstream targets was demonstrated to be involved in PlGF mediated chemotaxis. PI3K-inhibitors, as well as function blocking antibodies against VEGFR-1 reduced this activation (Tchaikovski 2008). **(b)** Direct linkage of VEGFR-1 signalling to integrin induced activation of FAK might be involved in PlGF mediated signalling. FAK activation is known to be involved in cellular migration and formation of lamellopodia and filopodia by activation of the downstream molecule $p130^{Cas}$ (Playford 2004). Lesslie and colleagues identified the family of Src kinases as link between VEGF-A mediated VEGFR-1 signalling and integrin signalling, resulting in specific activation of FAK, $p130^{Cas}$ (Lesslie 2004) and the small GTPase Rac-1 (Playford 2004). Activation of PI3K as well as FAK may be further enhanced by Nrp-1, acting as co-receptor for VEGFR-1. Recent publications demonstrated a direct role of Nrp-1 in VEGF-A-induced phosphorylation of $p130^{Cas}$ and endothelial cell migration (Evans 2011). Furthermore, Nrp-1 was shown to directly interact with integrins to promote integrin internalization and recycling, resulting in cell migration (Valdembri 2009).

According to the literature, PlGF induced migratory signals might be mediated via activation of two main signalling cascades: either by activation of VEGFR-1 signalling and activation of phosphoinositide 3-kinase (PI3K) (Fig 21a), or by regulation of the focal adhesion kinase (FAK) and activation of its effectors via (co-)activation of integrins and/or VEGFR-1 (Fig 21b). These signals might be enhanced by co-receptors as heparan sulphate-proteoglycans (HSPGs) or Nrp-1, and can be distinguished by distinct downstream signalling proteins.

2.11.1 Activation of Akt and Erk-1/2 by PlGF-2 is independent from its heparin binding domain

To analyse, whether the activation of PI3K and its downstream targets is involved in the heparin-binding domain mediated migratory and chemotactic response to PlGF in endothelial cells, serum-starved HUVE cells or PAE/Nrp-1 cells were stimulated with either rhPlGF-2 or the mutant rhPlGFStop and the phosphorylation pattern of VEGFR-1 (Tyr_{1213}), Akt (Ser_{473}) and Erk-1/-2 (Thr_{202}/Tyr_{204}) was analysed. Additionally, the involvement of PI3K in PlGF downstream signalling was tested by use of wortmannin, which inhibits the activation of PI3K/Akt.

Western blot analysis revealed activation of all tested kinases in HUVE cells upon stimulation with rhPlGF-2 or rhPlGFStop, and therefore confirmed that rhPlGF proteins expressed in HEK293 cells were functional and able to induce signal transduction. Both PlGF forms strongly activated VEGFR-1 phosphorylation at Tyr_{1213} after 5 minutes and the signal was sustained for at least 30 minutes, even though a slight decrease in intensity was observed upon treatment with rhPlGFStop (Fig 22a). Equal loading is demonstrated by Akt and Erk-1/2 loading control, as all samples were subjected to the same SDS-gel. Independent of the presence of the heparin-binding domain, rhPlGF-2 and rhPlGFStop strongly increased phosphorylation of both Erk-1 and Erk-2 after 5 minutes, as compared to the negative and the positive control (rhVEGF-A_{165}) which is in line with an early activation with VEGFR-1. Signal intensity decreased to basal levels at later time points (Fig 22a).

Phosphorylation of Akt after 5 minutes of stimulation was markedly increased when cells were treated with either rhPlGF-2 or rhPlGFStop, as compared to the negative control. The signal strength was similar to the rhVEGF-A_{165} treated positive control. After 20 and 30 minutes of stimulation with either rhPlGF-2 or rhPlGFStop phosphorylation decreased to basal levels (Fig 22a).

As the chemotactic response of PAE/Nrp-1 cells toward rhPlGF-2 was significantly increased as compared towards rhPlGFStop (Fig 17a,b), the role of Nrp-1 overexpression for heparin-binding domain mediated PlGF signal transduction was

analysed. Similarly as seen for stimulation of HUVE cells, both isoforms increased the phosphorylation of Erk-1 and Erk-2 at 5 and 20 minutes of stimulation as compared to the untreated control (Fig 22b). Signal intensity was not altered among isoforms, and declined after 30 minutes. Analysis of Akt phosphorylation at Ser_{473} revealed a delayed onset of activation in PAE/Nrp-1 cells as compared to HUVE cells. Slightly increasing after 5 minutes of stimulation, PlGF treatment significantly enhanced and prolonged phosphorylation at 20 and 30 minutes (Fig 22c). In addition, pre-incubation with the PI3K-inhibitor wortmannin indicated an involvement of PI3K in PlGF-mediated signalling, as the phosphorylation of its downstream target Akt was decreased upon wortmannin-treatment (Fig 22c). Observed effects were heparin-binding domain independent, as the phosphorylation intensity was not altered among isoforms.

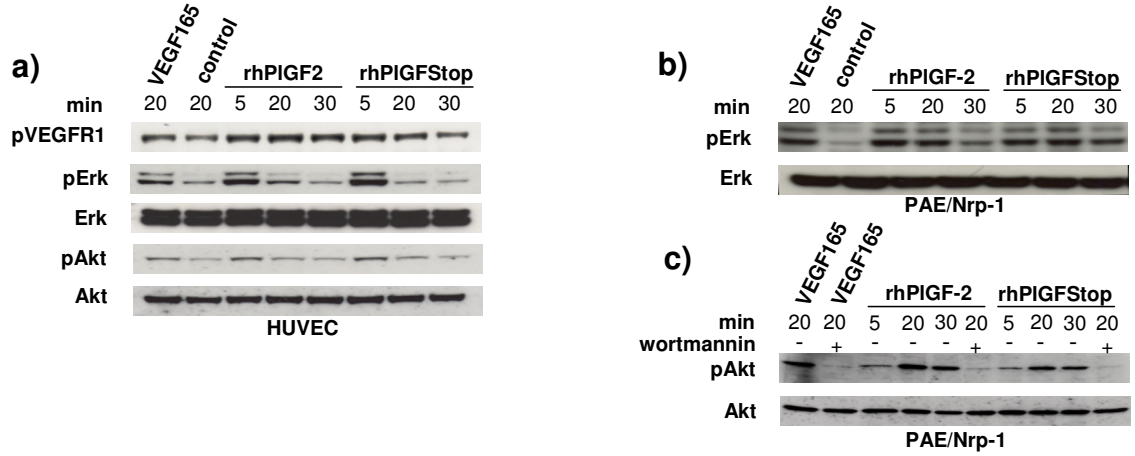

Figure 22: Akt and Erk-1/2 are activated by rhPlGF but not differential regulated by the heparin-binding domain. Western blot analysis of PI3K signal transduction in **(a)** HUVE cells or **(b,c)** PAE/Nrp-1 cells stimulated with 100 ng/mL rhPlGF-2 or rhPlGFStop. 50 ng/mL rhVEGF-A_{165} and starvation medium were used as positive and negative control, respectively. Samples were subjected to SDS-PAGE under reducing conditions and detected by specific antibodies. Phosphorylation of PI3K and downstream targets was analysed by antibodies directed against **(a)** phospho VEGFR-1 (Tyr_{1213}), **(a,b)** phospho Erk1/2 (Thr_{202}/Tyr_{204}), total Erk1/2, **(a,c)** phospho-Akt (Ser_{473}) and total Akt. **(c)** Involvement of PI3K was investigated by inhibition of Akt phosphorylation by wortmannin (200nM).

Analysis of the activation of PI3K and its downstream targets indicated that PlGF is able to activate the tested kinases independently of its heparin-binding domain. PI3K therefore might be involved in PlGF mediated migration, but appears not to be responsible for the differences found in the chemotactic activity. Both forms were able to induce VEGFR-1, Erk-1/-2 and Akt phosphorylation to a comparable or even higher level as observed for rhVEGF-A_{165}. Involvement of PI3K was demonstrated indirectly, by the use of the PI3K-inhibitor wortmannin and the observed reduced phosphorylation of Akt.
Interestingly, overexpression of Nrp-1 on PAE/Nrp-1 cells appears to increase signal strength and duration of phosphorylation of Erk-1/-2 and Akt as compared to HUVE cells (Fig 22b,c). Nevertheless, its overexpression did not alter the phosphorylation profile due

to the presence of the heparin-binding domain in rhPlGF-2 treated samples. Thus, binding to Nrp-1 appears not to be directly involved in a heparin-binding domain induced activation of PI3K and its downstream targets in this context.

2.11.2 Increase of pro-angiogenic response induced by rhPlGF-2 might be mediated by the focal adhesion kinase

FAK mediated activation and signalling to induce chemotaxis is quite complex due to a variety of possibly involved receptors and interacting adapters, kinases and phosphatases that might participate in signal transduction.

To analyse the possible role of FAK regulation in PlGF induced signalling and migration, the level of FAK phosphorylation at $Tyr_{576/577}$ was examined in HUVE cells. These sites are phosphorylated upon binding of members of the Src family of protein tyrosine kinases to FAK (Schaller MD 1994, Calalb MB 1995). As interaction of integrins with components of the extracellular matrix may have a strong impact on FAK activation, cells were seeded on either fibronectin- or collagen I-coated cell-culture dishes prior to stimulation.

Independent of differential coating, rhPlGF-2 and rhPlGFStop both increased FAK phosphorylation at early time points as compared to control, without apparent differences in signal strength among the two stimuli (Fig 23a). Similarly, phosphorylation of downstream targets Src and $p130^{Cas}$ was activated to a comparable degree by both isoforms. Both, rhPlGF-2 and rhPlGFStop increased and sustained phosphorylation of the Src kinase on Tyr_{416} as compared to the negative control when cells were seeded on collagen I (Fig 23a).

Downstream of FAK, the activation of the multimer adapter protein $p130^{Cas}$ was analysed by its phosphorylation at Tyr_{165}, which has been demonstrated to be dependent on both, activation of FAK and Src. Independent of the heparin-binding domain, both isoforms increased phosphorylation on fibronectin at early time points (5 and 15 minutes), but signal intensity was comparable to control samples after 30 minutes (Fig 23 a). When HUVE cells were seeded on collagen I coated cell-culture dishes, phosphorylation was equal between control and stimulus. (Fig 23a). As these were preliminary results, experiment has to be repeated to confirm the results.

Overall, both forms only slightly increased phosphorylation of the tested proteins in HUVE cells at early time points, and revealed no major differences due to presence of the heparin-binding domain. In this cell system, integrin activation by coating with specific adhesion substrates appeared to play a minor role.

Although Nrp-1 is known to be expressed by HUVE cells, its expression level might be

too low to have a major impact on activation of the FAK. To address this question, the PlGF mediated signal transduction in Nrp-1 transfected PAE cells (PAE/Nrp-1) was analysed and compared to signalling taking place in untransfected PAE cells (Fig. 23b). Indeed, Nrp-1 transfected cells grown on cell-culture treated dishes, revealed a clear and time-dependent increase in FAK phosphorylation upon stimulation with rhPlGF-2. The phosphorylation was dramatically decreased compared to control sample after 5 minutes, but phosphorylation strongly increased after 15 minutes and climaxed after 30 minutes. In contrast, stimulation with rhPlGFStop resulted in a slight increase in FAK phosphorylation over control and a sustained intensity at all time points (Fig. 23b, upper panel). By contrast, overall phosphorylation was markedly reduced in untransfected PAE cells.

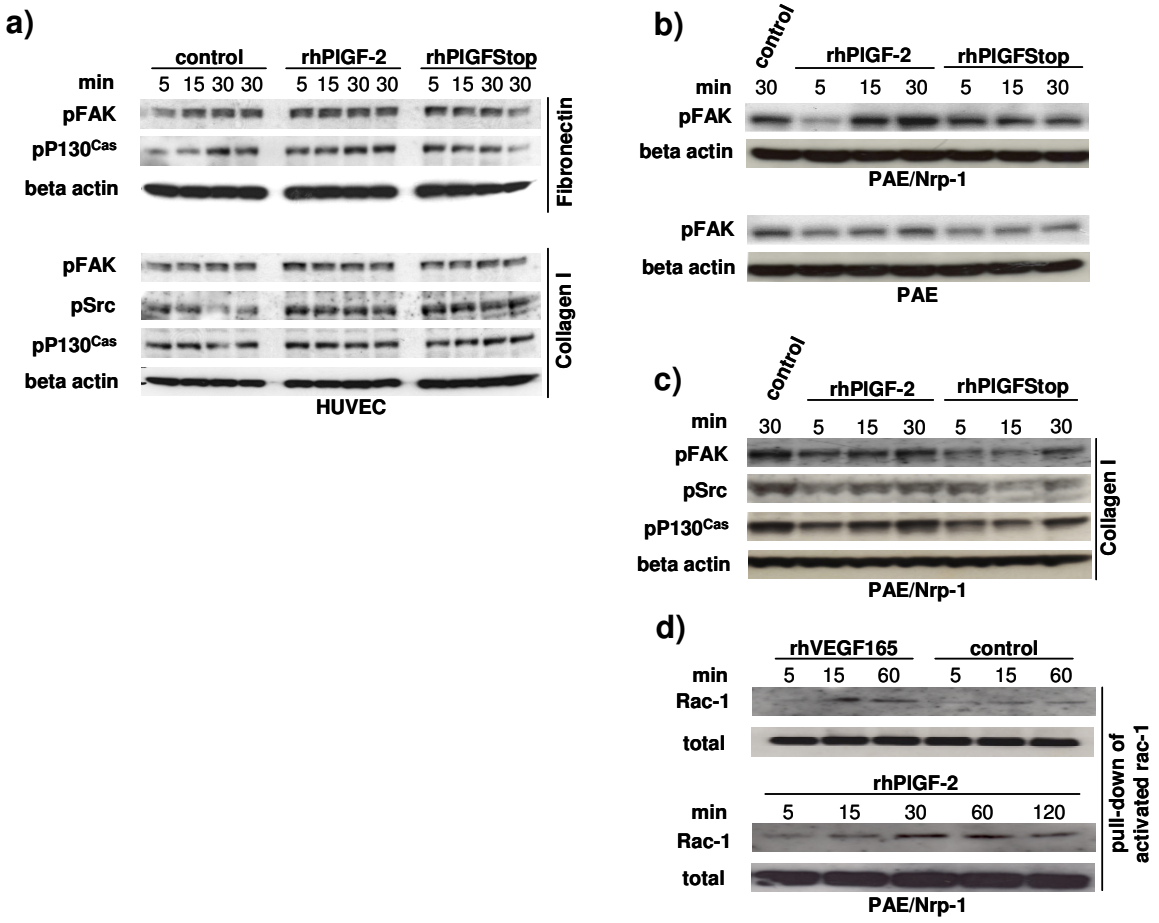

Figure 23: FAK activation is regulated by rhPlGF-2 and its heparin-binding domain under conditions of increased Nrp-1 expression. Western blot analysis of FAK signalling in **(a)** HUVE cells or **(b-d)** PAE/Nrp-1 cells stimulated with 100 ng/mL rhPlGF-2 or rhPlGFStop. 50 ng/mL rhVEGF-A_{165} and starvation medium were used as positive and negative control, respectively. Samples were subjected to SDS-PAGE under reducing conditions and kinase activation was detected by specific antibodies. Phosphorylation of FAK and its downstream targets was analysed by antibodies directed against **(a-c)** phospho-FAK ($Tyr_{576/577}$), **(a,c)** phospho-$p130^{Cas}$ (Tyr_{165}), **(a,c)** phospho-Src (Tyr_{416}); β-actin was used as loading control. Cell culture dishes were coated with either collagen I or fibronectin, as indicated. **(d)** To detect levels of activated Rac-1 in PAE/Nrp-1, a Rac-1 pull-down assay was performed using Pak-crib as bait.

Although rhPlGF-2 induced a time-dependent increase in phosphorylation, signal intensity was very low, and maximal phosphorylation after 30 minutes did not exceed control levels. rhPlGFStop was not able to increase phosphorylation (Fig. 23b, lower panel). As overexpression of Nrp-1 in PAE cells clearly increased rhPlGF-2 mediated FAK phosphorylation as compared to rhPlGFStop, the heparin-binding domain in co-operation with Nrp-1 might be a critical component in PlGF-2 induced migratory signals. As Nrp-1 expression altered FAK phosphorylation in response to the PlGF-2-dependent presence of the heparin-binding domain, PAE/Nrp-1 cells were used to analyse phosphorylation of FAK, Src and $p130^{Cas}$ upon stimulation with rhPlGF-2 or rhPlGFStop on collagen I coated dishes (Fig 23c). When cells were stimulated on collagen I, the phosphorylation pattern markedly differed among the isoforms. Following stimulation with rhPlGF-2, FAK phosphorylation increased in a time-dependent manner and climaxed at 30 minutes. In contrast, PlGFStop failed to induce phosphorylation at 5 and 15 minutes and only slightly activated FAK at 30 minutes of stimulation. Results obtained for phosphorylation of Src-family members revealed a similar pattern to FAK phosphorylation among cells stimulated with rhPlGF-2. The increase of phosphorylation was time-dependent, and resulted in a maximum intensity after 30 minutes. Stimulation with rhPlGFStop induced Src phosphorylation only after 5 minutes, whereas prolonged incubation had no pronounced effect. Phosphorylation of $p130^{Cas}$ was induced by both isoforms, and climaxed at 30 minutes. Induction by rhPlGF-2 resulted in a clear increase in signal intensity over time. In general, signals induced by rhPlGFStop were weaker, and a clear induction only became obvious after 30 minutes of stimulation. Interestingly, the control sample revealed a high base level for all analysed phospho-proteins, which has to be analysed in detail (Fig 23c). Analysis has to be repeated to confirm the results.
Activation of the small GTPase Rac-1 by $p130^{Cas}$ has been demonstrated to be one of the multiple mechanisms to mediate chemotactic signals upon phosphorylation of $p130^{Cas}$ (Burridge K 2004). To measure the rate of Rac-1 activation, a pull-down assay using PAK-Crip, a peptide of a binding partner of activated Rac-1 was performed. Indeed, rhPlGF-2 was able to activate Rac-1 to a comparable degree as observed upon rhVEGF-A_{165} stimulation, which serves as a positive control (Fig 23c). rhPlGF-2 activated Rac-1 in a time-dependent manner, starting at 15 minutes of incubation, climaxing at 60 minutes and decreasing after 120 minutes. No signal was detectable for the negative control. As the rhPlGFStop was not tested yet, these preliminary results may not clarify the role of the heparin-binding domain for PlGF mediated chemotactic responses, but strongly argue for its involvement in a PlGF-mediated chemotactic response.

For a PlGF mediated regulation of the FAK and its downstream effectors, the presence of the heparin-binding domain as well as an overexpression of Nrp-1 appeared to be crucial. Whereas both isoforms induced activation of FAK, Src and $p130^{Cas}$ with comparable strength in HUVE cells, rhPlGF-2 markedly increased signal intensity as compared to rhPlGFStop in PAE/Nrp-1 cells.

3 Discussion

The focus of this project was to evaluate the role of the heparin-binding domain of PlGF-2 in the regulation of PlGF-mediated biological activities, with regard to angiogenesis during wound healing. As confirmed by western blot and mass-spectrometric analysis, PlGF is a target of proteolytic processing by the serine protease plasmin. The resulting loss of the C-terminus markedly reduced PlGF-2 mediated activities *in vitro* and *in vivo*. As truncation of PlGF-2 evoked a comparable, reduced cellular response as compared to the short isoform PlGF-1, proteolytic processing appears to constitute a second mechanism of regulation for PlGF-mediated activities, besides alternative mRNA splicing.

3.1 Proteolytic processing of PlGF by plasmin results in the loss of the heparin-binding domain

Similar as observed for VEGF-A, the expression of the PlGF gene gives rise to different isoforms that are mainly distinguished by the presence or absence of a basic heparin-binding domain in the C-terminal region of the protein. This domain has been proposed to be involved in the binding of heparin/heparan sulphate and in the interaction with the co-receptor Nrp-1 to regulate cellular activities (Migdal 1998), but a detailed analysis remained to be elucidated.

In this project, we demonstrated that proteolytic processing of rhPlGF-2 might provide a second mechanism of regulation of PlGF-mediated bioactivity by cleavage of the heparin-binding domain. As under chronic non-healing wound conditions a highly proteolytic milieu and excessive processing of growth factors may be responsible for a disturbed wound angiogenesis (Eming 2007), we analysed the protease sensitivity of PlGF with regard to the serine protease plasmin. Incubation of rhPlGF-2 with plasmin resulted in a C-terminal degradation and in formation of a stable core fragment, which was resistant to further processing. Analysis of the cleavage fragments by LC-MS/MS analysis revealed multiple cleavage sites within the heparin-binding domain and the sequence of exon 7, finally resulting in the loss of the heparin-binding domain by cleavage between Lys_{118} and Met_{119}. This cleavage appeared to be successive from the C-terminus, as we detected intermediate cleavage product by western blot analysis, using an antibody directed against the N-terminus of PlGF. All but one fragment (Gly_{128}-Lys_{137}) were detected in both samples analysed by LC-MSMS. This fragment was not generated by unspecific cleavage but it rather appeared to be an intermediate cleavage product, as it revealed additional sites in its sequence. To investigate the kinetics of PlGF-2 by plasmin, a detailed analysis would be necessary, but this was not in focus of this project. As the heparin-binding domain was completely degraded by plasmin, an inhibitory effect of fragments of the heparin-binding domain by competitive binding to

receptors may therefore be excluded.

As the cleavage site closest to the N-terminus is located within exon 5, processing by plasmin might affect all PlGF isoforms. In line with this hypothesis, we were able to demonstrate, that plasmin also cleaves rhPlGF-1 in exon 5, which resulted in the loss of a sequence, which is mainly coded by exon 7. The stable N-terminal core-fragment formed upon final cleavage at Lys118/Met119 in both isoforms retained its basal structural features such as intra- and intermolecular disulfide bonds, and glycosylation sites.

Interestingly, this regulation of activity appears to be highly consistent among VEGF-family members. Besides high structural similarities and a comparable regulation by alternative splicing, the activity of VEGF-A_{165} has been demonstrated to be regulated by plasmin-mediated proteolytic processing, resulting in the loss of the heparin-binding domain and formation of a plasmin-resistant core-fragment (Lauer 2002). This truncated form of VEGF-A exhibited a markedly reduced angiogenic activity (Roth 2006). Similarly to PlGF, the VEGF-A_{165}-cleavage site closest to the N-terminus is located in exon 5 and therefore common to all VEGF-A isoforms. Furthermore, this site revealed a high compliance in its amino acid composition to the one identified in PlGF, with regard to their chemical properties ($KDR_{110}A_{111}R$ in VEGF-A versus $REK_{118}M_{119}K$ in PlGF).

Regulation of activity by proteolytic processing and cleavage of the heparin-binding domain therefore might provide a common mechanism within the VEGF-family. As the heparin-binding domain is predicted to enhance PlGF-mediated activities by gradient formation or recruitment of co-receptors, plasmin-mediated cleavage demonstrates a second form of regulation besides alternative splicing.

3.2 PlGF is upregulated during skin repair and proteolytically processed in exudates obtained from non-healing wounds

PlGF expression has been reported to be upregulated during wound healing in mouse and human, as compared to expression levels in non-wounded skin (Failla 2000, Cianfarani 2005). In line with this data, we demonstrated an increase of PlGF protein level in exudates obtained from healing human wounds. As this level is strongly increased in comparison to serum levels, the rise of PlGF can be attributed to a local expression. The PlGF-protein level in non-healing wounds was increased as compared to all time points analysed for normal healing progression, although this difference was not statistically significant. Similar differences were observed for the protein level of VEGF-A in human wounds, where an upregulation in non-healing wounds was detected as compared to healing ones (Lauer 2000). These observations may indicate an upregulation in expression to compensate the decrease in growth factor activity due to proteolytic processing. The relevance of proteolytic processing of PlGF in the non-healing wound *in vivo* was demonstrated by western blot analysis. Similarly as observed

for VEGF-A_{165}, PlGF-2 retained its structural integrity in exudates obtained from wounds with normal healing progression, whereas it was degraded in exudates obtained from non-healing human wounds, which reflects a dysregulated protease activity (Roth 2006). Although not analysed in detail, this processing of PlGF-2 appeared to be plasmin-dependent, as the degradation pattern could be reproduced *in vitro* using human plasmin. However, to address the role of plasmin in the degradation of PlGF in detail, the integrity of PlGF-2 in wound exudates has to be analysed by the use of specific inhibitors for plasmin. As several proteases are upregulated under conditions of impaired wound healing, they might contribute to a degradation of PlGF. Possible interesting candidates would be neutrophil elastase or the family of MMPs, whose activity is highly upregulated under these conditions (Nwomeh 1998). Furthermore, a subset of MMPs was shown to degrade VEGF-A in a comparable manner as demonstrated for plasmin, resulting in a markedly reduced binding capacity to matrix components and distinct angiogenic activity (Lee 2005).
Taken together these data confirm the relevance of PlGF-degradation *in vivo*, and strongly argue for the possibility of a common mechanism of proteolytic processing in the VEGF family.

To overcome negative effects of proteolytic processing, the generation of a plasmin-resistant form of PlGF-2 would be beneficial. As demonstrated for VEGF-A_{165}, such a mutant retains its stability in the proteolytic milieu of non-healing wounds and promotes wound angiogenesis (Lauer 2002, Roth 2006). The generation of a mutant, plasmin resistant form of PlGF-2 to improve stability may be complicated, as plasmin generates multiple cleavage sites within the heparin-binding domain. Both mutant forms of PlGF-2 (rhPlGF-$2^{lys\text{-}pro}$ and rhPlGF-$2^{lys\text{-}ala}$) generated by site directed mutagenesis at Lys_{118} did not prevent the degradation of the heparin-binding domain, as observed for mutation of the corresponding site in VEGF-A_{165} (Lauer 2002). A different presentation of plasmin cleavage sites within the heparin-binding domain might be the reason. To achieve plasmin resistance, the exchange of a variety of basic amino acids or amino acid sets has to be tested. The mutation of a set of basic residues comprises the risk, that this domain partly could lose its specific pattern of basic amino acids and therefore its binding capacity to certain molecules. In addition, extensive mutagenesis might affect folding and interface presentation within the heparin-binding domain.

3.3 The binding of PlGF isoforms to GAGs is mediated by the C-terminal domain encoded by exon 6 and 7

By use of Surface Plasmon Resonance spectroscopy, the C-terminal domain of rhPlGF-1 and PlGF-2 was clearly identified as a critical component for the binding to heparin, heparan sulphate, and chondroitin sulphate. Interestingly, this interaction appeared not to be solely dependent on the expression of the heparin-binding domain encoded by exon 6, but to a high degree on the sequence encoded by exon 7. As rhPlGF-1 revealed a binding strength, which was in average only 2-3 fold less intense as compared to rhPlGF-2, the heparin-binding domain seemed to have an enhancing effect, rather than an exclusive role for GAG-interaction. The results for rhPlGF-1 were surprising, as it was predicted to be unable to bind to heparin due to the lack of the heparin-binding domain. Two groups demonstrated that in contrast to PlGF-2, PlGF-1 is not able to bind to heparin-sepharose (Hauser 1993, Park 1994). Although SPR analysis provides the more sensitive method, binding experiments to heparin-Sepharose should be repeated, following the authors protocol.

rhPlGFStop, which lacks the heparin-binding domain as well as the sequence encoded by exon 7 was unable to bind to any of the tested GAGs. As it is identical to rhPlGF-1 apart from 13 C-terminal amino acids, this observation further highlighted the role of the sequence encoded by exon 7. In addition, its inability to bind to the tested GAGs proved that the core-fragment does not participate in a direct interaction. As the sequence lacking in rhPlGFStop is short and consists of only four basic amino acid residues, an analysis of critical amino acids could be performed easily by site-directed mutagenesis.

The high similarities in the binding strength among rhPlGF-1 and rhPlGF-2 were surprising, as the differential isoform expression was thought to play an essential role in extracellular patterning, similar as observed for VEGF-A. Upon secretion, the VEGF-A isoforms have been demonstrated to have a differential diffusability, which appears to be crucial for the establishment of a gradient and vascular patterning (Carmeliet 1999, Maes 2002, Ruhrberg 2002, Stalmans 2002, Gerhardt 2003). Whereas VEGF-A_{188} was sequestered directly upon secretion, VEGF-A_{121} is predicted to have no GAG-binding capacity and to be freely diffusible. VEGF-A_{165} has an intermediate binding capacity.

Our results appear to argue against a formation of a clear gradient among the isoforms, as at least rhPlGF-1 and rhPlGF-2 revealed a comparable binding strength for the tested GAGs. Nevertheless, we cannot rule out a differential binding to other GAGs. Therefore, analysis of additional GAGs might be an interesting topic, as a potential difference in the binding strength among the isoforms might help to identify areas of local and distinct sequestration.

Our results identified the sequence coded by exon 7 as a critical determinant for an interaction between PlGF and the tested GAGs. The heparin-binding domain of rhPlGF-2 appears to enhance this interaction, but not to be the exclusive binding-interface.

3.4 Heparin enhances the interaction between Nrp-1 and PlGF-2

As plasmin processing markedly affected the binding capacity of both, rhPlGF-1 and rhPlGF-2 to GAGs, the binding of the various PlGF forms to the co-receptor Nrp-1 was assessed. We measured a moderate binding strength between rhPlGF-2 and Nrp-1 by Surface Plasmon Resonance spectroscopy, which was largely enhanced in the presence of heparin. These data are in line with results obtained from cross-linking experiments (Migdal 1998). In contrast to rhPlGF-2, rhPlGFStop did not show any binding to Nrp-1, which again underlines the essential role of the C-terminus for the binding capacity of PlGF. Unfortunately, a precise characterization of the binding of rhPlGF-1 to Nrp-1 is not existent, as the measured binding curves in our experiments had a bad resolution. Therefore, the measurements have to be repeated. While predicted not to bind to Nrp-1, several evidences argue for a binding of rhPlGF-1 to this co-receptor. First, VEGF-A_{121} the VEGF-A isoform lacking the heparin-binding domain was recently shown to bind directly to Nrp-1 in a heparin-independent fashion. The last C-terminal amino acids coded by exon 8 appeared to be the critical components, as this interaction was largely competed by Tuftsin, a synthetic tetrapeptide, which is very similar to the C-terminus of VEGF-A and PlGF. In addition, VEGF-A_{165b}, which expresses the heparin-binding domain but an alternative C-terminal end, is unable to interact with Nrp-1 (Cebe Suarez 2006, Pan 2007a, Vander Kooi 2007). Second, Migdal and co-workers analysed the binding of PlGF to Nrp-1 by cross-linking experiments on HUVE cells, as mentioned above. Although they awarded PlGF-1 a minor role in Nrp-1 binding, they observed that PlGF-1 slightly competes with ^{125}I-PlGF-2 for the binding to Nrp-1 on HUVE cells (Migdal 1998). As these experiments were performed in a cellular system, this method may not control all aspects for a proper binding and is less sensitive as compared to SPR spectroscopy. In addition, the same group demonstrated an essential role of the PlGF heparin-binding domain as well as of the sequence encoded by exon 7. By generation of synthetic peptides, corresponding to either the first 15 amino acids of exon 6 (heparin-binding domain) or exon 7, they largely inhibited the binding of ^{125}I-PlGF-2 to Nrp-1. To clearly confirm a direct interaction between PlGF-1 and Nrp-1, our SPR-measurements have to be repeated.

The major question in this context is how the heparin-binding domain differentially regulates the biological function of PlGF-2. Vander Kooi and co-workers established a model to explain the role of the heparin-binding domain for the interaction between VEGF-A_{165}, Nrp-1, and the VEGFRs, which may be partially adaptive for PlGF-2. At least two factors likely contribute to the critical role of the heparin-binding domain of VEGF-A and are required for heparin binding. First, the heparin-binding domain may be pivotal to extend the C-terminal Nrp-binding region from the VEGF-A core-protein sufficiently, to

allow unencumbered access to the Nrp-1 dimer. Second, the heparin-binding domain provides an additional binding-interface for heparin and supports the interaction between heparin and Nrp-1. The length of the saccharide-chain appears to be crucial for the binding strength, as an optimal chain length of 22 and 24 monosaccharide units of heparin have been demonstrated to optimize the binding between VEGF-A_{165} or PlGF-2 to Nrp-1, respectively (Mamluk 2002). The heparin-binding domain of VEGF-A_{165} therefore might serve as a prolonged and continuous GAG-binding interface as compared to VEGF-A_{121}, which then is sufficient to recruit Nrp-1 to the VEGFRs (Vander Kooi 2007). For VEGF-A, Nrp-1 and VEGFR-2 this hypothesis has been proven. In dependence of the heparin-binding domain, the complex of VEGF-A_{165}/heparin/Nrp-1 was able to cluster with VEGFR-2. This complex largely enhanced the interaction between the receptors and the ligand and resulted in an increased phosphorylation of VEGFR-2. Nrp-1-bound VEGF-A_{121} failed to induce this complex (Pan 2007a). Combined binding studies with VEGFR-1, Nrp-1 and PlGF-1 or PlGF-2 would be needed to confirm a similar mechanism of Nrp-1 recruitment to VEGFR-1, mediated by PlGF-2 and its heparin-binding domain.

For a detailed structural analysis, the crystal structure of PlGF-1 and -2 would be helpful, but up to date only 3D-models of the core-protein are available for PlGF and VEGF-A. This strongly argues for the possibility, that the C-terminus is flexible and therefore may exhibit a low degree of tertiary structure, which does not allow crystallization. This might account for the high accessibility for proteases within the heparin-binding domain. Both 3D-models of the core-protein reveal highly basic patches of amino acids at the surface of the core-fragments. These patches may be supportive for an interaction of PlGF with GAGs or Nrp-1. However, our experiments investigating the interaction between rhPlGFStop and GAGs or Nrp-1 reveal, that these basic regions alone are not sufficient due to the lack of the C-terminus.

Our findings strongly indicate, that the interaction of PlGF-2 with Nrp-1 is mediated by its C-terminal domain and significant enhanced in the presence of heparin. The observed inability of rhPlGFStop to bind to Nrp-1 strongly suggests that a reduction of PlGF-2 activity after plasmin digestion is caused by loss of its Nrp-1 binding capacity.

3.5 The mechanisms of PlGF-mediated activities

To analyse the direct role of the heparin-binding domain for PlGF-induced cellular function, the chemotactic activity, as well as the capacity to induce sprouting of endothelial cells was assessed by a direct comparison of the different forms of PlGF. In both *in vitro* assays performed, rhPlGF-2 significantly increased the cellular response, as compared to PlGF forms that lack the heparin-binding domain encoded by exon 6.

According to the literature, the PlGF-induced cellular responses may be mediated by several mechanisms, that may in part be regulated by alternative expression of the heparin-binding domain or its proteolytic degradation: by activation of the VEGFR-1, by recruitment of the co-receptor Nrp-1 to VEGFR-1, by induction of signal transduction via Nrp-1 alone or by linkage of the VEGFR-1 system to integrin signalling.

3.5.1 VEGFR-1 is activated independently of the C-terminal domain of PlGF encoded by exon 6 and 7

The role of VEGFR-1 for the recruitment of several cell types has been demonstrated by gene-deletion experiments, in which cells defective for VEGFR-1 or ligand failed to be recruited in response to VEGF-A_{165} or PlGF-2 (Park 1994, Clauss 1996, Ishida 2001, Hattori 2002, Luttun 2002). VEGFR-1 is therefore believed to be directly involved in migration of endothelial cells, monocytes and macrophages as well as pericytes and precursor cells derived from the bone marrow. Exact mechanisms are unknown, but this recruitment appears to be highly dependent on the expression of Nrp-1, as its gene silencing by siRNA completely abolished cellular recruitment in response to VEGF-A_{165} (Zacchigna 2008). VEGFR-1 is therefore believed to work in concert with Nrp-1 rather than to promote directed migration solely. This hypothesis is supported by the fact, that the various isoforms of VEGF-A induce distinct cellular responses due to differential expression of the heparin-binding domain, although the binding to VEGFR-1 appears to be not affected by this domain.

Similarly to VEGF-A, the minimal interface of PlGF that mediates the binding to the VEGFR-1 was identified by crystallization of Ig-like domains-2 and -3 of VEGFR-1 in interaction with PlGF and by detailed mutagenesis experiments. All critical amino acids involved in a direct interaction to VEGFR-1 are located in the core-protein of PlGF encoded by exon 1-5 (Christinger 2004, Errico 2004). Different to VEGF-A, glycosylation at Asn_{84} appears to be critical for the PlGF-binding to the VEGFR-1. A role of the heparin-binding domain for the direct interaction to VEGFR-1 was not analysed on the structural level so far, but as PlGF-1 and PlGF-2 reveal a comparable binding strength to VEGFR-1 independent of the heparin-binding domain (Yamazaki 2006), it appears not to influence the binding by direct interaction. Due to the fact, that all critical determinants for the interaction between PlGF and VEGFR-1 are located within the core-protein of PlGF, it is likely, that proteolytic processing of PlGF-2 or expression of PlGF-1 (lacking the heparin-binding domain) will not largely affect binding and activation of VEGFR-1, but cannot completely excluded.
In line with these predictions, both rhPlGFStop and rhPlGF-2 activated VEGFR-1 by phosphorylation at Tyr_{1213} to a comparable degree, which is thought to be the main site for phosphorylation upon ligand binding (Autiero 2003). Receptor-activation as well as

activation of the downstream targets Akt and Erk-1/-2 revealed no differences, therefore this signal transduction cascade may not be reasonable for the significant increased cellular responses observed upon stimulation with rhPlGF-2. As Akt and Erk-1/-2 have been demonstrated to be involved in monocyte migration upon activation of VEGFR-1 (Tchaikovski 2008), they might have a role in induction of an increased general motility (Fig 24), rather than being involved in signal transduction for directed migration.

The idea, that VEGFR-1 activation alone may not be responsible for the increased cellular response induced by PlGF-2 and its heparin-binding domain is supported by the data obtained from *in vitro* experiments. Neither rhPlGF-1 nor rhPlGF-2 was able to induce a significant chemotactic response on PAE cells, which solely express the VEGFR-1 and lack Nrp-1 expression. Although PlGF is known to induce the recruitment of several cell types that express VEGFR-1 (as mentioned above), this expression alone appears to be not sufficient to mediate the chemotactic effect of PlGF-2.

Analysis of the potency to induce endothelial sprouting revealed that all isoforms increased the cumulative sprouting length as compared to the negative control. Furthermore, all PlGF isoforms appeared to stabilize the spheroid. This effect seems to be, at least in part independent of the heparin-binding domain. This phenomenon may be explained by activity as a survival factor, which might be induced by VEGFR-1 signalling alone (Adini 2002, Cai 2003). Nevertheless, the clear increase in the cumulative sprouting length and the sprout number in response to rhPlGF-2 cannot be explained by VEGFR-1 signalling alone.

To clearly eliminate a role of the heparin-binding domain for the induction of a distinct signalling via VEGFR-1 alone, a screen on all phosphorylation sites of VEGFR-1 would be necessary.

3.5.2 Nrp-1 expression is important for PlGF-2 mediated chemotaxis and endothelial sprouting

The role of Nrp-1 for angiogenesis is undisputable, as homozygous deletion as well as overexpression resulted in severe vascular defects (Kitsuwaka T 1995, Kawasaki 1999, Takashima 2002). Strong evidence points to a role of Nrp-1 in cell migration, adhesion and morphogenesis in response to VEGF-A, as neutralizing antibodies that specifically prevent VEGF-A binding to Nrp-1, blocked endothelial cell sprouting and neo-vascularization *in vitro* (Pan 2007a). Nrp-1 was demonstrated to bind different VEGF-A isoforms independently of the heparin-binding domain, but its recruitment and clustering with the VEGFRs appears to be mediated by ligands bearing a heparin-binding domain in a GAG-dependent fashion (Pan 2007a, Vander Kooi 2007).

In line with these findings, we observed a significant increase in the chemotactic response induced by rhPlGF-2 in Nrp-1/PAE cells, whereas untransfected PAE cells failed to respond to rhPlGF-2. Expression of VEGFR-1 solely therefore appears to be not

sufficient to induce a chemotactic response. Furthermore, we clearly identified the heparin-binding domain as a critical determinant for the induction of chemotaxis on endothelial cells, as both isoforms lacking the heparin-binding domain failed to induce directed migration. Although an involvement of Nrp-1 in rhPlGF-2 induced chemotaxis is demonstrated by loss of the migratory response in untransfected PAE cells, inhibitory antibodies should prove its role on PAE/Nrp-1 cells.

These results were confirmed by analysis on HUVE cells, which are known express both receptors. Whereas rhPlGF-2 induced a robust chemotactic response, a lack of the heparin-binding domain appears to largely inhibit chemotaxis. Interestingly, Migdal and co-workers directly compared the chemotactic response of PlGF-1 and PlGF-2 on HUVE cells in the Boyden chamber assay, which did not reveal clear differences among the two isoforms (Migdal 1998). Although a comparable experimental setting was utilised, the authors used collagen IV to coat the porous membranes, whereas the cells were exposed to collagen I in the experiments presented here. Of more importance, the authors did not detect VEGFR-1 expression on HUVE cells in cross-linking experiments. It is known, that primary HUVE cells lose their ability to express VEGFR-1 with increasing passage number, and therefore a lack of VEGFR-1 may be reasonable for a failure of an induction of migration on that account (Shibuya 2001).

Besides its migratory effects, Nrp-1 was demonstrated to be involved in VEGF-A_{165}- and VEGF-A_{121}-induced vascular sprouting (Pan 2007a). Although VEGF-A_{121} was less effective in sprout induction, both isoforms induced tubular outgrowth in a Nrp-1 dependent fashion, as it was markedly reduced by an inhibitory Nrp-1-antibody. This antibody had no effect on spouting induced by a truncated form of VEGF-A (VEGF-A_{109}). As VEGF-A_{109} is unable to bind Nrp-1, sprouting appears to be induced, at least in part, independent of Nrp-1. Interestingly, these data exactly reflect our results obtained from spheroids, stimulated with rhPlGF-1, rhPlGF-2, and rhPlGFStop: a clearly increased sprout number in spheroids stimulated with rhPlGF-2 and a reduced, but comparable sprouting in rhPlGF-1 and rhPlGFStop stimulated spheroids. Although a direct role of Nrp-1 has to be analysed by use of inhibitory antibodies, it is likely that the observed increase in sprout number is induced by a heparin-binding domain mediated bridging of Nrp-1 and VEGFR-1. This hypothesis has to be confirmed by either co-immunoprecipitation of VEGFR-1 and Nrp-1 and/or an altered phosphorylation of VEGFR-1 upon stimulation with PlGF-2 or PlGF-1/PlGFStop.

Besides acting as a direct co-receptor, which is bridged to the VEGFRs in a heparin-binding domain-/GAG-dependent fashion, Nrp-1 is predicted to induce cellular responses independent of, or in parallel with the VEGFRs. Such activation of Nrp-1 induced signalling might be induced independently of the heparin-binding domain. Wang *et al*. demonstrated, that EGF can induce migration of endothelial cells expressing a

fusion protein consisting of the extracellular domain of EGFR (epidermal growth factor receptor) fused to the transmembrane and intracellular domain of Nrp-1. This induction of migration appeared to involve activation of the PI3K/Akt axis (Wang 2003). To analyse, if this is a possible mechanism, by which PlGF-2 might differentially induce the observed chemotactic response on endothelial cells, we stimulated PAE/Nrp-1 cells with either rhPlGF-2 or rhPlGFStop and analysed the phosphorylation of Akt by western blot analysis. Both forms clearly induced Akt phosphorylation to a comparable degree. As Akt phosphorylation was inhibited by wortmannin, it appears to be PI3K-dependent. rhPlGFStop is not able to bind to Nrp-1, therefore the observed phosphorylation may not be caused by Nrp-1 mediated signalling. Nevertheless, we cannot rule out, that other signalling cascades might be directly activated by Nrp-1 upon ligand binding. To analyse a role of Nrp-1 signalling independently of VEGFR-1, the use of inhibitory antibodies to prevent VEGFR-1 activation may help to identify possible signal transduction targets of Nrp-1.

Our results clearly support the essential role of Nrp-1 in rhPlGF-2 induced chemotaxis and sprout induction. As the lack of the heparin-binding domain significantly attenuated this cellular response, it appears to be highly regulated by alternative splicing as well as plasmin-dependent processing.

3.5.3 The heparin-binding domain of PlGF-2 modulates potential integrin-mediated activation of downstream kinases

Integrins are known to be crucial surface molecules, which are essential for adhesion and migration by binding to components of the extracellular matrix and intracellular re-organization of the cytoskeleton. Lesslie and colleagues observed a possible mechanism, by which VEGF-A_{165} specifically induced chemotaxis of a human carcinoma cell line by activation of FAK and its downstream target $p130^{Cas}$. They identified the family of Src-kinases as linker between VEGF-A mediated VEGFR-1 signalling and integrin signalling (Lesslie 2006). As $p130^{Cas}$ activation requires integrin-mediated FAK phosphorylation at Tyr_{397} as well as Src-induced FAK phosphorylation at $Tyr_{576/577}$, it appears to be highly dependent on both pathways.

In line with these results, we observed a slight activation of FAK, Src-family kinases and $p130^{Cas}$ upon PlGF stimulation of HUVE cells. This induction of phosphorylation appeared to be independent of the heparin-binding domain, as these effectors revealed a comparable phosphorylation pattern upon stimulation with either rhPlGF-2 or rhPlGFStop. Interestingly, in PAE/Nrp-1 cells rhPlGF-2 clearly increased FAK phosphorylation as compared to rhPlGFStop, whereas this phosphorylation was markedly decreased in untransfected PAE cells. In conclusion, Nrp-1 may enhance the

rhPlGF-2 induced phosphorylation in a heparin-binding domain-dependent fashion, whereas rhPlGFStop induces a weak phosphorylation by solely activating VEGFR-1. Similar to FAK phosphorylation, rhPlGF-2 increased activation of $p130^{Cas}$ and Src family kinases, as compared to rhPlGFStop. These differences among the isoforms were even more pronounced, when cells were seeded on collagen I, underlining the role of integrin activation. Based on these findings, a co-activation of integrin-mediated signalling and rhPlGF-2 induced VEGFR-1/Nrp-1 signal transduction may be responsible for the observed increase in chemotaxis. The involvement of integrin-mediated signalling has to be proven by specific antibodies. Although the results of FAK-mediated directed migration in response of rhPlGF-2 have to be verified and compared to rhPlGF-1, this mechanism may provide a reasonable explanation for a distinct heparin-binding domain mediated *in vitro* activity of PlGF-2.

Upon activation, VEGFR-1 has been demonstrated to interact with a variety of SH-2 adapter proteins such as Grb2, Crk, and Nck. As these adapters are able to bind and trans-phosphorylate FAK (for review see Playford 2004, Mitra 2006), the collaboration between PlGF-2 induced VEGFR-1/Nrp-1 signalling and integrin mediated signals may be changed or fine-tune to promote differential cellular responses such as tube-formation. Detailed analysis on VEGFR-1 phosphorylation and activation of adapter-kinases will help to identify exact mechanisms of interaction of these two pathways.

Our data indicates a collaboration of integrin- and VEGFR-1/Nrp-1-mediated signal transduction to promote PlGF-2 induced chemotaxis. This assumption is supported by an increased activation of FAK and downstream kinases induced PlGF-2 and its heparin-binding domain.

3.6 rhPlGF-2 increases wound angiogenesis and promotes granulation tissue formation in diabetic mice

In diabetes, numerous aspects of the normal wound healing response are impaired and include dysfunction in the inflammatory response, a reduced granulation tissue formation, and impaired angiogenesis. In part, a dysregulation of proteases may be responsible. To investigate the role of either alternative mRNA splicing or proteolytic processing for the *in vivo* activity of PlGF to promote angiogenesis during wound healing, we topically applicated the different PlGF forms onto the wound bed and wounds were analysed microscopically at day 10 and day 14 post wounding.

Results obtained by H&E-staining and immunohistochemical staining clearly demonstrated, that rhPlGF-2 treatment improves granulation tissue formation and angiogenesis in diabetic mice. As rhPlGF-1 and rhPlGFStop induced a significantly reduced response in these parameters, the observed effects appear to be heparin-

binding domain dependent and to be regulated by alternative splicing as well as proteolytic processing. Nevertheless, both isoforms slightly increased granulation tissue formation and angiogenesis, as compared to vehicle treated controls. Cianfarani *et al*. obtained comparable results in streptozotocin-induced diabetic mice. The authors observed an accelerated wound closure rate, a slight increase in granulation tissue and an improved angiogenic response by either transgenic overexpression of PlGF-1 in the skin (K14 promoter) or adenoviral transfer of PlGF-1 to the wound site (Cianfarani 2006). A direct comparison of the results is difficult, as streptozotocin-induced diabetic mice appear to have a retarded healing response as observed in our diabetic mice. Whereas in their model wounds were not closed before day 16, in our diabetic mice all wounds were already closed at day 10. As we did not analyse the effect of PlGF-treatment before day 10, we cannot conclude on an accelerated closure response. Therefore, analysis has to be performed at earlier time points. By analysis of granulation tissue formation and maturation, the authors observed an increase in area as well as in cellularity in adenoviral treated mice. The granulation tissue appeared to be more mature in response to PlGF-1, revealed a high degree of collagen content, and was highly populated with fibroblasts and monocytes/macrophages. As recruitment of VEGFR-1$^+$ cells is known to be induced by PlGF, these results appear to be a direct effect of PlGF treatment (Park 1994; Clauss 1996, Hattori 2002). Similarly, we observed a slight but not significant increase in granulation tissue formation in wounds treated with either rhPlGF-1 or rhPlGFStop. As corresponding stainings are under investigation at the moment we can just speculate, but a PlGF induced recruitment of VEGFR$^+$ fibroblasts and monocytes/macrophages to the wound site appears to be reasonable. This cell recruitment seems to be further increased by rhPlGF-2. A heparin-binding domain mediated mechanism therefore appears to be responsible for the significant increase in granulation tissue and might include Nrp-1 signalling.

In streptozotocin-induced diabetic mice, adenoviral PlGF-1 treatment significantly improved vascularization of granulation tissue and vessel coverage with pericytes/smooth muscle cells at day 7 post wounding. This data might coincide with our results, although we analysed vascularization of granulation tissue at later time points. At day 10 post wounding, we observed a slightly increased vessel density in rhPlGF-1 and rhPlGFStop treated wounds as compared to vehicle treated controls, which is even more pronounced in rhPlGF-2 treated wound. These differences among isoforms become even more obvious at day 14 post wounding. Interestingly, the vessel density of rhPlGF-2 treated wounds remains stable between day 10 and day 14, whereas vessels in rhPlGF-1 or rhPlGFStop treated wounds and control wounds appear to regress. The significant differences in vessel density between PlGF-1 treatment and vehicle control at

day 7, observed by Cianfarani *et al*., might be adapted by vessel regression at later time points. To underline this hypothesis, we have to analyse vessel density in earlier phases of healing progression.

The increased persistence of vasculature observed in rhPlGF-2 treated wounds as compared to rhPlGF-1, rhPlGFStop or vehicle control, especially at day 14, may have several reasons. The most obvious one is the significant increase in perivascular cells. These VEGFR-1$^+$ cells are known to be recruited in response to PlGF (Carmeliet 2001). In line, we observed a slight increase in the desmin positive area in rhPlGF-1 and rhPlGFStop treated wounds at day 10. As this recruitment was significantly enhanced by rhPlGF-2, a heparin-binding domain dependent mechanism appears to be reasonable. As this recruitment resulted in augmented vessel coverage with pericytes, rhPlGF-2 might promote vessel stabilization and maturation. A second mechanism might be the induction of anti-apoptotic gene expression in endothelial cells (Adini 2002). Adini and colleagues have demonstrated, that mPlGF-2 induced survivin expression on endothelial cells during tumor formation, and therefore promoted endothelial cell survival rather than vessel formation. An additive effect of both mechanisms might be conceivable. Analysis of the gene-expression profile among the different PlGF-forms therefore might be in interesting topic.

Our findings clearly demonstrate that rhPlGF-2 promotes angiogenesis and formation of granulation tissue. As treatment with either rhPlGF-1 or rhPlGFStop revealed a significant reduced response, the PlGF mediated activities appear to be regulated by alternative splicing as well as proteolytic processing. The involvement of Nrp-1 and/or and altered gene-expression in response to the heparin-binding domain of PlGF remains to be elucidated.

3.7 Model for PlGF-induced signal transduction

The findings of this study clearly demonstrate that the heparin-binding domain of PlGF-2 stimulates endothelial cell functions *in vitro* and promotes angiogenesis and granulation tissue formation *in vivo*. The model presented in Figure 24 provides a possible mechanism, by which PlGF-2 might mediate its chemotactic activity.

Supported by western blot analysis (Fig 22a), binding and activation of VEGFR-1 appears to be independent of the heparin-binding domain or the sequence encoded by exon 7 (Fig 24a), as demonstrated by rhPlGFStop (core-fragment) induced receptor-phosphorylation. This binding resulted in the activation of the PI3K/Akt axis, which may promote increased random migration, but failed to induce directionality, as observed for rhPlGF-1 and rhPlGFStop in the Boyden chamber assay. In contrast, rhPlGF-2 increased chemotaxis in an Nrp-1-dependent fashion. Reasonable might be VEGFR-

1/Nrp-1 clustering. For complex formation, the heparin-binding domain of PlGF-2 as

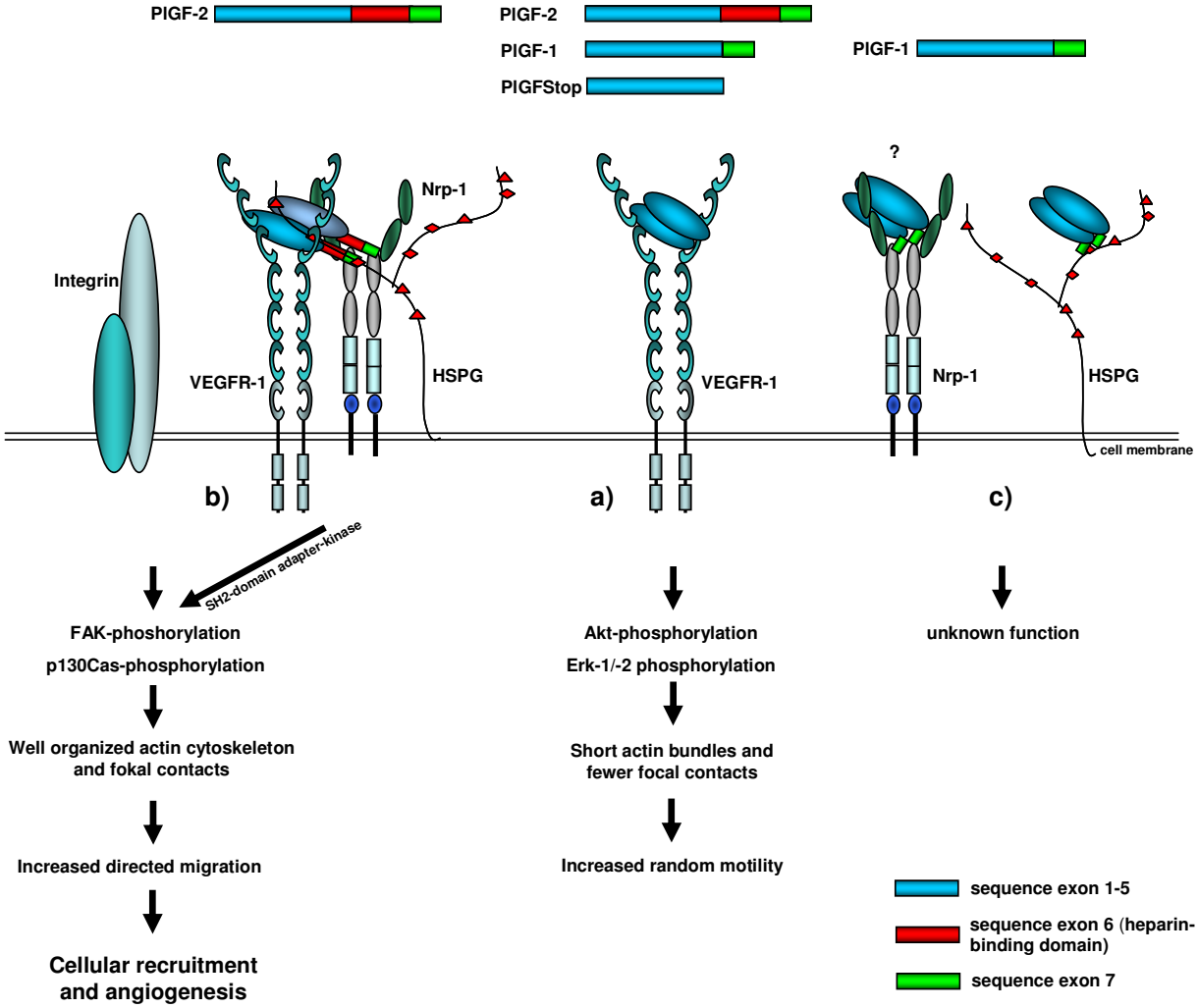

Figure 24: Model for heparin-binding domain dependent or independent induction of endothelial cell activity in response of PlGF. (a) Independent of the C-terminal heparin-binding domain and the sequence encoded by exon 7, the PlGF core-protein can bind and activate the VEGFR-1. This interaction results in activation of the PI3K/Akt axis to promote random migration. **(b)** In contrast, PlGF-2 promotes clustering of VEGFR-1 and Nrp-1 in dependence of its heparin-binding domain and the presence of GAGs. This altered VEGFR-1 activation supports the interaction of VEGFR-1- and integrin-induced signal transduction to promote FAK phosphorylation. The collaboration between integrins and VEGFR-1/Nrp-1/GAG/PlGF-2 is mediated by SH-2-domain adapter kinases such as Src-kinases, which induce distinct FAK phosphorylation. FAK activation initiates a defined downstream signalling pathway and directed motility. **(c)** PlGF-1 has the capability to bind to GAGs, activate VEGFR-1 and probably interacts with Nrp-1, but it appears that these interactions are not sufficient to promote chemotaxis and sprouting. Potentially, the absence of the heparin-binding domain prevents VEGFR-1/Nrp-1/GAG clustering. A possible function of PlGF-1 binding to Nrp-1 or GAGs remains to be elucidated.

well as GAGs are essential to bridge these two receptors. In turn, enhanced or altered VEGFR-1 phosphorylation activates certain SH-2-domain adapter-kinases such as Src (Fig 23c). These kinases work in concert with activated integrins to promote a distinct FAK phosphorylation pattern and induction of cytoskeletal re-organization and directed motility (Fig 24b).

PlGF-1 has the capability to interact with VEGFR-1, GAGs and probably with Nrp-1 (Fig

24c), but it appears, that this binding is not sufficient to promote chemotaxis or endothelial sprouting. Potentially, the absence of the heparin-binding domain prevents VEGFR-1/Nrp-1/GAG clustering, similarly as observed for VEGF-A_{121} (Pan 2007, Vander Kooi 2007). The function of its GAG-binding- and predicted Nrp-binding-capacity remains to be elucidated. Signal transduction mediated via Nrp-1 cannot be excluded.

This model of a linked VEGR-1/integrin- mediated signal transduction may be adaptive for other cellular responses triggered by PlGF-2, such as tubulogenesis. Induced by differential GAG-binding, VEGFR-1/Nrp-1 clustering upon PlGF-2 binding might result in a change in SH-2-domain adapter-protein activation such as Grb-2 or Nck (see Figure 5). In collaboration with activated integrins, this might promote an altered FAK phosphorylation pattern and a varied cellular response.

4 Methods

4.1 Material

4.1.1 Equipment

Bacterial shaker (Ceromat R)	Braun, Melsungen, Germany
Cell Inkubator (HERAcell 150i)	Thermo Fisher Scientific Inc., Waltham, USA
Centrifuges:	
Eppendorf 5424	Eppendorf, Hamburg, Germany
Eppendorf 5415R	Eppendorf, Hamburg, Germany
Cryostat (Cryocut 180)	Leica, Heidelberg, Germany
Cryostat (Microm HM 560)	Thermo Fisher Scientific Inc., Waltham, USA
DNA-gelelectrophoresis chamber	PEQLAB Biotechnologie, Erlangen, Germany
Film-developer (Curix60)	Agfa, Cologne, Germany
ELISA plate reader (Victor^3)	PerkinElmer, Waltham, MA, USA
Magnetic stirrer Ikamag	Janke & Kunkel, Staufen, Germany
Microscope:	
Light microscope (DM 4000B)	Leica Camera AG, Solms, Germany
Light microscope (Eclipse TS100)	Nikon, Melville, NY, USA
Fluorescense microscope Nicon (A1)	Nikon, Melville, NY, USA
PCR-Thermocycler (T-3000)	Biometra, Düsseldorf, Germany
Photometer (Biophotometer)	Eppendorf, Hamburg, Germany
Plate shaker (KS250basic)	Janke & Kunkel, Staufen, Germany
Power supply (Feather Volt 500)	Stratagene, Heidelberg, Germany
Razor	Wella, Darmstadt, Germany
Weighing machine (Adventurer)	OHAUS, USA
Special accuracy weighing machine (explorer)	OHAUS, USA
SDS-gel electrophoresis chamber (Xcell *SureLock*™ Mini-Cell & Blotting module)	Invitrogen Ltd., Paisley, UK
Thermomixer (compact)	Eppendorf, Hamburg, Germany
UV-visualizer (Eagle Eye)	Stratagene, Heidelberg, Germany
Vortex-mixer (Vortex genie 2)	Scientific Industries, USA
Water bath	Julabo, Seelbach, Germany
Work bench (Safe 2000)	Thermo Fisher Scientific Inc., Waltham, MA USA

4.1.2 Cell culture material, media and supplements

Materials for cell culture were supplied from Greiner (Solingen) und Renner (Dannstadt)

Penicillin/Streptomycin	Biochrom, Berlin, Germany
DMEM (Dulbecco´s modified Eagle´s Medium)	Gibco, Eggenstein, Germany
EGM-2 (Endothelial cell growth medium +supplements)	Lonza, Basel, Switzerland
Ham`s F12	PAA Laboratories, Austria
Ham`s F12/DMEM GlutaMAX	Invitrogen Ltd., Paisley, UK
PBS (phosphate buffered saline w/o Ca^{2+})	PAA Laboratories, Austria
FCS (Fetal calf serum)	PAA Laboratories, Austria
L-Glutamin	Biochrom, Berlin, Germany
Trypsin	Gibco, Eggenstein, Germany
Methyl cellulose	Sigma-Aldrich, USA
Collagen type I (rat tail)	BD Biosciences, Heidelberg, Germany
Fibronectin (human)	BD Biosciences, Heidelberg, Germany
PVDF membranes (8 µm pore size)	Millipore Corporation, Billerica, USA
Puromycin	Invitrogen Ltd., Paisley, UK

Escherichia coli-Culture:

Agar	Life Technologies, Eggenstein, Germany
Ampicillin	Sigma-Aldrich, USA
Hefeextrakt	Life Technologies, Eggenstein, Germany
Pepton	Life Technologies, Eggenstein, Germany

4.1.3 Chemicals, proteins and enzymes

All chemicals had analytical grade and were supplied from Sigma-Aldrich (USA), Roth (Karlsruhe), Merck (Darmstadt), Riedel de Haen (Seelze) or Life Technologies (Eggenstein). Other materials, chemicals and systems were supplied from:

SDS-electrophoresis und protein detektion:

BCA Protein Assay Reagent Kit	Pierce Protein Research Products, Thermo Scientific
Bromphenolblue	Merck, Darmstadt, Germany
Western Lightning Chemiluminsecence Reagent	Perkin Elmer, USA

Molecularweight-standards:	
SeeBlue Plus2 pre-stained	Invitrogen Ltd., Paisley, UK
Page Ruler pre-stained	Fermentas GmbH, St. Leon-Rot, Germany
Tween 20	Merck, Darmstadt, Germany
QuantikinePlGF-Elisa	R & D Systems, Wiesbaden, Germany
SilverQuest silver-staining Kit	Invitrogen Ltd., Paisley, UK
Membranes and films:	
Hybond C Extra	Amersham, Braunschweig, Germany
Immobilon-p (PVDF)	Millipore Corporation, Billerica, USA
Hyperfilm ECL	Amersham, Braunschweig, Germany
Nucleic-acid isolation and Purification	
Quiaex II (Gelextraction Kit)	Qiagen, Hilden, Germany
Qiaprep Spin Miniprep Kit	Qiagen, Hilden, Germany
Qiaprep Plasmid Midiprep Kit	Qiagen, Hilden, Germany
PCR-purification kit	Qiagen, Hilden, Germany
peqGOLD 50 bp DNA ladder	Peq lab, Erlangen, Germany
peqGOLD 1 kb DNA ladder	Peq lab, Erlangen, Germany
Proteinase K	Peq lab, Erlangen, Germany
Immunohistochemistry:	
Haematoxylin	Thermo Shandon, USA
Polysine glas slides	Menzel Gläser, Braunschweig, Germany
Proteinpurification:	
Strep-Tactin Superflow sepharose	IGA BioTAGnology, USA
Ni-NTA fastflow	GE Healthcare, Fairfield, CT, USA
Gelatine sepharose	GE Healthcare, Fairfield, CT, USA
Dialysis tubes	GE Healthcare, Fairfield, CT, USA
FuGene HD transfection reagent	Roche, F. Hoffmann-La Roche Ltd, Basel, Switzerland
Streptavidin-Agarose	Novagen/Merck KGaA, Darmstadt, Germany
Proteins, enzymes and GAGs:	
Recombinant human PlGF-1 and PlGF-2	Reliatech, Braunschweig, Germany
Plasmin (human plasma)	Merk, Darmstadt, Germany
α2-antiplasmin (human plasma)	Sigma-Aldrich, USA

recombinant human VEGF-A_{165}	Reliatech, Braunschweig, Germany
recombinant human Nrp-1	R & D Systems, Wiesbaden, Germany
Heparin	Sigma-Aldrich, USA
Heparan sulphate	Celsius, Ohio, USA
Chondroitin sulphate	Sigma-Aldrich, USA
PAK-CRIB-peptid	Kindly provided by Prof. C. Niessen
Taq-DNA-polymerase	Bio-budget Technologies, Krefeld, Germany
Nhe I	Fermentas GmbH, St. Leon-Rot, Germany
Bam HI	Fermentas GmbH, St. Leon-Rot, Germany
Calf intestine alkaline phosphatase	Fermentas GmbH, St. Leon-Rot, Germany
T4-ligase	Fermentas GmbH, St. Leon-Rot, Germany
PMSF	Sigma-Aldrich, USA
Mammalian protease inhibitor cocktail	Sigma-Aldrich, USA
PhosStop phosphatase inhibitor cocktail	Roche, F. Hoffmann-La Roche Ltd, Basel, Switzerland

Other systems and chemicals

Agarose	Life Technologies, Eggenstein, Germany
QuickChange II XL Side-directed mutagenesis Kit	Stratagene, Heidelberg, Germany
Quickdiff staining kit	DADE Behring, USA
Synthetic olignonucleotides	MWG-Biotech, Ebersberg, Germany
TOPO TA Cloning Kit	Invitrogen Ltd., Paisley, UK

Chemicals used for mouse experiments

Keatnest S (25mg/ml)	Park Davies, USA
Rompun 2%	Bayer, Leverkusen, Germany
Bepanthen Roche	Roche, Eppstein, Germany
Biopsy punches (5-8 mm)	Stiefel, Offenbach, Germany

Dokumentation of mouse-experiments:

Dental Eye mit Diafilm von Kodak	Olympus, Japan
Sony Digicam DSC-707	Sony, Japan

4.1.4 Antibodies

Primary antibodies

Name	Source	Company	Dilution
Western blot			
hPlGF (reducing, AA1-20)	rabbit (polyclonal)	Reliatech, Braunschweig	1:150
hPlGF (non-reducing)	rabbit (polyclonal)	Reliatech, Braunschweig	1:150
total hFlt-1 (clone BK302, AA1251-1338)	mouse (monoclonal)	Upstate technologies	1:1000
p-hFlt-1 (Tyr1213)	rabbit (polyclonal)	Upstate technologies	1:1000
p-FAK (Tyr 676/577)	rabbit (polyclonal)	Cell signalling technology	1:1000
total PI3K (p85)	rabbit (polycolnal)	Cell signalling technology	1:1000
p-PI3K (p55 Tyr 199/p85 Tyr 458)	rabbit (polyclonal)	Cell signalling technology	1:1000
p-Src family (Tyr 416)	rabbit (monoclonal)	Cell signalling technology	1:1000
p-P130Cas (Tyr 165)	rabbit (polyclonal)	Cell signalling technology	1:1000
total AKT	rabbit (polyclonal)	Cell signalling technology	1:1000
p-Akt (Ser473)	rabbit (polyclonal)	Cell signalling technology	1:1000
total Erk1/2	rabbit (polyclonal)	Cell signalling technology	1:1000
p-Erk1/2 (Thr202/Tyr204)	rabbit (monoclonal)	Cell signalling technology	1:1000
β-actin	mouse (monoclonal)	Santa Cruz biotechnology	1:1000
total hRac1 (Klon 23A8)	mouse (monoclonal)	Sigma-Aldrich, USA	1:500
hNrp1 (A12)	mouse (monoclonal)	Santa Cruz biotechnology	1:1000
Immunohistochemnistry			
CD31/PCAM-1	Rat (monoclonal)	BD Biosciences, Heidelberg, Germany	1:1000
desmin	Mouse (moncolnal)	Dako, Glostrup, Denmark	1:1000

Secondary antibodies

Name	Source	Company	Dilution
Western blot			
swine-α-rabbit HRP	swine (polyclonal)	Dako, Glostrup, Denmark	1:1000
rabbit-α-mouse HRP	rabbit (polyclonal)	Dako, Glostrup, Denmark	1:1000
Immunohistochemistry			
goat-α-rat Alexa594	goat (polyclonal)	Invitrogen Ltd, Paisley, UK	1:500
goat-α-mouse Alexa488	Goat (polyclonal)	Invitrogen Ltd, Paisley, UK	1:500

4.1.5 Vector maps

4.1.5.1 pCEP

D722

5` A GCT CGT TTA GTG AAC CGT CAG ATC TCT AGA AGC TGG GTA CCT TAA GGC GCC AGC
3` TGA TCA AGC TTC TGC CTG CCG CCT GCC TGC CTG CCA CTG AGG GTT CCC AGC ACC

BM 40 signal sequence

ATG AGG GCC TGG ATC TTC TTT CTC CTT TGC CTG GCC GGG AGG GCT CTG GCA GCC
TAC TCC CGG ACC TAG AAG AAA GAG GAA ACG GAC CGG CCC TCC CGA GAC CGT CGG

8xHIS-tag

CCG CTA GAG GGC AGC GGC CAT CAC CAT CAC CAC CAT CAT CAT AGC AGC GGC CTG
GGC GAT CTC CCG TCG CCG GTA GTG GTA GTG GTG GTA GTA GTA TCG TCG CCG GAC

Nhe I

replaced by PCR-insert

GTG CCG CGC GGC AGC GCT AGC ATG GCG CGC CCG TAC GCC GAC GCG GCC GCT CGA
CAC GGC GCG CCG TCG CGA TCG TAC CGC GCG GGC ATG CGG CTG CGC CGG CGA GCT

Bam HI

Strep-tag

GGC CGG CAA GGC CGG ATC CAT CGA AGG GCG CAG CGC TTG GAG CCA CCC TCA GTT
CCG GCC GTT CCG GCC TAG GTA GCT TCC CGC GTC GCG AAC CTC GGT GGG AGT CAA

Strep-tag

CGA GAA AGG TGG AGG TTC CGG AGG TGG ATC TGG AGG TGG TTC ATG GAG CCA CCC
GCT CTT TCC ACC TCC AAG GCC TCC ACC TAG ACC TCC ACC AAG TAC CTC GGT GGG

*

ACA GTT CGA AAA ATA A 3`
TGT CAA GCT TTT TAT T 5`

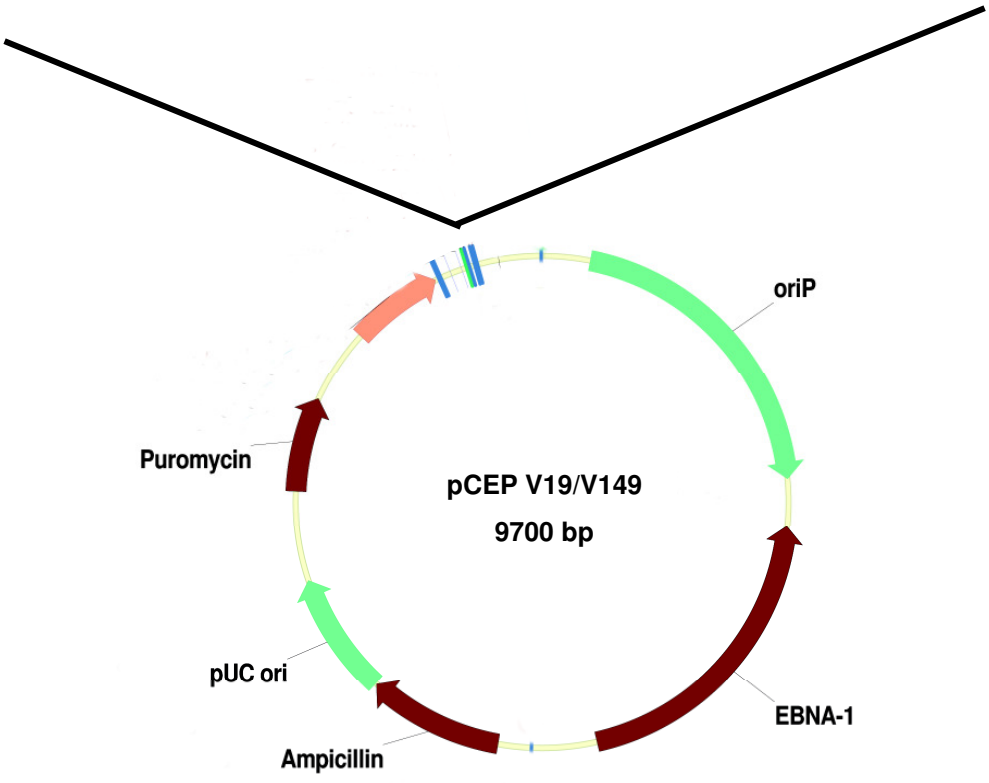

The empty vectors pCEP V19 and pCEP V149 were generated and kindly provided by Manuel Koch (Medical faculty, Institute of Biochemistry II, University of Cologne)

4.1.5.2 pCR II TOPO

M13 reverse primer — Sp6 Promoter

```
5` CAG GAA ACA GCT ATG ACC ATG ATT ACG CCA AGC TAT TTA GGT GAC ACT ATA GAA
3` GTC CTT TGT CGA TAC TGG TAC TAA TGC GGT TCG ATA AAT CCA CTG TGA TAT CTT
```

Nsi I *Hin*d III *Kpn* I *Sac* I *Bam*H I *Spe* I

```
TAC TCA AGC TAT GCA TCA AGC TTG GTA CCG AGC TCG GAT CCA CTA GTA ACG GCC
ATG AGT TCG ATA CGT AGT TCG AAC CAT GGC TCG AGC CTA GGT GAT CAT TGC CGG
```

*Bst*X I *Eco*R I *Eco*R I *Eco*R V

```
GCC AGT GTG CTG GAA TTC GCC CTT  PCR-  AAG GGC GAA TTC TGC AGA TAT
CGG TCA CAC GAC CTT AAG CGG GAA  product  TTC CCG CTT AAG ACG TCT ATA
```

*Bst*X I *Not* I *Xho* I *Nsi* I *Xba* I *Apa* I

```
CCA TCA CAC TGG CGG CCG CTC GAG CAT GCA TCT AGA GGG CCC AAT TCG CCC TAT
GGT AGT GTG ACC GCC GGC GAG CTC GTA CGT AGA TCT CCC GGG TTA AGC GGG ATA
```

T7 Promoter — M13 (-20) Forward Primer

```
AGT GAG TCG TAT TAC AAT TCA CTG GCC GTC GTT TTA CAA CGT CGT GAC TGG GAA 3`
TCA CTC AGC ATA ATG TTA AGT GAC CGG CAG CAA AAT GTT GCA GCA CTG ACC CTT 5`
```

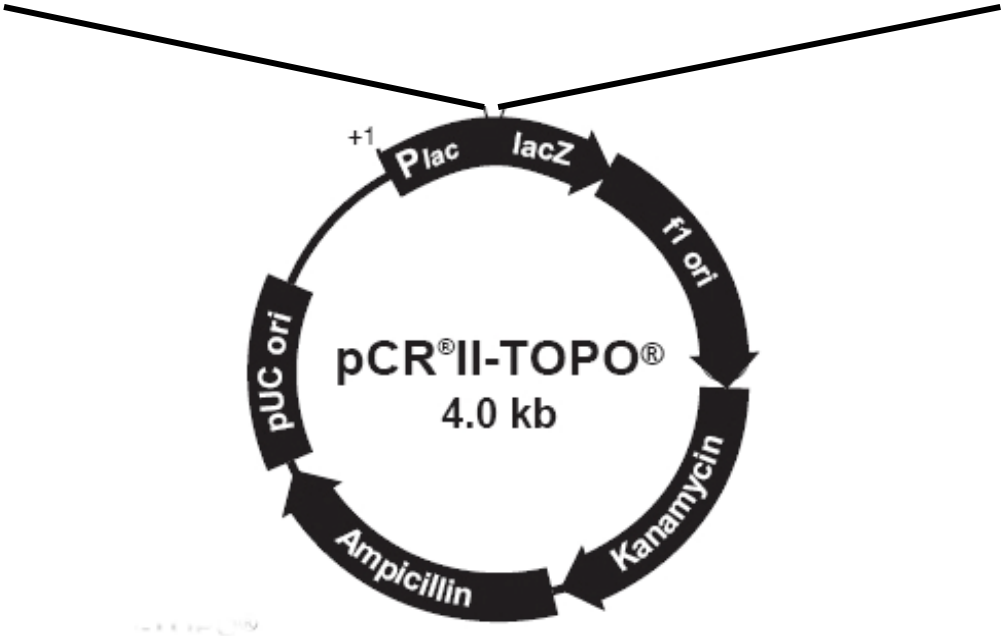

4.1.6 Oligonucletides

name	sequence
PlGF fw	5`GCAGCTAGCGCAGACGGGAGGCTGCCTGCTGTGCCCCCCCAGCAG
PlGF-2 rev	5´CAGGGATCCCCTCCGGGGAACAGCATCGCCGCACAGGTG
PlGF-1 rev	5´CAGGGATCCCCTCCGGGGAACAGCATCGCC
PlGFStop rev	5`TGCGGATCCCTACTACTTCTCCCGCAGAGGCCGGCATTCG
PlGFmutPro fw	5`TGCCGGCCTCTGCGGGAGCCTATGAAGCCGGAAAGG
PlGFmutPro rev	5`CCTTTCCGGCTTCATCGGCTCCCGCAGAGGCCGGCA
PlGFmutAla fw	5`TGCCGGCCTCTGCGGGAGGCGATGAAGCCGGAAAGG
PlGFmutAla rev	5`CCTTTCCGGCTTCATCGCCTCCCGCAGAGGCCGGCA
D722	5`AGCTCGTTTAGTGAACCGTCAG
M13(-20) fw	5`GTAAAACGACGGCCAG
M13 rev	5` CAGTATCGACAAAGGAC

4.2 Cell culture and media

4.2.1 Bacterial cell culture

Cultivation of *E.coli* was performed under selective conditions. For selection of recombinant bacteria, the LB-broth was supplemented with ampicillin at a final concentration of 0.1 mg/mL. For preparation of agar plates 1.5% Agar-Agar was added to the medium. Liquid cultures of bacteria were incubated in LB-medium supplemented with ampicillin and grown overnight at 37°C, shaking. Bacteria grown on agar plates were incubated at 37°C for 16-18 hours. Clones on agar plates were stored 4°C for short periods.

4.2.1.1 Competent bacteria

To transform *E.coli,* bacteria were induced to be competent for DNA-uptake by $CaCl_2$ (Cohen *et al*., 1972). 2 mL of bacteria suspension of an overnight culture were cultured in 100 mL LB-medium resulting in an OD_{600} of 0.03-0.04, grown at 37°C on an orbital shaker (300 rmp) to reach an OD_{600} of 0.3-0.4, and then incubated on ice for 15 minutes. Cells were harvested by centrifugation (5 minutes at 3000g, 4°C), and the cell pellet was resuspended in 30 mL RF I solution, incubated on ice for 15-30 minutes and collected by centrifugation. The cell pellet was then resuspended in 8 mL cold RF II and for 15 minutes incubated on ice. Cells were aliquoted and snap-frozen in liquid nitrogen, and stored at -80°C.

***RF I**: 100mM RbCL, 50 mM $MnCl_2$, 30 mM KAC, 10 mM $CaCl_2$, 15% Glycerine*

***RF II**: 10 mM MOPS, 10 mM RbCl, 75 mM $CaCl_2$, 15% Glycerine*

4.2.1.2 Preparation of Escherichia coli frozen stocks

For long-term storage of recombinant *E.coli* clones, 1 mL of the bacteria culture was harvested by centrifugation, the supernatant was discarded and the pellet was resuspended in 2xpYT containing 50% Glycine (w/v). The stocks were stored at -80°C.

4.2.1.3 Escherichia coli strains

***E. coli* strain**	**Genotype**
DH5α	F- φ80lacZΔM15 Δ(lacZYA-argF) U169 recA1 endA1 hsdR17 (rk-, mk+) galphoA supE44 λ- thi-1 gyrA96 relA1
XL10-Gold®	TetR Δ(*mcrA*)*183* Δ(*mcrCB-hsdSMR-mrr*)*173 endA1 supE44 thi-1 recA1 gyrA96 relA1 lac* Hte [F´ *proAB lacI*q*ZΔM15* Tn*10* (TetR) Amy CamR]*a*

4.2.1.4 Media

LB (Luria Broth) medium and agar: *1% peptone, 0.5% yeast extract, 1% NaCl, (optional 1.5% select agar*

SOC medium: *0.5% yeast extract, 2% peptone, 10mM NaCl, 2.5 mM KCl, 10 mM $MgCl_2$, 10 mM $MgSO_4$, 20 mM glucose*

2x YT medium: *1.6% tryptone, 1% yeast extract, 0,5% NaCl*

Antibiotics: *Ampicillin (0.1 mg/mL)*

4.2.2 Eukaryotic cell culture

All work with eukaryotic cells was performed under sterile conditions and all used solutions were autoclaved or sterile filtered prior to use, to avoid bacterial contamination. All media or solutions were brought to room temperature or 37°C before use. Cells were cultured at 37°C, 5% CO_2 and 60% humidity.

4.2.2.1 Cultivation of Human Umbilical Vein Endothelial cells (HUVE-cells)

Primary human endothelial cells isolated from the umbilical vein are a pooled batch from three different donors (Lonza). Cells were cultured in EGM-2 medium (supplemented with 2% fetal calf serum (FCS), several growth factors, 1% glutamine, and 100 U/mL Penicillin/Streptomycin) in 10 cm cell culture treated culture dishes.

HUVE cells were detached with 0.1% (w/v) Trypsin/0.002% (w/v) EDTA at 70-90% confluency and splitted in an adequate manner. To minimize the rate of differentiated cells, all experiments were performed using cells below passage 5. Experimental cells were starved 12 hours before starting the experiment. Starvation medium was EGM-2 medium supplemented with 1% FCS without supplemental growth factors.

4.2.2.2 Cultivation of Porcine Aortic Endothelial (PAE) cells

PAE cells are immortalized endothelial cells, originally isolated from porcine aorta. Besides wild-type cells, stably transfected PAE cells with human Nrp-1 (PAE/Nrp) were used. These cells were cultured in Ham`s F12 medium supplemented with 10% FCS, 1% glutamine and 100 U/mL Penicillin/Streptomycin in 10 cm cell culture treated dishes. A 70-90% confluency, cells were splitted 1:4. Experimental cells were starved 12 hours before starting the experiment using serum-free Ham`s F12.
PAE and PAE/Nrp-1 cells were kindly provided by Prof Dr. Michael Klagsbrun, Boston.

4.2.2.3 Cultivation HEK293 Ebna cells

HEK293 *Ebna* is an immortalized cell line originally derived from human embryonic kidney cells. These cells additionally carry the *Ebna* gene, that allows an increased transient expression rate when transfected with an adequate expression vector.
Untransfected cells were cultivated in standard medium (DMEM supplemented with 10% FCS, 1% glutamine and 100 U/mL Penicillin/Streptomycin) at 37°C in 75 cm^2 cell culture treated flasks. The cells were transfected using FuGene HD to express recombinant protein. Transfected cells were cultured in GlutaMAX™ in cell culture flasks coated with 30 µg/mL collagen I during collection of supernatant to promote an efficient adhesion of the cells. Depending on the method of protein purification, the medium was supplemented with FCS (strep-tag) or cells were cultured serum-free (his-tag) under serum-free conditions. For the selection of positive clones, the antibiotic puromycin was added to the medium.
HEK293 *Ebna* cells were kindly provided by Prof. Dr. Manuel Koch (Institute for Biochemistry, University of Cologne).

4.2.2.4 Mycoplasma test

To detect mycoplasma, in a regular time lag a mycoplasma test was performed at regular intervals. For detection, several thousand cells were cultured for 2 days in chamber slides, washed, and fixed for 20 minutes at room temperature (methanol/glacial acetic acid 3:1). For staining, cells were incubated in DAPI-solution (1 µg/mL) at room temperature for 15 minutes. In case of contamination with Mycoplasma, cells show – beside their own fluorescent nucleus – fluorescent “dots” within the cytoplasm.

4.2.3 Cell culture based assays

4.2.3.1 Chemotactic activity in the Boyden chamber assay

A modified Boyden chamber assay was used to analyse the chemotactic potency of a certain molecule or protein.

Two chambers divided by a porous membrane (Nucleopore, 8 µm pore size) were filled with a potentially chemoattractant molecule on the one side of the membrane, and cells are seeded on the other side. By this setup a gradient is created, that might induce directed migration (chemotaxis) of the cells through the membrane towards the maximum of concentration.

To create optimal conditions for migration, the membrane was coated with collagen I (BD, rat tail, 30 µg/mL) at 4°C overnight. For each condition, 200 µl of starvation medium supplemented with or without different PlGF-forms (100 ng/mL) were filled into the lower chamber and sealed with the coated membrane by assembling of the Boyden chamber. Complete-medium was used as positive control. $2.5x10^5$ starved cells were seeded in starvation medium into the upper chamber and incubated for 4.5 hours at 37°C.

After incubation, the membranes were collected and cells on the upper side were removed to exclude cells that had not migrated through the pores by directed migration. Afterwards, the membrane was stained with a variant of Romanowski staining (Quickdiff, DADE Behring) and analysed by light-microscopy. For this, 10 randomly chosen pictures at 10x-magnification were taken and cells were counted using ImageJ. All experiments were performed under identical conditions and at least in triplicates. Statistical analyses were performed with help of GraphPadPrism5 software.

4.2.3.2 3D-spheroid-sprouting assay

To analyse the competence of a growth factor to induce endothelial sprouting, spheroid were pre-formed and embedded into collagen I gels. For spheroid formation, HUVE cells were detached, counted, and seeded in 100 µL 20% methylcellulose/80% growth medium into a 96-roundbottom plate (NUNC, untreated plate). After 24 hours of incubation at 37°C, spheroids were harvested and 50 spheroids/gel were seeded into 500 µL of a non-polymerized collagen I gel (2 mg/mL) in 24-well plates. After polymerization, 100 µL rhPlGF in starvation medium was pipetted onto the gel at a final concentration of 40 ng/mL. rhVEGF-A_{165} with a final concentration of 5 ng/mL served as positive control. After 24 hours incubation at 37°C, 10 randomly chosen spheroids were analysed for each condition at 20-fold magnification using a Nikon bright field microscope. Cumulative sprouting length and number of sprouts/spheroid was measured using ImageJ. Statistical analysis was performed using GraphPadPrism5.

4.2.3.3 Sample preparation for analysis of cell signalling by western blotting

Cells were seeded in appropriate number into cell-culture dishes and grown to 70% confluency in adequate supplemented medium under optimal cell culture conditions. In case of matrix-based experiments, plates were coated with either collagen type I (rat tail) or human fibronectin (10 µg/mL each) for 3 hours at 37°C. Afterwards, cells were starved overnight in serum- and supplement-free medium (0.5% FCS for HUVE cells). Cells were washed with PBS and stimulated with 100 ng/mL rhPlGF-variants at 37°C, for times as indicated. Unsupplemented medium served as a negative control. Cells were lysed in RIPA-buffer supplemented with various protease inhibitors and phosphatase inhibitors, and the lysate was incubated with shaking for 1 hour at 4°C. The sample was pre-cleared by centrifugation at maximum speed for 10 minutes at 4°C, and concentration was determined by BCA-assay to ensure equal loading on SDS-gel.

RIPA buffer: *50 mM Tris/HCl (pH 7.4), 1% NP-40, 0.25% Na-deoxycholate, 150 mM NaCl, 1 mM EDTA, 1 mM PMSF, 1µg/mL Aprotinin, 1µg/mL Leupeptin , 1µg/mL Pepstatin, 1 mM Na3VO4, 1 mM NaF, 1 tablet PhosphoStop/10 mL RIPA-buffer*

4.2.3.4 Rac-1 pull-down

The Rac-1 pull-down-assay was performed, to determine the amount of activated, GTP-bound Rac-1. All used solutions used were cooled down on ice. Starved PAE/Nrp-1 were stimulated as described above, washed in PBS, and lysed in 700 µL Rac-1-lysis-buffer. After constant rotation at 4°C for 45 minutes, supernatant was pre-cleared by centrifugation at 4°C, 50 µL supernatant was taken for analysis of total-Rac-1 and 30 µL streptavidin-coupled agarose beats were added to the remaining sample. The sample was incubated for additional 45 minutes at 4°C under rotation, to allow interaction between the biotin-motif and streptavidin-beats. The beats were collected by centrifugation and washed with 1 mL Rac-1-lysis-buffer three times. After evolvement of all liquid, agarose-beats were resuspended with 20 µL sample-buffer and heated at 95°C for 10 minutes. By determination of the protein content in the corresponding total-Rac-1 sample by BCA-assay, the volume of the pull-down samples were normalized and subjected to SDS-PAGE and western blotting.

Rac-1-lysis buffer: *50mM Tris-HCl, pH 7,4; 100mM NaCl; 10mM MgCl2, 1% NP-40, PMSF (1:100), Mammalian protease inhibitor cocktail (100); prior to cell lysis, 2 µL PAK-CRIB-peptide for each sample was added to the lysis buffer*

4.3 Molecular biological methods

4.3.1 Polymerase-chain-reaction (PCR)

The polymerase-chain reaction is a method to amplify specific DNA sequences selectively, that are restricted by binding of two primers to a DNA-matrix (Mullis 1987). Primers have to hybridize to one of the strand in 5`-3` direction and flank the sequence of interest. During this work, PCR was used to amplify PlGF cDNA from placental total RNA (kindly provided by Prof. Dr. Manuel Koch). As resulting PCR products were used for cloning, primers for the different PlGF forms included a sequence with restriction sites for the restriction enzymes Nhe I and Bam HI. Additionally, the forward primer includes a sequence that allows a proteolytic cleavage of the N-terminal his-tag after protein expression by FactorXa.

Reaction:

ddH_2O	39.5 µL
dNTP (10 mM)	1 µL
Taq buffer (10x)	5 µL
forward primer (10 µM)	1 µL
backward primer (10 µM)	1 µL
cDNA	1 µL
Taq-polymerase (1 U/µL)	0.5 µL

Reaction was incubated in a thermo block using the following conditions:

PCR-program:

Initial denaturation	94°C	2 min	
denaturation	94°C	30 s	35 cycles
annealing	65°C	30 s	
elongation	72°C	1.5 min	
final elongation	72°C	5 min	

PlGF primers:

PlGF forward (common to all PlGF forms)

5` GCA GCT AGC GCA GAC GGG AGG CTG CCT GCT GTG CCC CCC CAG CAG 3`

NheI FaktorXa

PlGF reverse

PlGF-1

5´CAG GGA TCC CCT CCG GGG AAC AGC ATC GCC 3´

BamHI

PlGF-2

5´CAG GGA TCC CCT CCG GGG AAC AGC ATC GCC GCA CAG GTG 3´

BamHI

PlGFStop

5`TGC GGA TCC CTA CTA CTT CTC CCG CAG AGG CCG GCA TTC G 3`

BamHI 2xstop

4.3.2 Quantification of nucleic acid

DNA has an absorption maximum at 260 nm, and it is possible to calculate the concentration of nucleic acid by measurement of the absorption in a UV-spectral photometer. An absorption of 1 at 260 nm reflects a concentration of 50 µg/mL double strand DNA. As proteins have their absorptions maximum at 280 nm, the quotient $absorption_{260}/absorption_{280}$ can be used to assess the purity of the DNA-sample. The purity of a DNA-sample should have a value between 1.8 and 2.0. As a test for quality, several dilutions of the sample were separated on an agarose-gel, and where visualized and analysed by UV-light.

4.3.3 Gelelectrophoresis of nucleic acids

To dissolve and/or purify isolated DNA, a native, horizontal gel electrophoresis was performed using 1-2% agarose gels. TE buffer was used as gel- and running buffer. The agarose was boiled in TE buffer, supplemented with 1 µg/mL ethidium bromide, and filled into the electrophoresis chamber. After polymerization, the gel was covered with running buffer, and samples diluted in 5x Bromphenolblue sample buffer-solution at a final concentration of 0.001% and loaded into the gel pockets. Electrophoresis was performed at 100 V and resulting DNA-bands were visualized by UV-light.

TE-buffer: *10mM Tris (pH8 with HCl), 1mM EDTA*

5x Bromphenolblue (0.001%): *30% Glycerine in 50 mM EDTA*

4.3.4 Gel extraction of nucleic acids

To purify specific DNA-bands out of a DNA solution, the sample was separated on an agarose-gel, the DNA-band was cut out of the gel and the gel-slice was purified using the QIAEX II Gel Extraction Kit (Qiagen, Hilden) following the manufacturer's instructions. This method is required after restriction of a PCR-product or a vector for following cloning, to remove cleaved nucleotides or DNA-fragments.

4.3.5 Cloning of DNA-fragments

Cloning of DNA-fragments into bacterial vectors provides one of the most essential tools in biology. It allows the expression of foreign or artificial proteins in bacterial or eukaryotic cells and therefore is either used to produce and purify large amounts of the protein of interest or force cells to produce a protein and directly analyse its effect on cellular processes. During this work expression-vectors were produced carrying the sequence of human PlGF forms, to purify recombinant proteins from transfected HEK293 *Ebna* cells

4.3.5.1 Restriction of DNA-fragments

To selectively clone a DNA-fragment into a vector both – vector and DNA-fragments have to react with endonucleases (type II), which create specific complementary cohesive ends on the digested DNA. These restriction enzymes have specific recognition sites for restriction and produce “blunt” or “cohesive” ends. If vector and DNA-fragment are restricted in the same way, this allows a site directed ligation of the fragment into the vector (see 4.3.5.2). In this work, all fragments and vectors were restricted with Nhe I and Bam HI, which create cohesive ends.

Recognition sites:

Nhe I	Bam HI
5`GCT AGC3`	5`GGA TCC3`
3`CGA TCG5`	3`CCT AGG5`

The restriction sites were chosen, as insertion at this sites in the multiple cloning site of the vector are “in frame” and allows a correct protein expression of the vector sequence (signal peptide and tags) and fragment.

As both enzymes use the same buffer system, double digestion of the PCR-fragments and the expression vectors (pCEP V19 and pCEP V146; see 4.1.5.1) were performed:

Restriction reaction

DNA (PCR product or vector, approximately 5 µg)	10 µL
ddH_2O	34 µL
Tango buffer (10x)	5 µL
Bam HI (10U/µL)	2 µL
Nhe I (10U/µL)	2 µL

The reaction was incubated at 37°C for 6 hours followed by heating to 85°C for 20 minutes to heat-inactivate the restriction enzymes. The restricted vector-DNA was analysed on an agarose-gel.

4.3.5.2 Ligation of restricted DNA-fragments

After restriction, the vector-DNA was incubated with 1U of calf intestine alkaline phosphatase for 2 hours at 37°C. This phosphatase dephosphorylates 5`-ends of linearized vectors and is used to avoid spontaneous auto-ligation. The reaction was heat-inactivated at 85°C, and the sample was purified by gel extraction prior to ligation.
For the ligation of the PCR-fragment into the vector, a molar ratio of 1:3 of vector to insert was used. The amount of insert DNA was calculated by the formula:

$$(ng_{vector} \times kb_{insert}) / (kb_{vector} \times \text{molar ratio}_{vektor/insert}) = ng_{insert}$$

For standard ligation, 200 ng of vector-DNA were used.

Ligation reaction:

Vector DNA (200 ng)	x µL
calculated ng insert-DNA	x µL
T4-Ligase buffer, 10x	2 µL
T4-Ligase (5 U/µl)	2 µL
ddH2O	Up to 20 µL

The reaction was incubated at 16°C overnight and heat-inactivated for 20 min at 60°C.

4.3.5.3 Transformation of competent E.coli with vector-DNA and identification of recombinant clones

Heat-shock transformation was used to transform the competent *E.coli* strain DH5α. 5-10 µl ligation reaction were carefully mixed with 100 µL bacteria suspension and incubated for 20 minutes on ice. To induce a heat-shock, Cells were incubated at 42°C for 2 minutes and cooled down on ice. 900 µL pre-warmed LB-medium was added, and cell suspension was incubated for 1 hour at 37°C with shaking. Afterwards, transformed bacteria were plated on LB_{Amp}-plates and incubated overnight at 37°C for selection.
Only transformed bacteria are able to grow on LB_{Amp}-plates. Single colonies were picked from the plates and transferred to 2 mL liquid LB_{Amp}, grown overnight with shaking for the selection of positive clones (see 4.3.5.5).

4.3.5.4 TOPO TA cloning

For TOPO TA cloning a kit from Invitrogen was used. This system provides a high-efficient cloning strategy for direct insertion of a Taq-polymerase amplified PCR product. Taq polymerase adds a single deoxy-adenosine to the 3`end of PCR products, whereas the linearized provided vector (pCR®II-TOPO®) has a 3`thymidine overhang. The provided topoisomerase I is covalently bound to the vector and is therefore able to ligate the unrestricted PCR product directly into the vector. Cloning was performed by following the manufacturer's instructions. Identification of positive clones was performed as described above.

4.3.5.5 Isolation of Plasmid-DNA from E.coli

Plasmid preparations were performed to identify positive clones after bacterial transformation and to confirm a proper ligation of the insert the vector. Low scale plasmid preparations were performed using the Plasmid mini prep Kit, for large scale preparations the Plasmid midi prep kit was used (Qiagen, Hilden, Germany) following the manufacturer's instructions.

4.3.6 Site-directed mutagenesis

To produce rhPlGF-variants with a mutated the plasmin cleavage site, the QuickChange®II XL Site-Directed Mutagenesis Kit (Stratagene) was used. To facilitate the cloning procedure, pCR®II-TOPO® carrying the PlGF-2 sequence were used for mutagenesis. The principle of this method is the use of a mutagenic primer directed replication of both plasmid strands and therefore results in the insertion or deletion of a mutation into the newly replicated plasmid. To eliminate parental DNA, the product was treated with the endonuclease Dpn I. Mutated, complementary primers were generated by flanking the desired mutation with at least 15 correct bases at each site.

Original PlGF-2

5` TGC GAA TGC CGG CCT CTG CGG GAG AAG ATG AAG CCG GAA AGG AGG 3`

C E C R P L R E K M K P E R R

PlGF-2 mutPro

5` TGC GAA TGC CGG CCT CTG CGG GAG CCG ATG AAG CCG GAA AGG AGG 3`

C E C R P L R E P M K P E R R

PlGF-2 mutPro forward

5` TGC CGG CCT CTG CGG GAG CCG ATG AAG CCG GAA AGG 3`

PlGF-2 mutPro reverse

5` CCT TTC CGG CTT CAT CGG CTC CCG CAG AGG CCG GCA 3`

PlGF-2 mutAla

5` TGC GAA TGC CGG CCT CTG CGG GAG GCG ATG AAG CCG GAA AGG AGA 3`

C E C R P L R E A M K P E R R

PlGF-2 mutAla forward

5` TGC CGG CCT CTG CGG GAG GCG ATG AAG CCG GAA AGG 3`

PlGF-2 mutAla reverse

5` CCT TTC CGG CTT CAT CGC CTC CCG CAG AGG CCG GCA 3`

The resulting mutated Plasmids were transformed into XL10-gold (high efficiency). All preparations followed the manufacturer's instructions.

4.3.7 DNA sequencing

To ensure correct ligation of the PCR-insert into the vector in accordance with the vector`s reading frame, and to exclude nucleotide exchanges, plasmids isolated from positive clones where sequenced in a service laboratory. For sequencing, either the PlGF specific reverse primer (see 4.3.1) or the vector specific forward primer D722 (pCEP4 V143 and pCEP4V19) was used. Analysis of ligation into pCR®II-TOPO® and site directed mutagenesis was performed by the use of standard M13 primers. The obtained sequence was analysed by alignment with the expected DNA sequence using ChromasLite and VectorNTI software.

pCEP forward primer D722:

5` AGC TCG TTT AGT GAA CCG TCA G 3`

4.4 Biochemical methods

4.4.1 Colorimetric quantification of total protein

To quantify the total protein concentration in a solution, the BCA (bicinchroninic acid) assay from Pierce® was used. It was mainly used to determine the protein concentration in cell lysate to ensure equal loading prior gel electrophoresis and immuno-blotting. It combines the reduction of Cu^{2+} to Cu^{1+} by protein in alkaline medium with the colorimetric detection of the cuprous cation by bicinchroninic acid.
Procedure was performed according to the manufacturer`s manual, and protein concentration was determined using a BSA-standard-curve.

4.4.2 Quantification of PlGF by ELISA (Enzyme-linked immuno-sorbent assay)

To determine the concentrations of human PlGF forms in different solutions (human samples, cell culture supernatants, protein purifications) a Quantikine-sandwich ELISA System (R&D Systems, Wiesbaden, Germany), following the manufacturer's manual.

4.4.3 Sodiumdodecyl-sulphate-polyacrylamide-gelelectrophoresis (SDS-PAGE)

SDS-PAGE was performed following a modified protocol of Laemmli (1970). Samples were resolved in adequate amounts of LDS-sample buffer, which contained 20% β-mercapto-ethanol for reduced samples and heated for 10 minutes to 95°C. Thereafter, the samples were resolved on a 4-12% reducing Bis-Tris pre-cast SDS-PAGE gel (NuPAGE® Novex®, Invitrogen) and electrophoresis was performed at 200 V for around 45 minutes in the Xcell SureLock® Mini-Cell system. MES buffer was used as running buffer. Upon protein separation, the gels were either stained directly by coomassie- or silver-staining, or transferred to a PVDF-membrane to detect immuno-reactive products.

4x-LDS-sample buffer (pH 8.5): *100 mM Tris HCl, 140 mM Tris base, 2% LDS, 10% Glycerol, 0.5 mM EDTA, 0.2 mM SERVA Blue G250, 0,2 mM Phenol Red*

MES buffer (pH 7.3): *2.5 mM MES, 2.5 mM Tris base, 0.005% SDS, 0.005 mM EDTA*

4.4.4 Silver-staining

Silver staining of SDS-PAGE gels provides an easy and very sensitive method to detect low concentrations of proteins. This method was used to detect cleavage products of PlGF after plasmin digestion, as specific antibodies for the C-terminal part of PlGF are not available. The staining was performed following the manufacturer's instructions (SilverQuest, Invitrogen).

4.4.5 Coomassie-brilliant blue staining

Coomassie-brilliant-blue G-250 staining is another method to stain protein gels directly, with sensitivity of >0.3 µg. It was mainly used to test supernatants of HEK293 cells for protein expression and to verify the sample purity after recombinant protein purification. Gels were stained by 30-60 minutes of incubation in coomassie-brilliant-blue solution on an orbital shaker. Gels were washed briefly in H_2O and unspecific background was removed overnight in destaining solution. As this dye unspecifically binds to the basic side chains of amino acids, gel resolved protein bands retain the colour after destaining.

Coomassie staining solution: *0.01% Coomassie blue R-250, 50% MeOH, 5% acetic acid*
Destaining solution: *10% MeOH, 10% acetic acid*

4.4.6 Protein-transfer and immunodetection

To detect immuno-reactive products proteins were immobilized by western blot transfer to a PVDF membrane (Immobilon-P, Millipore) using a tank blot system (SureLock System and Tank blot module, Invitrogen). All components were soaked with transfer-buffer (Invitrogen) and arranged air bubble-free between the graphite plates of the blotting module in the following order:

cathode
2 transfer sponges
4 pieces of Whatman paper
SDS-PAGE-gel
PVDF-membrane
4 pieces of Whatman paper
2 transfer sponges
anode

The PVDF membrane was activated with methanol for 5 minutes, washed with water and incubated in transfer buffer for 5 minutes before use. The transfer was performed for 1.25 hours at 30 V. As test for successful transfer and equal loading of the samples, the

membrane was stained with PonceauS.

To detect immuno-reactive products by binding of specific antibodies, the membrane was incubated in 5% dry milk in tris-buffered-saline, supplemented with Tween20 (TBS-T) for 45 minutes to block unspecific binding sites, followed by incubation with the primary antibody for either 1.5 hours at room temperature or overnight at 4°C. After washing the membrane with TBS-T, the membrane was incubated with a HRP conjugated secondary antibody and washed again. Detection was performed using the enhanced chemiluminescence western blot detection system (Amersham Bioscience Europe GmbH), following the manufacturer's manual. Chemiluminescence was detected by exposing the membrane to an x-ray film.

Transfer buffer (pH 7,2): *25 mM Bicine, 25 mM Bis-Tris (base free), 1 mM EDTA*

Tris-buffered saline (TBS) (pH 7.6): *0.5M Tris base, 1.5 M NaCl (optional for TBS-T: 0.05%Tween-20)*

4.4.7 Generation of recombinant PlGF-proteins

4.4.7.1 Transfection of HEK293 cells

Transfection of the eukaryotic cell line HEK293 was performed using the transfection reagent FugeneHD (Roche), following the supplier`s recommendations.

For each transfection $1x10^6$ cells/well were seeded on a collagen I coated 6-well plate (Nunc) and incubated at 37°C until reaching a confluency of around 60-80%. 2 µg of the Plasmid-DNA to be transfected was incubated with varying volume of FugeneHD (3-10 µL) in 100 µL serum-free DMEM for 15 minutes at room temperature and pipetted to the cells. After 24 hours at 37°C, the cells were washed, and successfully transfected cells were selected in GlutaMAX™ by addition of puromycin (2 µg/mL). Positive clones were expanded in triple-flasks. Depending on the method of protein purification cells were incubated in medium with or without FCS. Supernatant was collected every second day for up to 2 weeks, filtered and stored at -80°C until purification.

4.4.7.2 Sample preparation for protein purification

Independently of the method of purification, PMSF (1 mM) was added to the thawed cell culture supernatants to avoid proteolytic degradation of the recombinant proteins at a final concentration of 25 mM. Prior to purification of his-tagged proteins, NaH_2PO_4 (pH 9.5) and Tween-20 with final concentrations of 12.5 mM and 0.005% respectively, were added to the supernatant to create an alkaline solution. Supernatant was filtered (Schleicher and Schuell) and subjected to gravity flow. To pre-clear the cell culture supernatant, a gelatine-sepharose (GE healthcare) column was used. For tag-specific

purification, either Ni-sepharose (his-tagged proteins) or Strep-tactin (for strep-tagged proteins) was used, as specified below. All purification steps are performed at 4°C. Sample preparation and protein purification were performed using a protocol, which was kindly provided by Prof. Dr. Manuel Koch.

4.4.7.3 Strep-Tactin®affinity chromatography protein purification

The Strep-tag purification is based on the highly selective binding of an engineered Streptavidin (Strep-Tactin; IBA-go), to Strep-tag II fusion protein under physiological conditions and was used to purify PlGF-1 and PlGF-2.

Before adding the cell supernatant to the Strep-Tactin columns (normally 2 mL Strep-Tactin matrix/2 L supernatant), the matrix was equilibrated with one column volume (CV) washing buffer by gravity flow. After the supernatant has entered the column (4°C), it was washed 5 times with 1 CV. Bound strep-tag fusion protein was eluted in 6 steps using 0.5 CV elution buffer. Protein content and purity was visualized by Coomassie staining. Positive fraction were pooled and dialysed against 5 L PBS overnight at 4°C.

For regeneration of the matrix, 3 times 5 CV regeneration buffer was subjected to the column followed by two washing steps with 4 CV of washing buffer. The resign was overlaid with 2 mL washing buffer and stored at 4°C.

Washing buffer: *100 mM Tris-HCl pH8, 150 mM NaCl, 1 mM EDTA*

Elution buffer: *100 mM Tris-HCl pH8, 150 mM NaCl, 1 mM EDTA, 2.5 mM desthiobiotin*

Regeneration buffer: *100 mM Tris-HCl pH8, 150 mM NaCl, 1 mM EDTA, 1mM HABA*

4.4.7.4 Immobilized metal ion affinity chromatography

Immobilized metal ion affinity chromatography (IMAC) exploits the interaction between chelated transition metal ions and side-chains of certain amino acids, mainly histidine, on proteins. In general, Ni^{2+} is the preferred metal ion for purification of his-tagged proteins. Ni-Sepharose 6 Fast Flow (Amersham Pharmacia Biotech) was used for purification.

After loading of the Ni-Sepharose 6 Fast Flow onto the column (2 mL matrix/2 L supernatant), it was washed and equilibrated with 3 CV sterile deionised H_2O and binding buffer, respectively. The supernatant was applied to the column overnight at 4°C. The resign was washed with 10 CV binding buffer, followed by a stepwise elution by increasing concentrations of imidazole in binding buffer.

Protein content and purity of the eluted his-tag fusion protein was visualized by Coomassie-brilliant-blue staining. Positive fraction were pooled and dialysed against 5 L PBS overnight at 4°C.

For regeneration, the resign was washed with 30 CV sterile deionised H_2O and 30 CV binding buffer, and regenerated by 5 CV of a 100 mM Imidazole solution. Resign was overlaid with 2 mL binding buffer and stored at 4°C

Binding buffer: *20 mM Tris, 300 mM NaCl (pH8)*

Elution buffer: *20 mM Tris, 300 mM NaCl, Imidazole (serial dilutions from 250 mM to 10 mM)*

4.4.8 Surface Plasmon Resonance (SPR) Spectroscopy

To analyse the binding capacity of different PlGF forms to glycosaminoglycans (GAGs) and the interaction between PlGF and Nrp-1, the SPR-Spectrometer BIAcore 2000 from BIAcore was used. All pre-tests, couplings to the SA-chips and measurements were performed at room temperature. Before any measurement or coupling, the system was equilibrated with running or coupling buffer to get a constant baseline. The first flow chamber of every chip was used as a reference. BIAcore measurements were performed by Dr. Daniela Zwolanek, Biochemistry II, Medical Faculty, University Cologne.

4.4.8.1 Determination of PlGF/GAG-interaction

Surface Plasmon Resonance spectroscopy was performed using a BIAcore 2000 (BIAcore AB) system, in collaboration with Prof. Dr. Manuel Koch. Measurement of protein-GAG interactions were carried out following well-established procedures (Ricard-Blum et al., 2004). Briefly, heparan sulphate (Celsius), chondroitin sulphate (Sigma-Aldrich) or heparin (Sigma-Aldrich) was biotinylated in a stoichometric ratio of 1:10 with biotin/LC-hydrazide (Pierce) following the manufacturers recommendations. Biotinylated GAG chains were diluted in HEPES running buffer and immobilized on a streptavidin coated sensor chip (SA-Chip, BIAcore) at a flow rate of 5 µl/min, until an immobilization of ~500 RU was reached. Experiments were carried out using serial dilutions (300 nM, 100 nM, 30 nM, 10 nM and 3 nM) of rhPlGF-1, -2 and rhPlGFStop diluted in running buffer. The analyte was passed over the sensor chip with a constant flow rate of 30 µl/min for 300 sec, dissociation was measured over 500 sec. Fittings of the data, overlay plots and calculation of K_D-values were done with BIAevaluation software 4.1 estimating a 1:1 model

HEPES running-buffer (pH 7,4): *20 mM HEPES, 150 mM NaCl, 2 mM $CaCl_2$ (degassed and filter-sterilized), 0.005% (v/v) P20*

4.4.8.2 Determination of PlGF/Nrp-1 interaction

Experiments were run on a BIAcore 2000 using a CM5 sensor surface. First, the chip was activated by use of EDC/NHS and coupling buffer in a ratio of 1:1 as activating reagents. The degree of coupling was set to approximately 1500 resonance units (RU). Remaining reactive groups were inactivated with ethanolamine, and rPlGF-1, rhPlGF-2, and rhPlGFStop were coupled on chip surface at a flow rate of 5µl/min. The following binding experiments with rhNrp-1 as soluble analyte were performed at a flow rate of 30 µL/min and with concentrations ranging from 1 to 300 nM rhNrp-1 in HEPES running buffer. The analyte was passed over the sensor chip with a constant flow rate of 30 µl/min for 300 sec, dissociation was measured over 500 sec. Between different experimental cycles, the bound proteins were washed from the sensor surface with 2 M NaCl in running buffer. In a second experimental setting, 100 nM rhNrp-1 was pre-incubated with increasing concentrations of unfractionated heparin (0-100 µg/mL) prior to analysis. Fittings of the data, overlay plots and calculation of K_D-values were done with BIAevaluation software 4.1 estimating a 1:1 model.

HEPES running-buffer (pH 7,4): *20 mM HEPES, 150 mM NaCl, 2 mM $CaCl_2$ (degassed and filter-sterilized), 0.005% (v/v) P20*

Coupling buffer (pH 5); *25 mM NaAC (pH 5 with acetic acid)*

4.4.9 Analysis of the plasmin cleavage sites in PlGF

4.4.9.1 Digestion of PlGF-protein by plasmin

To examine, whether PlGF is a target of the serine protease plasmin, 600 ng of rhPlGF-1 and -2 were incubated with 0.02 U/mL of plasmin for defined periods of at 37°C. The reaction was stopped by the addition of sample buffer and heating to 95°C. Afterwards, samples were subjected to SDS-gel electrophoresis and silver-staining (see 2.4.4).
For western blot analysis, 200 ng of rhPlGF-2 (Reliatech) were incubated with 0.02-0.00002 U/mL of plasmin in plasmin buffer for 30 minutes at 37°C. Reaction was stopped by the addition of Laemmli-sample buffer and heating to 95°C. To detect immuno-reactive cleavage products western blotting was performed using a primary rabbit anti-PlGF antibody, directed against the first 20 N-terminal amino acids. The primary antibody was recognized by HRP-labelled swine anti-rabbit secondary antibody.

Plasmin-buffer: *50mM Tris/HCl (pH 8)*

4.4.9.2 Mass spectrometric analysis for identification of the PlGF cleavage site

4.4.9.2.1 Sample preparation

rhPlGF-2 expressed in HEK293 cells (25 µg in 200 µL plasmin buffer) was incubated with 40 µL Ni-sepharose beats for 15 minutes at room temperature to bind to the N-terminal 6x-his-tag, followed by incubation in 80 µL plasmin (final concentrations: 0.04 or 0.008 U/mL in plasmin buffer) for 5 or 30 minutes at 37°C, respectively. Conditions were chosen to ensure specificity. Beats were collected by centrifugation for 5 minutes at 13.500 rpm and 4°C, and the supernatants were analysed by LC-MS/MS, as described below.

4.4.9.2.2 LC-MS/MS of plasmin-cleaved PlGF

Liquid chromatography (LC)-MS data were acquired on a Q-TofII quadrupole-TOF mass spectrometer (Micromass, Manchester, United Kingdom) equipped with a Z spray source. Samples were introduced by an Ultimate Nano-LC system (LC Packings, Amsterdam, The Netherlands) equipped with the Famos autosampler and the Switchos column-switching module. The column setup comprises a 0.3-mm-by-1-mm trapping column and a 0.075-by-150-mm analytical column, both packed with 3 µm Atlantis dC18 (Waters). Samples were diluted 1:10 in 0.1% TFA. A total of 10 µl was injected onto the trap column and desalted for 1 min with 0.1% TFA and a flow rate of 10 µl/min. The 10 port valve switched the trap column into the analytical flowpath, and peptides were eluted onto the analytical column by using a gradient of 2% acetonitrile (ACN) in 0.1% FA to 40% ACN in 0.1% FA over 65 min and a column flow rate of ca. 200 nl/min, resulting from a 1:1,000 split of the 200 µl/min flow delivered by the pump. The electrospray ionization (ESI) interface comprised an uncoated 10 µm i.d PicoTip spray emitter (New Objective) linked to the HPLC flowpath using a 7 µl dead volume stainless steel union mounted onto the PicoTip holder assembly (New Objective). Stable nanospray was established by the application of 1.7 to 2.4 kV to the stainless steel union. The data-dependent acquisition of MS and tandem MS (MS/MS) spectra was controlled by the Masslynx 4.0. Survey scans of 1.4 s covered the range from *m/z* 400 to 1,400. Doubly and triply charged ions rising above a given threshold were selected for MS/MS experiments. In MS/MS mode, the mass range from m/z 40 to 1,400 was scanned in 1.4 s, and 4 scans were added up for each experiment. Micromass-formatted peak lists were generated from the raw data by using the Proteinlynx software module.
A database search using a local installation of MASCOT 1.9 and a custom database containing the sequence of recombinant PlGF-2 was used for a fast identification of PlGF-2 derived peptides. No enzyme specificity was used for the database search.

Since it was expected, that the sequence stretch of interest contains a pair of oxidised cysteines, cysteine oxidation was allowed as optional modification. Results reported by the search engine were verified by manual inspection of the deconvo.

4.4.9.3 Human wound exudates

Wound exudates analysed were obtained from patients in the dermatologic clinic, presenting with non-healing chronic *ulcera crura* due to venous insufficiency or from patients with normally healing cutaneous wounds (excisional wounds of the lower leg awaiting wound closure by secondary intention). To accumulate the exudate, the wound was covered with a semi-permeable polyurethane film (Hyalofilm, Hartmann, Heidelberg, Germany) for a maximum of 8 hours. A maximum of 1 mL exudate per wound was usually obtained. Following exudate collection fluids were centrifuged (10 min, 13,000 x g, 4°C) to remove insoluble material, and supernatants were frozen at -80°C until use.

4.4.9.3.1 Incubation of PlGF-protein in human wound exudate

To analyse the stability of the wild-type isoform PlGF -2, it was incubated in wound fluids obtained from patients with healing or non-healing (chronic) wounds.
200 ng rhPlGF (Reliatech) were incubated with 3 µL wound exudate in a total volume of 20 µL at 37°C (time as indicated). Reaction was stopped by addition of reducing sample buffer and heating at 95°C. Immuno-reactive products were detected by western blotting using a PlGF-specific primary (rabbit anti-human PlGF, 1:1000; Reliatech) and a HRP-conjugated secondary antibody (swine anti-rabbit-HRP, 1:1000; DAKO).

4.5 Mice

4.5.1 Mouse strain

C57BLKS/J-m+/+Lepr^{db} (db/db) mice were obtained from The Jackson Laboratory (Bar Harbor, Maine, USA) and caged individually under standard pathogen-free conditions in the animal care facility of the CMMC, Cologne. Male mice were 10-12 weeks of age at the start of the experiments.

4.5.2 Isolation of genomic tail DNA

To verify the genotype of the experimental db/db mice, genomic DNA was isolated out of tail tissue obtained from three-week-old mice. Therefore, 0.5 cm tail tissue was lysed in 500 µL lysis buffer, supplemented with 10 µL Proteinase K (20 mg/mL) and incubated with shaking at 55°C over night. The Lysate was centrifuged for 8 minutes at 14000rpm and the supernatant was mixed with 1000 µL ethanol. To wash the precipitate, it was

transferred into 750 µL of 70% ethanol, and incubated for 5 minutes. Subsequently, the DNA was dried by air for 15 minutes, and dissolved in 150 µL TE-buffer with constant shaking at 50°C overnight. To identify the exact genotype, 3 µL of the resulting DNA-solution were used to perform PCR.

To verify the genotype, the PCR-product was restricted with RSA I. Primers are chosen to amplify a part of genomic DNA, which carries the point mutation responsible for a shift in the reading frame. This shift causes the loss of the splicing site at the exon/intron border of exon 12 but in addition causes formation of a RSA I restriction site. It therefore enables a clear identification of the mutation by restriction analysis

Lysis Buffer: *50 mM Tris (pH 7.8), 50 mM EDTA, 100 mM NaCl, 5 mM Spermidin, 2% SDS*
TE-buffer: *10mM Tris (pH8 with HCl), 1mM EDTA*

4.5.3 Genotyping protocol

PCR-program:

initial denaturation	95°C	5 min	
denaturation	95°C	30 s	35 cycles
annealing	52°C	30 s	
elongation	72°C	30 s	
final elongation	72°C	5 min	

Primer for genotyping PCR

forward	5´-AGAACGGACACTCTTTGAAGTCTC-3´
backward	5´-CATTCAAACCATAGTTTAGGTTTGTGT-3´

4.5.4 Excisional wounding and PlGF treatment in diabetic mice

To analyse the role of PlGF and its heparin-binding domain for wound healing and angiogenesis *in vivo* two independent wound healing experiments were performed and tissue was harvested at day 10 and day 14 post wounding. In total 6 mice per condition and time point were analysed. Mice were anesthetized under Ketanest/Rompun (Ketanest S, Park Davies GmbH, Karlsruhe, Germany/Rompun 2%, Bayer, Leverkusen, Germany). The animals' backs were shaved and four full-thickness punch-biopsy wounds with a diameter of 6 mm and 5 mm apart from each other were created. Immediately after wounding and for the following 7 days, wounds were treated by topical application of 1 µg/wound of rhPlGF-1, rhPlGF-2 or rhPlGFStop in a total volume of 5 µL, or PBS as a vehicle control. Solution was allowed to adsorb for at least 1 hour before the animal was placed back into its cage. Wound closure was monitored by photographs

taken daily during the time of healing and analysed using the Imaging Software Lucia G 4.80 (Dental Eye, Olympus, Japan; Imaging Software Lucia G 4.80, Laboratory Imaging Ltd., Prague, Czech Republic). Animals were sacrificed and wound tissues were harvested 10 and 14 days after wounding. Wound tissue was excised and the wound area bisected in caudocranial direction and the tissue was either fixed overnight in 4% paraformaldehyde in phosphate buffered saline (PBS), or embedded in OCT compound (Tissue Tek, Miles, IN), immediately frozen in liquid nitrogen, and stored at -80 °C. Histological analysis was performed on serial sections (14-18 µm cryo-sections) from the central portion of the wound.

4.5.4.1 Haematoxylin/eosin staining on paraffin embedded sections

For paraffin sections, wounds were fixed in formalin, embedded in paraffin and cut into 6 µm sections, and were stained with haematoxylin/ eosin (H&E). H&E is commonly used in histology for overview sections. Eosin stains eosinophilic structures like cytoplasm and protein pink, and erythrocytes red. Haematoxylin stains basophilic structures such as nucleic acids blue to purple. Sectioning and staining was performed according to established standard protocols at the histology core facility of the dermatology compartment of the University Hospital of Cologne.

4.5.4.1.1 Morphometric analysis of H&E stained sections

For the quantification of classical wound parameters (amount of granulation tissue, distance between the ends of panniculus carnosus, length of epithelial tongue), serial images of the entire wound area were taken using a Nikon eclipse E800 fluorescence microscope, and assembled in Adobe Photoshop CS5 (Adobe, Dublin, Ireland). Using the image analysis program ImageJ (Wayne Rasband, National Institute of Mental Health, Bethesda, MD, USA), the parameters were analysed.

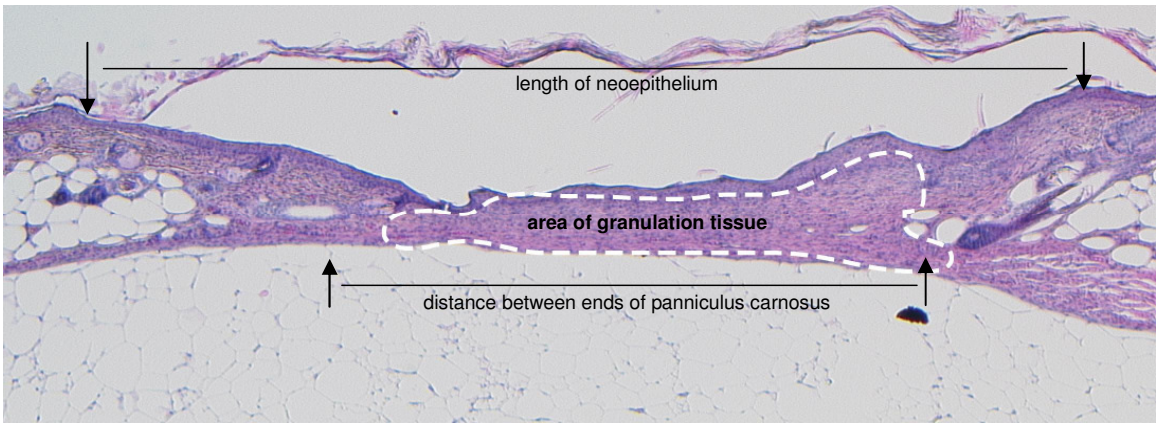

Figure 25: Wound analysis by determination of characteristic parameters.

4.5.4.2 Staining for CD31 and desmin on cryo-sections

For cryosections, wounds were embedded in OCT compound (TissueTek) and frozen. 15 µm thick sections were fixed in cold acetone and used for immunohistochemistry.
Wound sections were blocked in 10% normal goat serum and probed with antibodies directed against desmin (DAKO Glostrup, Denmark, 1:1000 in 1% BSA), a marker for pericytes, and CD31 (BD Pharmingen, 1:1000 in 1% BSA), a marker for endothelial cells. Primary antibodies were detected with Alexa Flour® 488 or 594 coupled secondary antibodies (Invitrogen, 1:500 in 1% BSA), and nuclei of cells were stained with DAPI (1 µg/mL).

4.5.4.2.1 Quantification of wound angiogenesis on CD31 and desmin stained sections

For the quantification of classical wound parameters (amount of granulation tissue, distance between the ends of panniculus carnosus, length of epithelial tongue), serial images of the entire wound area were taken using a Nikon eclipse E800 fluorescence microscope, and assembled in Adobe Photoshop CS5 (Adobe, Dublin, Ireland). Using the image analysis program ImageJ (Wayne Rasband, National Institute of Mental Health, Bethesda, MD, USA), the channels were split, regions exhibiting a positive signal were selected manually via the thresholding tool, and the area was determined. The desmin- and CD31-positive areas were analysed as percentage to the overall area of granulation tissue and as total positive stained area within the granulation tissue. Measurements were performed several times.

4.6 Statistical analysis

Data is presented as mean ± SEM. A p value < 0.05 was considered significant. Statistical analyses were performed using GraphPad Prism 5 (GraphPad Software Inc., La Jolla, CA, USA. Significance was analysed using unpaired Student's t-test for Gaussian distribution.

5 References

Abramsson A, Kurup S, Susse M, Yamada S, Lindblom P, Schallmeiner E, Stenzel D, Sauvaget D, Ledin J, Ringvall M, Landegren U, Kjellen L, Bondjers G, Li JP, Lindahl U, Spillmann D, Betzlotz C, Gerhardt H. Defective N-sulfatation of heparan sulfate proteoglycans limits PDGF-BB binding and pericyte recruitment in vascular development. *Genes Dev*. 2007 Feb 1;21(3):316-31

Adini A, Kornaga T, Firoozbakht F, Benjamin LE. Placental growth factor is a survival factor for tumor endothelial cells and macrophages. *Cancer Res* 2002;62:2749-52.

Alitalo K, Carmeliet P. Molecular mechanisms of lymphangiogenesis in health and disease. *Cancer Cell* 2002;1, 219-227.

Ancelin M, Chollet-Martin S, Herve M, Legrand C, Benna J, Perrot-Applanat M. VEGF189 induces human neutrophil chemotaxis in extravascular tissue via an autocrine amplification mechanism. *Lab Invest* 2004;84:502–12.

Armulik A, Abramsson A, et al. Endothelial/pericyte interactions. *Circ Res*. 2005;97(6): 512-523.

Asahara T, Takahashi T, Masuda H, Kalka C, Chen D, Iwaguro H, et al. VEGF contributes to post-natal neovascularization by mobilizing bone marrow-derived endothelial progenitor cells. *EMBO J* 1999;18:3964-72

Ash JD, Overbeek PA. Lens-specific VEGF-A expression induces angioblast migration and proliferation and stimulates angiogenic remodeling. *Dev Biol*. 2000;223:383–398.

Astrof S, Hynes RO. Fibronectins in vascular morphogenesis. *Angiogenesis* 2009;12:165–175

Autiero, M, Luttun A, Tjwa M & Carmeliet P. Placental growth factor and its receptor, vascular endothelial growth factor receptor-1: novel targets for stimulation of ischemic tissue revascularization and inhibition of angiogenic and inflammatory disorders. *J. Thromb. Haemost.* 2003; 1, 1356–1370.

Autiero M, Waltenberger J, Communi D, Kranz A, Moons L, Lambrechts D, Kroll J, Plaisance S, De Mol M, Bono F, Kliche S, Fellbrich G, Ballmer-Hofer K, Maglione D, Mayr-Beyrle U, Dewerchin M, Dombrowski S, Stanimirovic D, Van Hummelen P, Dehio C, Hicklin DJ, Persico G, Herbert JM, Shibuya M, Collen D, Conway EM and Carmeliet P. Role of PlGF in intramolecular cross talk between the VEGF receptors Flt1 anf Flk1. *Nat. Med*. 2003;9: 936–943.

Bates DO and Harper SJ. Regulation of vascular permeability by vascular endothelial growth factors. *Vascul. Pharmacol*. 2002;39:225–237

Becker PM, Waltenberger J, Yachechko R, Mirzapoiazova T, Sham JSK, Lee CG, Elias JA and Verin AD. Neuropilin-1 Regulates Vascular Endothelial Growth Factor–Mediated Endothelial Permeability. *Circ Res.* 2005 Jun 24;96(12):1257-65

Benjamin LE, Glucose, VEGF-A, and diabetic complications. *Am J Pathol*. 2001 Apr; 58(4):1181-4.

Blotnick S, Peoples GE, Freeman MR, Eberlein TJ, Klagsbrun M. T lymphocytes synthesize and export heparin-binding epidermal growth factor-like growth factor and basic fibroblast growth factor, mitogens for vascular cells and fibroblasts: differential production and release by CD4+ and CD8+ T cells. *Proc Natl Acad Sci USA*. 1994; 91:2890–2894.

Braiman-Wiksman L, Solomonik I, et al. Novel insights into wound healing sequence of events. *Toxicol Pathol*. 2007;35(6): 767-779.

Brooks PC, Clark RA, et al. Requirement of vascular integrin alpha v beta 3 for angiogenesis. *Science* 1994a;264(5158): 569-571.

Brooks PC, Montgomery AM, et al. Integrin alpha v beta 3 antagonists promote tumor regression by inducing apoptosis of angiogenic blood vessels. *Cell* 1994b;79(7): 1157-1164.

Brown LF, Yeo K-T, Berse B, Yeo T-K, Senger DR, Dvorak HF, Van De Water L: Expression of vascular permeability factor (vascular endothelial growth factor) by epidermal keratinocytes during wound healing. *J Exp Med* 1992, 176:1375–1379

Broxmeyer HE et al. Myeloid progenitor cell regulatory effects of vascular endothelial cell growth factor. *Int.J.Hematol*. 1995;62,2003-215

Burridge K and Wennerberg K. Rho and Rac take center stage. Cell 2004;116, 167–179

Calalb MB, Polte TR, Hanks SK. Tyrosine phosphorylation of focal adhesion kinase at sites in the catalytic domain regulates kinase activity: a role for Src family kinases. *Mol Cell Biol*. 1995 Feb;15(2):954-63.

Cai H, Reed RR. Cloning and characterization of neuropilin-1-interacting protein: a PSD-95/Dlg/ZO-1 domain-containing protein that interacts with the cytoplasmic domain of neuropilin-1. *J. Neurosci*. 1999;19, 6519–6527

Cai J, Ahmad S, Jiang WG, Huang J, Kontos CD, Boulton M, Ahmed A. Activation of Vascular Endothelial Growth Factor Receptor-1 Sustains Angiogenesis and Bcl-2 Expression Via the

Phosphatidylinositol 3-Kinase Pathway in Endothelial Cells. *Diabetes*. 2003 Dec;52(12):2959-68

Cao Y, Chen H, Zhou L, Chiang MK, Anand-Apte B, Weatherbee JA, et al. Heterodimers of placenta growth factor/vascular endothelial growth factor. Endothelial activity, tumor cell expression, and high affinity binding to Flk-1/KDR. *J Biol Chem* 1996a;271:3154–62.

Cao Y, Ji WR, Qi P and Rosin A. Placenta growth factor: identification and characterization of a novel isoform generated by RNA alternative splicing. *Biochem. Biophys. Res. Commun*. 1997;235, 493–498

Carmeliet P, Ferreira V, Breier G, Pollefeyt S, Kieckens L, Gertsenstein M, Fahrig M, Vandenhoeck A, Harpal K, Eberhardt C, Declercq C, Pawling J, Moons L, Collen D, Risau W, Nagy A. Abnormal blood vessel development and lethality in embryos lacking a single VEGF allele. *Nature*. 1996;380:435– 439.

Carmeliet P, Ng YS, Nuyens D, Theilmeier G, Brusselmanns K,Cornelissen I, Ehler E, Kakkar VV, Stahlmans I, Mattot V, Perriard JC, Dewerchin M,Flammeng W, Nagi A, Lupu F, Moons L, Collen D, D`Amore PA,Shima DT. Impaired myocardial angiogenesis and ishemic cardiomyopathy in mice lacking the vascular endothelial growth factor isoforms VEGF164 and VEGF188. *Nat Med*. 1999 May;5(5):495-502

Carmeliet P. VEGF gene therapy: stimulating angiogenesis or angioma-genesis? *Nat Med* 2000, 6:1102–1103

Carmeliet P, Moons L, Luttun A, Vincenti V, Compernolle V, De Mol M, Wu Y, Bono F, Devy L, Beck H, Scholz D, Acker T, DiPalma T, Dewerchin M, Noel A, Stalmans I, Barra A, Blacher S, Vandendriessche T, Ponten A, Eriksson U, Plate KH, Foidart JM, Schaper W, Charnock-Jones DS, Hicklin DJ, Herbert JM, Collen D, Persico MG. Synergism between vascular endothelial growth factor and placental growth factor contributes to angiogenesis and plasma extravasation in pathological conditions. *Nat Med* 2001, 7:575–583

Cebe Suarez S, PierenM, Cariolato L, Arn S,HoffmannU, Bogucki A,Manlius C, Wood J, Ballmer-Hofer K. A VEGF-A splice variant defective for heparin sulphate and neuropilin-1 binding shows attenuated signalling through VEGFR-2. *Cell Mol Life Sci.* 2006; 63:2067–2077.

Chappell JC, Taylor SM, Ferrara N, Bautch VL. Local guidance of emerging vessel sprouts requires soluble Flt-1. *Dev Cell* 2009; 17:377–386.

Chen H, Chedotal A, He Z, Goodman CS and Tessier-Lavigne M. Neuropilin-2, a novel member of the neuropilin family, is a high affinity receptor for the semaphorins Sema E and Sema IV but not Sema III. *Neuron* 1997;19, 547–559

Chen TT, Luque A, Lee S, Anderson SM, Segura T, Iruela-Arispe ML. Anchorage of VEGF to the extracellular matrix conveys differential signaling responses to endothelial cells. *J Cell Biol.* 2010, 199 (4);595-609

Cheresh DA, Stupack DG. Regulation of angiogenesis: apoptotic cues from the ECM. *Oncogene* 2008;27(48): 6285-6298.

Christinger HW, Fuh G, de Vos AM and Wiesmann C. The chrystal structure of placenta growth factor in complex with domain2 of vascular endothelial growth factor receptor-1. *J. Biol. Chem*. 2004;279:10382-10388.

Cianfarani F, Zambruno G, Brogelli L, Sera F, Lacal PM, Pesce M,. Capogrossi MC, Failla CM, Napolitano M, Odorisio T. Placenta Growth Factor in Diabetic Wound Healing - Altered Expression and Therapeutic Potential. *Am J Pathol.* 2006 Oct;169 (4), 1167-1182

Clauss M, Weich H, Breier G, Knies U, Röckl W, Waltenberger J, et al. The VEGF receptor Flt-1 mediates biological activities. *J Biol Chem* 1996;271:17629–34.

Coffin JD, Poole TJ. Endothelial cell origin and migration in embryonic heart and cranial blood vessel development. *Anat Rec*. 1991;231:383–395.

Cohen T, Nahari D, Cerem-WeissL, Neufeld G, Levi B; Interleukin-6 induces the expression of vascular endothial growth factor. *J Biol Chem* 1996; 271: 736-741

Coleman DL. Thermogenesis in diabetes-obesity syndromes in mutant mice. *Diabetologia*.1982 Mar;22(3):205-11.

Collo G, Pepper MS. Endothelial cell integrin alpha5betal expression is modulated by cytokines and during migration in vitro. *J Cell Sci*. 1999; 112:569–578.

Colognato H, Yurchenco PD. Form and function: the laminin family of heterotrimers. *Dev Dyn* 2000;218:213–34.

Cunningham SA, Waxham MN, Arrate PM et al. Interaction of the Flt-1 tyrosine kinase receptor with the p85 subunit of phosphatidylinositol 3-kinase. *J Biol Chem* 1995;270:20254–20257

Cunningham SA, Arrate MP, Brock TA, Waxham MN, Interactions of FLT-1 and KDR with

phospholipase C%: identification of the phosphotyrosine binding sites. *Biochem. Biophys. Res. Commun.* 1997; 240, 635-639.

Davis GE, Camarillo CW. An alpha 2 beta 1 integrin-dependent pinocytic mechanism involving intracellular vacuole formation and coalescence regulates capillary lumen and tube formation in threedimensional collagen matrix. *Exp Cell Res*. 1996;224:39 –51.

Davis GE, Bayless KJ, Davis MJ, Meininger GA. Regulation of tissue injury responses by the exposure of matricryptic sites within extracellular matrix molecules. *Am J Pathol* 2000;156:1489–1498.

Dealey C. *The care of wounds: A guide for nurses*. Oxford; Malden, Mass. Blackwell Science. Electronic book 1999.

Dejana E, Languino LR, Polentarutti N, Balconi G, Ryckewaert JJ, Larrieu MJ, Donati MB, Mantovani A, Marguerie G. Interaction between fibrinogen and cultured endothelial cells. Induction of migration and specific binding. *J Clin Invest*. 1985;75:11–18.

Dejana E, Orsenigo F, Lampugnani MG. The role of adherens junctions and VE-cadherin in the control of vascular permeability. *J Cell Sci* 2008;121:2115–2122.

Dejana E, Tournier-Lasserve E, Weinstein BM. The control of vascular integrity by endothelial cell junctions: molecular basis and pathological implications. *Dev Cell* 2009;16:209–221.

De la Torre J, Sholar A (2006). Wound healing: Chronic wounds. Emedicine.com.

Deodato B, Arsic N, Zentilin L, Galeano M, Santoro D, Torre V, Altavilla D, Valdembri D, Bussolino F, Squadrito F, Giacca M: Recombinant AAV vector encoding human VEGF165 enhances wound healing. *Gene Ther* 2002, 9:777–785

Deodhar AK, Rana RE. Surgical physiology of wound healing: a review. *Journal of Postgraduate Medicine* 1997;43 (2): 52-56.

Deroanne CF, Hajitou A, Calberg-Bacq CM, Nusgens BV, Lapiere CM; Angiogenesis by fibroblast growth factor 4 is mediated through an autocrine up-regulation of vascular endothelial growth factor expression. *Cancer Res* 1997; 57: 5590-5597

De Vries C, Escobedo JA, Ueno H, Houck K, Ferrara N and Williams LT. The fms-like tyrosine kinase, a receptor for vascular endothelial growth factor. *Science* 1992;255, 989-991.

DiPietro LA, Burns AL. Wound Healing: Methods and Protocols. *Methods in Molecular Medicine*. (2003) Totowa, N.J. Humana Press. Electronic book.

DiSalvo J, Bayne ML, Conn G, Kwok PW, Trivedi PG, Soderman DD, et al. Purification and characterization of a naturally occurring vascular endothelial growth factor/placenta growth factor heterodimer. *J Biol Chem* 1995;270:7717–23.

Drake CJ, Fleming PA. Vasculogenesis in the day 6.5 to 9.5 mouse embryo. *Blood*. 2000;95:1671–1679.

Dvorak HF, Brown LF, Detmar M, Dvorak AM. Vascular permeability factor/vascular endothelial growth factor, microvascular hyperpermeability, and angiogenesis. *Am J Pathol* 1995;146:1029-39.

Eichler MJ, Carlson MA. Modeling dermal granulation tissue with the linear fibroblast-populated collagen matrix: A comparison with the round matrix model. *Journal of Dermatological Science*. 2005;41(2): 97-108. PMID 16226016.

Elson DA, Thurston G, Huang LE, Ginzinger DG, McDonald DM, Johnson RS, Arbeit JM. Induction of hypervascularity without leakage or inflammation in transgenic mice overexpressing hypoxia-inducible factor-1alpha. *Genes Dev*. 2001 Oct 1;15(19):2520-32.

Eming SA, Krieg T, et al. Inflammation in wound repair: molecular and cellular mechanisms. *J Invest Dermatol* 2007;127(3): 514-525.

Enenstein J, Waleh NS, Kramer RH. Basic FGF and TGF-beta differentially modulate integrin expression of human microvascular endothelial cells. *Exp Cell Res* 1992;203:499–503.

Errico M, Riccioni T, Iyer S, Pisano C, Acharya KR, Persico MG, De Falco S. Identification of Placenta Growth Factor Determinants for Binding and Activation of Flt-1 Receptor. *J Biol Chem.* 2004 Oct15;249(42):43929-39

Evans IM, Yamaji M, Britton G, Pellet-Many C, Lockie C, Zachary IC, Frankel P. Neuropilin-1 signaling through p130Cas tyrosine phosphorylation is essential for growth factor dependent migration of glioma and endothelial cells. *Mol Cell Biol*. 2011 Jan 19 (epub ahead of print)

Failla CM, Odorisio T, Cianfarani F, Schietroma C, Puddu P, Zambruno G: Placenta growth factor is induced in human keratinocytes during wound healing. *J Invest Dermatol* 2000, 115:388–395

Fantuzzi G, Faggioni R. Leptin in the regulation of immunity, inflammation, and hematopoiesis. *J Leukoc Biol.* 2000 Oct;68(4):437-46.

Ferguson JE, Kelley RW, Patterson C. Mechanisms of endothelial differentiation in embryonic vasculogenesis. *Arterioscler Thromb Vasc Biol*. 2005;25:2246 –2254.

Ferrara N, Henzel WJ. Pituitary follicular cells secrete a novel heparin-binding growth factor

References

specific for vascular endothelial cells. *Biochem. Biophys. Res. Commun*. 1989;161, 851–858

Ferrara N, Carver-Moore K, Chen H, Dowd M, Lu L, O'Shea KS, Powell-Braxton L, Hillan KJ, Moore MW. Heterozygous embryonic lethality induced by targeted inactivation of the VEGF gene. *Nature*. 1996;380:439–442.

Ferrara N, Davis-Smyth T. The biology of vascular endothelial growth factor. Endocr. Rev. 1997;18, 4–25

Ferrara N, Gerber HP, LeCouter J. The biology of VEGF and its receptors. *Nat Med* 2003; 9:669-76.

Finkenzeller G, Sparacio A, Technau A, Marme D, Siemeister G; Sp-1 recognition sites in the proximal promotor of the human vascular endothelial growth factor gene are essential for platelet-derived growth factor induced gene expression. *Oncogen* 1997; 15: 669-676

Folkman J, Klagsbrun M. Angiogenic factors. *Science* 1987;235:442-448.

Fong GH, Rossant J, Gertsenstein M, Breitman ML. Role of the Flt-1 receptor tyrosine kinase in regulating the assembly of vascular endothelium.*Nature*. 1995;376:66 –70.

Fong GH, L Zhang, et al. Increased hemangioblast commitment, not vascular disorganization, is the primary defect in flt-1 knock-out mice. *Development* 1999;126(13): 3015-3025.

Frank S, Hübner G, Breier G, Longaker MT, Greenhalgh DG, Werner S. Regulation of vascular endothelial growth factor expression in cultured keratinocytes: implications for normal and impaired wound healing. *J Biol Chem* 1995;270: 12607-13.

Frank S, Stallmeyer B, Kampfer H, Kolb N, Pfeilschifter J. Leptin enhances wound reepithelialization and constitutes a direct function of leptin in skin repair. *J Clin Invest*. 2000 Ag;106(4):501-9.

Freeman MR, Schneck FX, Gagnon ML. Peripheral blood T lymphocytes and lymphocytes infiltrating human cancers express vascular endothelial growth factor: a potential role for T cells in angiogenesis. *Cancer Res*. 1995;55, 4140–4145

Friesel RE, Maciag T. Molecular mechanisms of angiogenesis: fibroblast growth factor signal transduction. *FASEB J* 1995;9:919–925.

Fuchs E. Epidermal differentiation. *Curr Poin Cell Biol*. 1990; 2: 1028-1035

Fuchs E. Epidermal differentiation and keratin gene expression. *J Cell Sci Suppl*. 1993; 17:197-208.

Fujisawa H, Takagi S and Hirata T. Growth-associated expression of a membrane protein, neuropilin, in Xenopus optic nerve fibers. *Dev. Neurosci*. 1995; 17,343–349

Fukumura D, Xavier R, Sugiura T, et al. Tumor induced VEGF promoter activity in stromal cells. *Cell* 1998;94:715–25.

Galiano RD, Tepper OM, Pelo CR, Bhatt KA, Callaghan M, Bastidas N, Bunting S, Steinmetz HG, Gurtner GC: Topical vascular endothelial growth factor accelerates diabetic wound healing through increased angiogenesis and by mobilizing and recruiting bone marrow-derived cells. *Am J Pathol* 2004, 164:1935–1947

Gavard J, Patel V, et al. Angiopoietin-1 prevents VEGF-induced endothelial permeability by sequestering Src through mDia. *Dev Cell*. 2008;14(1): 25-36.

Gerber H, Dixit V, Ferrara N. Vascular endothelial growth factor induces expression of the antiapoptotic proteins bcl-2 and A1 in vascular endothelial cells. *J Biol Chem* 1998;273: 13313-6.

Gerber HP *et al.* VEGF regulates haematopoietic stem cell survival by an internal autocrine loop mechanism. *Nature* 2002;417, 954–958.

Gerhardt H, Golding M, Fruttiger M, Ruhrberg C, Lundkvist A, Abramsson A, Jeltsch M, Mitchell C, Alitalo K, Shima D, Betsholtz C. VEGF guides angiogenic sprouting utilizing endothelial tip cell filopodia. *J Cell Biol*. 2003 Oct;314(1):15-23

Gerhardt H, Ruhrberg C, Abramsson A, Fujisawa H, Shima D and Betsholtz C. Neuropilin-1 is required for endothelial tip cell guidance in the developing central nervous system. *Dev. Dyn.* 2004;231, 503–509

Giancotti FG, Ruoslahti E. Integrin signaling. *Science*. 1999;285:1028–1032.

Gluzman-Poltorak Z, Cohen T, Herzog Y, Neufeld G. Neuropilin-2 and Neuropilin-1 are receptors for 165-amino acid long form of vascular endothelial growth factor (VEGF) and of placenta growth factor-2, but only neuropilin-2 functions as a receptor for the 145 amino acid form of VEGF. *J Biol Chem* 2000;275:18,040–18,045.

Goad DL, Rubin J, Wang H, Tashjian AH, Patterson C; Enhanced expression of vascular endothelial growth factor in human SaOS-2 osteoblast like cells and murine osteoblasts induced by insulin-like growth factor 1. *Endocrinology* 1996; 137: 2262-2268

Goova MT, Li J, Kislinger T, Qu W, Lu Y, Bucciarelli LG, Nowygrod S, Wolf BM, Caliste X, Yan SF, Stern DM, Schmidt AM. Blockade of receptor for advanced glycation endproducts restores effective wound healing in diabetic mice. *Am J Pathol*. 2001 Aug;159(2):513-25.

Graeven U, Rodeck U, Karpinski S, Jost M, Andre N, Schmiegel W. Expression patterns of placenta growth factor in human melanocytic cell lines. *J Invest Dermatol* 2000;115:118—23.

Greenaway J, Lawler J, Moorehead R, Bornstein P, Lamarre J, Petrik J. Thrombospondin-1 inhibits VEGF levels in the ovary directly by binding and internalization via the low density lipoprotein receptor-related protein-1 (LRP-1). *J Cell Physiol* 2007;210:807–818.

Greenhalgh DG. The role of apoptosis in wound healing. *Int J Biochem Cell Biol.* 1998;30 (9): 1019–1030..

Grenache DG, Zhang Z, Wells LE, Santoro SA, Davidson JM, Zutter SA. Wound healing in the alpha2betal integrin-deficient mouse: alterted keratinocyte biology and dysregulated matrix metalloproteinase expression. *J Invest Dermatol* 2007;127:455–66.

Gu J, Tamura M, Pankov R, Danen EHJ, Takino T, Matsumoto K, Yamada KM. Shc and FAK Differentially Regulate Cell Motility and Directionality Modulated by PTEN. *J Cell Biol*. 1999; 146 (2):389-403

Gualandris A, Presta M. 1995. Transcriptional and posttranscriptional regulation of urokinase-type plasminogen activator expression in endothelial cells by basic fibroblast growth factor. *J Cell Physiol* 162:400–409.

Gurtner GC, Werner S, Barrandon Y, Longaker MT. Wound repair and regeneration.Nature 2008;453:314–21.

Hallmann R, Horn N, Selg M, Wendler O, Pausch F, Sorokin LM. Expression and function of laminins in the embryonic and mature vasculature. *Physiol Rev* 2005;85:979–1000.

Harris AL. Hypoxia -a key regulatory factor in tumour growth. *Nat Rev Cancer*. 2002 Jan;2(1):38-47.

Hattori K, Heissig B, Wu Y, Dias S, Tejada R, Ferris B, et al. Placental growth factor reconstitutes hematopoiesis by recruiting VEGFR1+ stem cells from bone-marrow microenvironment. *Nat Med* 2002;8:841-9.

Hauser S, Weich HA. A heparin-binding form of placenta growth factor (PGF-2) is expressed in human umbilical vein endothelial cells and in placenta. *Growth Factors* 1993;9:259-68.

Hellstrom M, Kalen M, et al. Role of PDGF-B and PDGFR-beta in recruitment of vascular smooth muscle cells and pericytes during embryonic blood vessel formation in the mouse. Development 1999;126(14): 3047-3055.

Hellstrom M, Phng LK, Hofmann JJ, et al. Dll4 signaling through Notch1 regulates formation of tip cells during angiogenesis. *Nature* 2007; 445:776–780.

Hiratsuka S, Minowa O, Kuno J, Noda T and Shibuya M. Flt-1 lacking the tyrosine kinase domain is sufficient for normal development and angiogenesis in mice. *Proc. Natl. Acad. Sci. USA* 1998;95, 9349-9354.

Hiratsuka S, Kataoka Y, Nakao K, Nakamura K, Morikawa S, Tanaka S, Katsuki M, Maru Y, Shibuya M. Vascular endothelial growth factor A (VEGF-A) is involved in guidance of VEGF receptor-positive cells to the anterior portion of early embryos. *Mol Cell Biol*. 2005;25:355–363.

Hoch RV and Soriano P.Roles of PDGF in animal development. *Development* 2003;130(20): 4769-4784.

Hopkinson-Woolley J, Hughes D, Gordon S, Martin P. Macrophage recruitment during limb development and wound healing in the embryonic and foetal mouse. *J Cell Sci*. 1994 May;107 (Pt 5):1159-67.

Houck KA, Ferrara N, Winer J, Cachianes G, Li B, Leung DW. The vascular endothelial growth factor family: identification of a fourth molecular species and characterization of alternative splicing of RNA. Mol. Endocrinol. 1991;5, 1806–1814

Howdieshell TR, Callaway D, Webb WL, et al. Antibody neutralization of VEGF inhibits wound granulation tissue formation. *J Surg Res* 2001;96:173–82.

Hübner G, Brauchle M, Smola H, Madlener M, Fässler R, Werner S. Differential regulation of pro-inflammatory cytokines during wound healing in normal and glucocorticoid-treated mice. *Cytokine*. 1996 Jul;8(7):548-56

Igarashi K, Isohara T, Kato T, Shigeta K, Yamano T, Uno I. Tyrosine 1213 of Flt-1 is a major binding site of Nck and SHP-2. *Biochem. Biophys.Res. Commun.* 1998; **246**, 95-99.

Ikeda E, Achen MG, Breier G and Risau W, Hypoxia-induced transcriptional activation and increased mRNA stability of vascular endothelial growth factor in C6 glioma cells. *J. Biol. Chem.* 1995;270:19761–19766.

Ishida A, Murray J, Saito Y, Kanthou C, Benzakour O, Shibuya M, et al. Expression of vascular endothelial growth factor receptors in smooth muscle cells. *J Cell Physiol* 2001;188:359-68.

Ito N, Wernstedt C, Engstrom U, Claesson-Welsh L. Identification of vascular endothelial growth factor receptor-1 tyrosine phosphorylation sites and binding of SH2 domain-containing molecules. *J. Biol. Chem.* 1998;273, 23410-23418.

References

Ito N, Huang K, Claesson-Welsh L. Signal transduction by VEGF receptor-1 wild type and mutant proteins. *Cell Signal* 2001;13:849–854

Iyer S, Leonidas DD, Swaminathan GJ et al. The crystal structure of human placenta growth factor-1 (PlGF-1), an angiogenic protein, at 2.0 A resolution. *J. Biol. Chem*. 2001;276, 12153-12161

Kämpfer H, Pfeilschifter J, Frank S. Expressional regulation of angiopoietin-1 and -2 and the tie-1 and -2 receptor tyrosine kinases during cutaneous wound healing: a comparative study of normal and impaired repair. *Lab Invest*. 2001 Mar;81(3):361-73.

Kanda S, Landgren E, Ljungstrom M, Claesson-Welsh L. Fibroblast growth factor receptor 1 induced differentiation of endothelial cell line established from tsA58 large T transgenic mice. *Cell Growth Differ* 1996; 7:383–395.

Kandel J, Bossy-Wetzel E, Radvanyi F, Klagsbrun M, Folkman J, Hanahan D. Neovascularization is associated with a switch to the export of bFGF in the multistep development of fibrosarcoma. *Cell* 1991;66:1095–1104.

Kawasaki T *et al.* A requirement for neuropilin-1 in embryonic vessel formation. *Development* 1999;126, 4895–4902.

Keck PJ, Hauser SD, Krivi G. Vascular permeability factor, an endothelial cell mitogen related to PDGF. *Science* 1989;246, 1309–1312

Keyt BA, Berleau LT, Nguyen HV, Chen H, Heinsohn H, Vandlen R, Ferrara N. The carboxy-terminal domain (111-165) of vascular endothelial growth factor is critical for its mitogenic potency. *J Biol Chem*. 1996 Mar 29;271(13):7788-95

Kim KY, Jeong SY, Won J, Ryu PD, Nam MJ. Induction of angiogenesis by expression of soluble type II transforming growth factor-beta receptor in mouse hepatoma. *J Biol Chem* 2001;276:38781-38786.

Kingsley DM. The TGF-beta superfamily: new members, new receptors, and new genetic tests of function in different organisms. *Genes Dev* 1994; 8:133–146.

Kishimoto J, Ehama R, Ge Y, Kobayashi T, Nishiyama T, Detmar M, et al. In vivo detection of VEGF promoter activity in transgenic mouse skin. *Am J Pathol* 2000;157:103–10.

Kitsukawa T, Shimono A, Kawakami A, Kondoh H and Fujisawa H. Overexpression of a membrane protein, neuropilin, in chimeric mice causes anomalies in the cardiovascular system, nervous system and limbs. *Development* 1995;121, 4309–4318.

Klagsbrun M, Takashima S and Mamluk R. The role of neuropilin in vascular and tumor biology. *Adv. Exp. Med. Biol*. 2002;515, 33–48

Knox SM, Whitelock JM. Perlecan: how does one molecule do so many things? *Cell Mol Life Sci* 2006;63:2435–45.

Koster MI. Making an epidermis. *Ann N Y Acad Sci* 2009;1170: 7-10.

Ku DD, Zaleski JK, Liu S, Brock TA. Vascular endothelial growth factor induces EDRF-dependent relaxation in coronary arteries. Am J Physiol. 1993 Aug;265(2Pt2):H586-92

Kubo H, Alitalo K. The bloody fate of endothelial stem cells. *Genes Dev.* 2003;17, 322–329.

Lacal PM, Failla CM, Pagani E, Odorisio T, Schietroma C, Falcinelli S, et al. Human melanoma cells secrete and respond to placenta growth factor and vascular endothelial growth factor. *J Invest Dermatol* 2000;115:1000—7.

Lange T, Guttmann-Raviv N, Baruch L, Machluf M, Neufeld G. VEGF162, a new heparin-binding vascular endothelial growth factor splice form that is expressed in transformed human cells. *J. Biol. Chem*. 2003;278, 17164–17169

Lansdown ABG, Sampson B, and Rowe A. Experimental observations in the rat on the influence of cadmium on skin wound repair. *Int J Exp Pathol*, 2001;82(1): 35-41.

Larsen M, Tremblay ML, Yamada KM. Phosphatases in cell-matrix adhesion and migration. Nat *Rev Mol Cell Biol*. 2003 Sep;4(9):700-11

Lauer G, Solberg S, Cole M, Flamme I, Stürzebecher J, Mann K, Krieg T, Eming SA. Expression and proteolysis of Vascular Endothelial Growth Factor is increased in chronic wounds. *J Invest. Dermatol*. 2000;115 (1), 12-18

Lauer G, Sollberg S, Cole M, Krieg T, Eming SA. Generation of a novel proteolysis resistant vascular endothelial growth factor165 variant by a site-directed mutation at the plasmin sensitive cleavage site. *FEBS letters* 2002;531:309-313

Lee S, Jilani SM, Nikolova GV, Carpizo D, Irula-Arisoe LM. Processing of VEGF-A by matrix metalloproteinases regulates bioavailability and vascular patterning in tumors. J Cell Biol 2005;169:681–691

Lee TH, Seng S, et al. Integrin regulation by vascular endothelial growth factor in human brain microvascular endothelial cells: role of alpha6beta1 integrin in angiogenesis. *J Biol Chem* 2006;**281**(52): 40450-40460.

Lerman OZ, Galiano RD, Armour M, Levine JP, Gurtner GC. Cellular dysfunction in the diabetic fibroblast: impairment in migration, vascular endothelial growth factor production, and response to hypoxia. *Am J Pathol*. 2003 Jan;162(1):303-12.

Lesslie DP, Summy JM, Parikh NU, Fan F, Trevino JG, Sawyer TK, Metcalf CA, Shakespeare WC, Hicklin DJ, EllisLM, Gallick GE. Vascular endothelial growth factor receptor-1 mediates migration of human colorectal carcinoma cells by activation of Src family kinases. *Br J Cancer*. 2006; 94(11):1710-7

Leung DW, Cachianes G, Kuang W J, Goeddel D V and Ferrara N. Vascular endothelial growth factor is a secreted angiogenic mitogen. *Science* 1989;246, 1306–1309

Levy AP, Levy NS, Goldberg MA. Post-transcriptional regulation of vascular endothelial growth factor by hypoxia. *J. Biol. Chem.* 1996;**271**, 2746-2753.

Levy NS, Chung S Furneaux H, Levy AP; Hypoxic stabilization of vascular endothelial growth factor mRNA by the RNA-binding protein HuR. *J Biol Chem* 1998; 273: 6417-6423

Li A, Dubey S, Varnes ML, Dave BJ, Singh RK. IL-8 directly enhanced endothelial cell survival, proliferation, and matrix metalloproteinases production and regulated angiogenesis. *J Immunol* 2003a;170:3369–76.

Li J, Perrella MA, Tsai JC, Yet SF, Hsieh CM, Yoshizumi M, Patterson C, Endege WO, Zhou F, Lee ME. Induction of vascular endothelial growth factor gene expression by interleukin-1 beta in rat aortic smooth muscle cells. *J Biol Chem*. 1995 jan 6;270(1):308-12

Li J, Zhou L, Tran HT, Chen Y, Nguyen NE, Karasek MA, et al. Overexpression of laminin-8 in human dermal microvascular endothelial cells promotes angiogenesis-related functions. *J Invest Dermatol* 2006;126:432–40.

Li Y, Madigan MC, Lai K, Conway RM, Billson FA, Crouch R, et al. Human uveal melanoma expresses NG2 immunoreactivity. *Br J Ophthalmol* 2003b;87:629–32.

Lobov IB, Renard RA, Papadopoulos N, et al. Delta-like ligand 4 (Dll4) is induced by VEGF as a negative regulator of angiogenic sprouting. *Proc Natl Acad Sci USA* 2007; 104:3219–3224.

Lorenz HP and Longaker MT (2003). Wounds: Biology, Pathology, and Management. Stanford University Medical Center.

Luttun A, Tjawa M, Moons L, Wu Y, Angelillo-Scherrer A, Liao F,. Nagy JA, Hopper A, Priller J, de Klerck B, Compernolle V,Daci E, Bohlen P, Dewerchin M, Herbert J-M, Fava R, Matthy P, Carmeliet G, Collen D, Dvorak HF,Hicklin DJ, Carmeliet P. Revascularization of ischemic tissues by PlGF treatment, and inhibition of tumor angiogenesis, arthritis and atherosclerosis by anti-Flt1. *Nature Med.*2002, 8 (8);831-840

Maes C, Carmeliet P, Moermans K, Stockmans I, Smets N, Collen D, Bouillon R, Carmetiet G. Impaired angiogenesis and endochondral tube formation in mice lacking the vascular endothelial growth facor isoforms VEGF164 and VEGF188. *Mech Dev*. 2002 Feb;111(1-2):61-73

Maglione D, Guerriero V, Viglietto G, Delli-Bovi P and Persico MG. Isolation of a human placenta cDNA coding for a protein related to the vascular permeability factor. *Proc. Natl. Acad. Sci. U.S.A.* 1991;88, 9267–9271

Maglione D, Guerriero V, Viglietto G et al. Two alternative mRNAs coding for the angiogenic factor, placenta growth factor (PlGF), are transcribed from a single gene of chromosome 14. *Oncogene* 1993;**8**, 925–931

Maisonpierre PC, Suri C, Jones PF, Bartunkova S, Wiegand SJ, Radziejewski C, Compton D, McClain J, Aldrich TH, Papadopoulos N, Daly TJ, Davis S, Sato TN, Yancopoulos GD. Angiopoietin-2, a natural antagonist for Tie2 that disrupts in vivo angiogenesis. *Science* 1997;277:55–60.

Malhotra R, Stenn KS, Fernandez LA, Braverman IM. The angiogenic properties of normal and psoriatic skin associate with the epidermis, not the dermis. *Lab Invest* 1989;61: 162-5.

Mamluk R, Gechtman Z, Kutcher ME, Gasiunas N, Gallagher J, Klagsbrun M. Neuropilin-1 Binds Vascular Endothelial Growth Factor 165, Placenta Growth Factor-2, and Heparin via Its b1b2 Domain. *J Biol. Chem*. 2002; 277 (27), 24818–24825

Marin-Padilla, M. Early vascularization of the embryonic cerebral cortex: Golgi and electron microscopic studies. *J. Comp. Neurol.* 1985;241:237–249.

Martin P. Wound healing – aiming for perfect skin regeneration. *Science* 1997;276:75–81.

Martin P and Leibovich. Inflammatory cells during wound repair: the good, the bad and the ugly. *Trends in Cell Biology* 2005;15 (11): 599-607.

Matsumoto T, Claesson-Welsh L. VEGF receptor signal transduction. *Sci.STKE*. 2001 Dec 11;112: re21.

Melter M, Reinders ME, Sho M. Ligation of CD40 induces the expression of vascular endothelial growth factor by endothelial cells and monocytes and promotes angiogenesis *in vivo*. *Blood*

References

2000;96, 3801–3808

Menke NB, Ward KR, et al. Impaired wound healing. *Clin Dermatol* 2007;25(1): 19-25.

Mercandetti M, Cohen AJ (2005). Wound Healing: Healing and Repair. Emedicine.com.

Meredith JE, Schwartz MA. Integrins, adhesion and apoptosis. *Trends Cell Biol*. 1997;7:146-150.

Miao HQ, Lee P, Lin H, Soker S, and Klagsbrun M (). Neuropilin-1 expression by tumor cells promotes tumor angiogenesis and progression. *FASEB J.* 2000;14 (15)**,**2532–2539

Midwood KS, Williams LV, and Schwarzbauer JE. Tissue repair and the dynamics of the extracellular matrix. *Int J Biochem Cell Biol.* 2004;**36** (6): 1031–1037. PMID 15094118

Migdal M, Huppertz B, Tessler S, Comforti A, Shibuya M, Reich R, Baumann H, Neufeld G. Neuropilin-1 Is a Placenta Growth Factor-2 Receptor. *J Biol Chem*. 1998; 273 (35), 22272–22278

Mirastschijski U, Haaksma CJ, Tomasek JJ and Ågren MS. Matrix metalloproteinase inhibitor GM 6001 attenuates keratinocyte migration, contraction and myofibroblast formation in skin wounds. *Exp Cell Res* 2004;299(2): 465-475. PMID 15350544

Mitra SK, Schlaepfer DD. Integrin-regulated FAK–Src signaling in normal and cancer cells. *Curr Opin Cell Biol*. 2006 Oct;18(5):516-23

Moldovan L, Moldovan NI. Role of monocytes and macrophages in angiogenesis. EXS 2005;(94):127-46

Montesano R, Orci L, Vassalli P. In vitro rapid organization of endothelial cells into capillary-like networks is promoted by collagen matrices. *J Cell Biol*. 1983;97:1648 –1652.

Muller YA, Li B, Christinger HW, Wells JA, Cunningham BC, de Vos AM. Vascular endothelial growth factor: crystal structure and functional mapping of the kinase domain receptor binding site. *Proc. Natl. Acad. Sci. U.S.A*. 1997;**94**, 7192–7197

Muller MJ, Hollyoak MA, Moaveni Z, La T, Brown H, Herndon DN, Heggers JP. Retardation of wound healing by silver sulfadiazine is reversed by Aloe vera and nystatin. *Burns* 2003;**29** (8): 834-836.

Murga M, Fernandez-Capetillo O, and Tosato G. Neuropilin-1 regulates attachment in human endothelial cells independently of vascular endothelial growth factor receptor-2. *Blood* 2005;Mar1;105(5):1992-9

Neufeld G, Cohen T, Shraga N, Lange T, Kessler O, Herzog Y. The neuropilins: multifunctional semaphorin and VEGF receptors that modulate axon guidance and angiogenesis. *Trends Cardiovasc Med* 2002;12:13-9.

Nagy JA, Vasile E, Feng D, Sundberg C, Brown LF, Detmar MJ, Lawitts JA, Benjamin L, Tan X, Manseau EJ, Dvorak AM, Dvorak HF. Vascular permeability factor/vascular endothelial growth factor induces lymphangiogenesis as well as angiogenesis. *J Exp Med* 2002, 196:1497–1506

Newby AC. Metalloproteinase expression in monocytes and macrophages and its relationship to atherosclerotic plaque instability. *Arterioscler Thromb Vasc Biol* 2008; 28:2108–2114.

Ng YS, Rohan R, Sunday ME, Demello DE, D'Amore PA. Differential expression of VEGF isoforms in mouse during development and in the adult. *Dev. Dyn.* 2001;220, 112-121.

Nguyen DT, Orgill DP, Murphy GF (2009). Chapter 4: The Pathophysiologic Basis for Wound Healing and Cutaneous Regeneration. *Biomaterials For Treating Skin Loss*. CRC Press (US) & Woodhead Publishing (UK/Europe), Boca Raton/Cambridge, p. 25-57. (ISBN 978-1-4200-9989-9, ISBN 978-1-84569-363-3)

Nissen NN, Polverini PJ, Koch AE, Volin MV, Gamelli RL, DiPietro LA. VEGF mediates angiogenic activity during the proliferative phase of wound healing. *Am J Pathol* 1998;152:1445–52.

Nwomeh BC, Liang HX, et al. Dynamics of the matrix metalloproteinases MMP-1 and MMP-8 in acute open human dermal wounds. *Wound Repair Regen* 1998;6(2): 127-134.

Odorisio T, Failla CM, Zambruno G. Molecular control of physiological skin angiogenesis.*Eur J Dermatol.* 2002 Nov-Dec;12(6):VII-X.

Ohki Y, Heissig B, Sato Y, Akiyama H, Zhu Z, Hicklin DJ, et al. G-CSF promotes neovascularization by releasing VEGF from neutrophils. *FASEB J* 2005;19:739–50.

Olsson AK, Dimberg A, Kreuger J, Claesson-Welsh L. VEGF receptor. Signaling – in control of vascular function. *Nat Rev Mol Cell* 2006;7:359–71.

Onesto C, Berra E, Grepin R, Pages G. Poly(A)-binding protein-interacting protein 2, a strong regulator of vascular endothelial growth factor mRNA. *J Biol Chem*. 2004 Aug 13;279(33):34217-26.

Orecchia A, Lacal PM, Schietroma C, Morea V, Zambruno G, Failla CM. VEGFR-1 is deposited in the ECM by endothelial cells and is a ligand for the a5b1 integrin. *J Cell Sci* 2003;116:3479–89.

Oura H, Bertoncini J, Velasco P, Brown LF, Carmeliet P, Detmar M. A critical role of placental growth factor in the induction of inflammation and edema formation. *Blood* 2003;101:560-7.

Ozawa K, Kondo T, Hori O, Kitao Y, Stern DM, Eisenmenger W, Ogawa S, Ohshima T. Expression of the oxygen-regulated protein ORP150 accelerates wound healing by modulating intracellular VEGF transport. *J Clin Invest*. 2001 Jul;108(1):41-50.

Paik JH, Skoura A, et al. Sphingosine 1-phosphate receptor regulation of N-cadherin mediates vascular stabilization. Genes Dev 2004;18(19): 2392-2403

Pan Q, ChatherY,Wu Y, RathoreN, Tong RK, PealeF, Bagri A, Tessier-Lavigne M, Koch AW, Watts RJ. Neuropilin-1 Binds to VEGF121 and Regulates Endothelial Cell Migration and Sprouting. *J Biol Chem*. 2007a; 282(32): 24049-56

Pan Q, Chanthery Y, Liang WC, Stawicki S, Mak J, Rathore N, Tong RK, Kowalski J, Yee SF, Pacheco G et al. Blocking neuropilin-1 function has an additive effect with anti-VEGF to inhibit tumor growth. *Cancer Cell* 2007b;11, 53–67

Papapetropoulos A, Fulton D, Mahboubi K, Kalb RG, O'Connor DS, Li F, Altieri DC, Sessa WC. Angiopoietin-1 inhibits endothelial cell apoptosis via the Akt/survivin pathway. *J Biol Chem* 2000;275:9102-9105.

Parenti A, Brogelli L, Filippi S, Donnini S, Ledda F. Effect of hypoxia on endothelial loss on vascular smooth muscle cell responsivenessto VEGF-A: role of Flt-1/VEGFR-1. *Cardiovasc Res* .2002 Jul;55(1):201-12

Park JE, Chen HH, Winer J, Houck KA, Ferrara N. Placenta growth factor. Potentiation of vascular endothelial growth factor bioactivity, in vitro and in vivo, and high affinity binding to Flt-1 but not to Flk-1/KDR. *J Biol Chem* 1994;269:25646–54.

Persico MG, Vincenti V, DiPalma T. Structure, expression and receptor-binding properties of PlGF. *Curr Top Microbiol Immunol* 1999;237:31–40.

Pertovaara L, Kaipainen A, Mustonen T, Orpana A, Ferrara N, Saksela O, Alitalo K. Vascular endothelial growth factor is induced in response to transforming growth factor-beta in fibroblastic and epithelial cells. *J Biol Chem*. 1995; 269: 6271-6274

Playford MP and Schaller MD. The interplay between Src and integrins in normal and tumor biology. *Oncogene* 2004; 23, 7928-7946

Plouet J, Moro F, Bertagnolli S. Extracellular cleavage of the vascular endothelial growth factor 189-amino acid form by urokinase is required for its mitogenic effect. *J. Biol. Chem*. 1997;272, 13390–13396

Polverini P, DiPietro LA, Dixit VM, Hynes RO, Lawler J. Thrombospondin-1 knock out mice show delayed organization and prolonged neovascularization of skin wounds. *FASEB J* 1995;9:A272.

Poschl E, Schlotzer-Schrehardt U, Brachvogel B, Saito K, Ninomiya Y, Mayer U. Collagen IV is essential for basement membrane stability but dispensable for initiation of its assembly during early development. *Development* 2004;131:1619–28.

Potter MD, Barbero S, et al. Tyrosine phosphorylation of VE-cadherin prevents binding of p120- and betacatenin and maintains the cellular mesenchymal state. *J Biol Chem* 2005;280(36): 31906-31912.

Proksch E, Brandner JM, et al. The skin: an indispensable barrier. *Exp Dermatol* 2008;**17**(12): 1063-1072.

Pugh CW, Ratcliffe PJ. Regulation of angiogenesis by hypoxia: role of the HIF system. *Nat. Med*. 2003;9:677–684.

Qi JH, Claesson-Welsh L. VEGF-Induced Activation of Phosphoinositide 3-Kinase Is Dependent on Focal Adhesion Kinase. *Exp Cell res*. 2001 Feb 1;263(1):173-82

Rafii S. *et al.* Contribution of marrow-derived progenitors to vascular and cardiac regeneration. *Semin. Cell Dev. Biol.* 2002;13, 61–67.

Ramjaun AR, Hodivala-Dilke K. The role of cell adhesion pathways in angiogenesis. *Int J Biochem Cell Biol* 2009;41:521–530.

Risau W, Flamme I. Vasculogenesis. *Annu Rev Cell Dev Biol*. 1995;11:73–91.

Robinson CJ, Mulloy B, Gallagher JT, Stringer SE. VEGF165-binding sites within heparansulphate encompass two highly sulphated domains and can be liberated by K5 lyase *J Biol Chem* 2006;281:1731–1740.

Romano Di Peppe S, Mangoni A, Zambruno G, Spinetti G, Melillo G, Napolitano M, Capogrossi MC: Adenovirus-mediated VEGF165 gene transfer enhances wound healing by promoting angiogenesis in CD1 diabetic mice. *Gene Ther* 2002, 9:1271–1277

Romo T and Pearson JM (2005). Wound Healing, Skin. Emedicine.com

Rook's Textbook of Dermatology, Seventh Edition, Blackwell Science Ltd (2008).

Rosenberg L, de la Torre J (2006). Wound Healing, Growth Factors. Emedicine.com. Accessed January 20, 2008

References

Rossiter H, Barresi C, Pammer J, Rendl M, Haigh J, Wagner EF, et al. Loss of vascular endothelial growth factor A activity in murine epidermal keratinocytes delays wound healing and inhibits tumor formation. *Cancer Res* 2004;64:3508-16.

Roth D, Piekarek M, Paulsson M, Christ H, Bloch W, KriegT, Davidson JM, Eming SA. Plasmin Modulates Vascular Endothelial Growth Factor-A-Mediated Angiogenesis during Wound Repair. *Am J Pathol*. 2006; 168 (2), 670-684.

Roy R, Zhang B, Moses MA. Making the cut: protease-mediated regulation of angiogenesis. *Exp Cell Res* 2006;312:608–22.

Ruhrberg C, Gerhardt H, Golding M. Spatially restricted patterning cues provided by heparin-binding VEGF-A control blood vessel branching morphogenesis. *Genes Dev*. 2002;16, 2684–2698

Ruoslahti E. RGD and other recognition sequences for integrins. *Annu Rev Cell Dev Biol* 1996;12:697–715.

Santoro MM and Gaudino G. Cellular and molecular facets of keratinocyte reepithelization during wound healing. *Experimental Cell Research* 2005;304 (1): 274-286. PMID 15707592.

Saunders WB, Bohnsack BL, et al. Coregulation of vascular tube stabilization by endothelial cell TIMP-2 and pericyte TIMP-3. *J Cell Biol* 2006;175(1): 179-191.

Sawano A, Takahashi T, Yamaguchi S, Aonuma M and Shibuya M. Flt-1 but not KDR/Flk-1 tyrosine kinase is a receptor for placenta growth factor (PlGF), which is related to vascular endothelial growth factor (VEGF). *Cell Growth Differ*. 1996;7:213-221.

Sawano A, Takahashi T, Yamaguchi S et al. The phosphorylated 1169-tyrosine containing region of Flt-1 kinase (VEGFR-1) is a major binding site for PLCγ. *Biochem Biophys Res Commun* 1997;238:487–491.

Schaller MD, Hildebrand JD, Shannon JD, Fox JW, Vines RR, Parsons JT. Autophosphorylationof the focal adhesion kinase, pp125FAK, directs SH2-dependent binding of pp60src. *Mol Cell Biol*. 1994 Mar;14(3):1680-8.

Schatteman GC & Awad O. Hemangioblasts, angioblasts, and adult endothelial cell progenitors. *Anat. Rec. A Discov. Mol. Cell Evol. Biol.* 2004; **276**, 13–21.

Schruefer R, Sulyok S, Schymeinsky J, Peters T, Scharffetter-Kochanek K, Walzog B. The proangiogenic capacity of PMN delineated by microarray technique and by measurement of neovascularisation in wounded skin of CD-18-deficient mice. *J Vasc Res* 2006;43:1–11.

Schweigerer L, Neufeld G, Friedman J, Abraham JA, Fiddes JC, Gospodarowicz D. Capillary endothelial cells express basic fibroblast growth factor, a mitogen that promotes their own growth. *Nature* 1987;325:257–259.

Senger DR, et al. Tumor cells secrete a vascular permeability factor that promotes accumulation of ascites fluid. *Science* 1983;219, 983-985.

Senger DR, Ledbetter SR, Claffey KP, Papadopoulos-Sergiou A, Peruzzi CA, Detmar M. Stimulation of endothelial cell migration by vascular permeability factor/vascular endothelial growth factor through cooperative mechanisms involving the alphavbeta3 integrin, osteopontin, and thrombin. *Am J Pathol*. 1996;149:293–305.

Senger DR, Claffey KP, Benes JE, Perruzzi CA, Sergiou AP, Detmar M. Angiogenesis promoted by vascular endothelial growth factor: regulation through α1β1 and α2β1 integrins. *Proc Natl Acad Sci U S A*. 1997;94:13612–13617.

Senger DR, Perruzzi CA, Streit M, Koteliansky VE, de Fougerolles AR, Detmar M. The alpha1beta1 and alpha2beta1 integrins provide critical support for vascular endothelial growth factor signaling, endothelial cell migration, and tumor angiogenesis. *Am J Pathol*. 2002;160:195–204.

Sepp NT, Li LJ, Lee KH, Brown EJ, Caughman SW, Lawley TJ, Swerlick RA. Basic fibroblast growth factor increases expression of the alpha v beta 3 integrin complex on human microvascular endothelial cells. *J Invest Dermatol* 1994;103:295–299.

Shibuya M, Yamaguchi S, Yamane A, Ikeda T, Tojo A, Matsushime H and Sato M. Nucleotide sequence and expression of a novel human receptor-type tyrosine kinase gene (flt) closely related to the fms family. *Oncogene* 1990;5: 519-524.

Shibuya M. Structure and dual function of vascular endothelial growth factor receptor-1 (Flt-1). *Int J Biochem Cell Biol*. 2001 Apr;33(4):409-20.

Shibuya M. Vascular endothelial growth factor receptor-1 (VEGFR-1/Flt-1):a dual regulator for angiogenesis. *Angiogenesis*. 2006;9(4):225-30

Shinkai A, Ito M, Anazawa H, Yamaguchi S, Shitara K, Shibuya M. Mapping of the sites involved in ligandassociation and dissociation at the extracellular domain of vascular endothelial growth factor receptor KDR. *J. Biol. Chem*. 1998;273, 31283-31288.

Shintani Y, Takashima S, Asano Y, Kato H, Liao Y, Yamazaki S, Tsukamoto O, Seguchi O, Yamamoto H, Fukushima T, Sugahara K, Kitakaze M, Hori M. Glycosaminoglycan modification of neuropilin-1 modulates VEGFR2 signaling. *EMBO J.* 2006 Jun12, 25(13):3045-55

Shoji W, Isogai S, Sato-Maeda M, Obinata M, Kuwada JY. Semaphorin3a1 regulates angioblast migration and vascular development in zebrafish embryos. *Development*. 2003;130:3227–3236.

Siekmann AF, Lawson ND. Notch signaling limits angiogenic cell behaviour in developing zebrafish arteries. Nature 2007; 445:781–784.

Sierra-Honigmann MR, Nath AK, Murakami C, Garcia-Cardena G, Papapetropoulos A, Sessa WC, Madge LA, Schechner JS, Schwabb MB, Polverini PJ, Flores-Riveros JR. Biological action of leptin as an angiogenic factor. *Science*. 1998 Sep 11;281(5383):1683-6.

Singer AJ, Clark RAF. Cutaneous wound healing. *N Engl J Med* 1999;341:738–46.

Smack DP, Korge BP. Keratin and keratinization." J Am Acad Dermatol 1994;30(1): 85-102.

Soker S, Fidder H, Neufeld G, Klagsbrun M. Characterization of Novel Vascular Endothelial Growth Factor (VEGF) Receptors on Tumor Cells That Bind VEGF165 via Its Exon 7-encoded Domain. *J Biol Chem*. 1996. 271(10);5761-5767

Stadelmann WK, Digenis AG, Tobin GR. Physiology and healing dynamics of chronic cutaneous wounds. *Am J Surg.* 1998 Aug;*176* (2): 26S-38S.

Stalmans I, Ng YS, Rohan R. Arteriolar and venular patterning in retinas of mice selectively expressing VEGF isoforms. *J. Clin. Invest*. 2002;109, 327–336

Stein I, Neeman M, Shweiki D, Itin A and Keshet E. Stabilization of vascular endothelial growth factor mRNA by hypoxia and hypoglycemia and coregulation with other ischemia-induced genes. *Mol. Cell Biol*. 1995;15:5363–5368.

Stratman AN, Malotte KM, et al. Pericyte recruitment during vasculogenic tube assembly stimulates endothelial basement membrane matrix formation. *Blood* 2009;114(24):5091-5101.

Streit M, Velasco P, Piccardi L, Spencer L, Brown LF, Janes L, et al. Thrombospondin-1 suppresses wound healing and granulation tissue formation in the skin of transgenic mice. *EMBO J* 2000;19:3272–82.

Streit M, Detmar M. Angiogenesis, lymphangiogenesis and melanoma metastasis. *Oncogene* 2003;22:3172-9.

Stupack DG. and Cheresh DA. ECM remodeling regulates angiogenesis: endothelial integrins look for new ligands. *Sci STKE* 2002 Feb12; 2002(119): pe7.

Suchting S, Freitas C, le Noble F, et al. The Notch ligand Delta-like 4 negatively regulates endothelial tip cell formation and vessel branching. *Proc Natl Acad Sci USA* 2007; 104:3225–3230.

Sundberg C, Nagy JA, Brown LF, Feng D, Eckelhoefer IA, Manseau EJ, Dvorak AM, Dvorak HF. Glomeruloid microvascular proliferation follows adenoviral vascular permeability factor/vascular endothelial growth factor-164 gene delivery. *Am J Pathol*. 2001 Mar;158(3):1145-60

Suri C, Jones PF, et al. Requisite role of angiopoietin-1, a ligand for the TIE2 receptor, during embryonicangiogenesis. *Cell* 1996;87(7): 1171-1180.

Swirski FK, Nahrendorf M, Etzrodt M, Wildgruber M, Cortez-Retamozo V, Panizzi P, Figueiredo J-L, Kohler RH, Chudnovskiy A, Waterman P, Aikawa E, Mempel TR, Libby P, Weissleder R, Pittet MJ. Identification of Splenic Reservoir Monocytes and Their Deployment to Inflammatory Sites. *Science*. 2009;325: 612-616.

Takagi S, Hirata T, Agata K, Mochii M, Eguchi G and Fujisawa H. The A5 antigen, a candidate for the neuronal recognition molecule, has homologies to complement components and coagulation factors. *Neuron* 1991;7:295–307

Takashima S *et al.* Targeting of both mouse neuropilin-1 and neuropilin-2 genes severely impairs developmental yolk sac and embryonic angiogenesis. *Proc. Natl Acad. Sci. USA* 2002;99:3657–3662.

Tan W, Palmby TR, Gavard J, Amornphimoltham P, Zheng Y, Gutkind S. An essential role for Rac1 in endothelial cell function and vascular development. *FASEB* J.2008 Jun;22(6):1829-38

Tanaka K, Yamaguchi S, Sawano A, et al. (1997) Characterization of the extracellular domain in the vascular endothelial growth factor receptor-1 (Flt-1 tyrosine kinase). *Jpn. J. Cancer Res.* 88, 867-876.

Tchaikovski V, Fellbrich G, Waltenberger J. The Molecular Basis of VEGFR-1 Signal Transduction Pathways in Primary Human Monocytes. *Artherioscler Thromb Vasc Biol*. 2008 Feb; 28(2):322-8

References

Terman BI et al. Identification of the KDR tyrosine kinase as a receptor for vascular endothelial cell growth factor. *Biochem. Biophys. Res. Commun*. 187, 1579-1586 (1992)

Thyboll J, Kortesmaa J, Cao R, Soininen R, Wang L, Iivanainen A, et al. Deletion of the laminin alpha4 chain leads to impaired microvessel maturation*. Mol Cell Biol* 2002;22:1194–202.

Tischer E, Mitchell R, Hartman T. The human gene for vascular endothelial growth factor. Multiple protein forms are encoded through alternative exon splicing. *J. Biol. Chem*. 1991;266, 11947–11954

Tomanek RJ, Ishii Y, Holifield JS, Sjogren CL, Hansen HK, Mikawa T. VEGF family members regulate myocardial tubulogenesis and coronary artery formation in the embryo. *Circ Res*. 2006;98:947–953.

Tredget EE, Ding J. Wound healing: from embryos to adults and back again. *Lancet* 2009;373(9671): 1226-1228.

Trompezinski S, Pernet I, Mayoux C, Schmitt D, Viac J. Transforming growth factor-_1 and ultraviolet A1 radiation increase production of vascular endothleial growth factor but not endothelin-1 in human dermal fibroblasts*. Br J Dermatol* 2000;143:539–545.

Valdembri D, Caswell PT, Anderson KI, Schwarz JP, Konig I, Astanina E, Caccavari F, Norman JC, Humphries MJ, Bussolino F, Serini G. Neuropilin-1/GIPC1 Signaling Regulates a5b1 Integrin Traffic and Function in Endothelial Cells. *PloS Biol*. 2009;12(2):187-93

Vander Kooi CW, Jusino MA, Perman B, Neau DB, Bellamy HD, Leahy DJ.Structural basis for ligand binding to neuropilin B domains. *Proc Natl Acad Sci USA*. 2007 Apr 10;104(15):6152-7

Velasco P, Lange-Asschenfeldt B. Dermatological aspects of angiogenesis. *Br J Dermatol* 2002;147:841-52.

Vernon RB, Sage EH. Between molecules and morphology: Extracellular matrix and creation of vascular form. *Am J Pathol*. 1995;147:873–883.

Vincent KA, Shyu KG, Luo Y, Magner M, Tio RA, Jiang C, Goldberg MA, Akita GY, Gregory RJ, Isner JM. Angiogenesis is induced in a rabbit model of hindlimb ischemia by naked DNA encoding an HIF-1alpha/VP16 hybrid transcription factor. *Circulation*. 2000 Oct 31;102(18):2255-61.

Vincenti V, Cassano C, Rocchi M, Persico G (1996) Assignment of the vascular endothelial growth factor gene to human chromosome 6p21.3. *Circulation* **93**, 1493–1495

Walmsley S*,* Advances in wound management*:* executive summary Clinica Reports*, PJB Publications, Ltd.,* London *(*2002*)*

Waltenberger J, Claesson-Welsh L, Siegbahn A, Shibuya M and Heldin CH, Different signal transduction properties of KDR and Flt-1, two receptors for vascular endothelial growth factor *J. Biol. Chem*., 269 (1994) 26988-26995

Wang L, Zeng H, Wang P, Soker S, Mukhopadhyay D. Neuropilin-1-mediated Vascular Permeability Factor/Vascular Endothelial Growth Factor-dependent Endothelial Cell Migration. *J Biol Chem* 2003; 278(49): 8848–48860

Weis SM, Cheresh DA. Pathophysiological consequences of VEGF-induced vascular permeability. *Nature* 2005;437:497–504

Weller K, Foitzik K, Paus R, Syska W, Maurer M. Mast cells are required for normal healing of skin wounds in mice. *FASEB J*. 2006 Nov;20(13):2366-8

Werner S, Smola H, Liao X, Longaker MT, Krieg T, Hofschneider PH, Williams LT; The function of KGF is morphogenesis of epithelium and reepitheliazation of wounds. *Science* 1994; 266: 819-822.

Wetzler C, Kampfer H, Stallmeyer B, Pfeilschifter J, Frank S. Large and sustained induction of chemokines during impaired wound healing in the genetically diabetic mouse: prolonged persistence of neutrophils and macrophages during the late phase of repair. *J Invest Dermatol.* 2000 Aug;115(2):245-53.

Whelan MC, Senger DR. Collagen I initiates endothelial cell morphogenesis by inducing actin polymerization through suppression of cyclic AMP and protein kinase A. *J Biol Chem*. 2003;278:327–334.

Wiesmann C, Fuh G, Christinger HW, Eigenbrot C, Wells JA and de Vos AM (1997) Chrystal structure at 1.7 Á resolution of VEGF in complex with domain 2 of Flt-1 receptor. *Cell* 91: 695-704

Witte MB and Barbul A.. Role of nitric oxide in wound repair. *Am J Surg.* 2002;183(4): 406-412.

Wong AL, Haroon ZA, Werner S, Dewhirst MW, Greenberg CS, Peters KG. Tie2 expression and phosphorylation in angiogenic and quiescent adult tissues. *Circ Res* 1997;81:567–574.

Wynn TA. Common and unique mechanisms regulate fibrosis in various fibroproliferative deseases.*J Clin Invest*. 2007;Mar; 117(3):524-9

Yamashita J, Itoh H, Hirashima M, Ogawa M, Nishikawa S, Yunugi T, et al. Flk-1-positive cells derived from embryonic stem cells serve as vascular progenitors. *Nature* 2000; 408:92—6.

Yamazaki Y, Morita T. Molecular and functional diversity of vascular endothelial growth factors. *Mol Divers*. 2006 Nov;10(4):515-27

Yang EY, Moses HL. Transforming growth factor beta1-induced changes in cell migration, proliferation, and angiogenesis in the chicken chorioallantoic membrane. *J Cell Biol* 1990;111:731–741.

Yang W, Ahn H, Hinrichs M, Torry RJ and Torry DS. Evidence of a novel isoform of placenta growth factor (PlGF-4) expressed in human trophoblast and endothelial cells. *J. Reprod. Immunol*. 2003;60, 53–60

Yano K, Oura H, Detmar M. Targeted overexpression of the angiogenesis inhibitor thrombospondin-1 in the epidermis of transgenic mice prevents ultraviolet-B-induced angiogenesis and cutaneous photo-damage. *J Invest Dermatol* 2002;118:800-5.

Young GD, Murphy-Ullrich JE. The tryptophan-rich motifs of the thrombospondin type 1 repeats bind VLAL motifs in the latent transforming growth factor-beta complex. *J Biol Chem* 2004;279:47633–47642.

Yuan F, Chen Y, Dellian M, Safabakhsh N, Ferrara N. Timedependent vascular regression and permeability changes in estabilished human tumor xenografts induced by anti-vascular endothelial growth factor/vascular permeability factor antibody. *Proc Natl Acad Sci USA* 1996;93:14765-70.

Yurchenco PD, Amenta PS, Patton BL. Basement membrane assembly, stability and activities observed through a developmental lens. *Matrix Biol* 2004;22:521–38.

Zacchigna S, Pattarini L, Zentilin L, Moimas S, Carrer A, Sinigaglia M, Arsic N, Tafuro S, Sinagra G, Giacca M. Bone marrow cells recruited through the neuropilin-1 receptor promote arterial formation at the site of adult neoangiogenesis in mice. *J Clin Invest*. 2008;118(6):2062-75

Zhang Z, Ramirez NE, Yankeelov TE, Li Z, Ford LE, Qi Y, Pozzi A, Zutter MM. α2β1 integrin expression in the tumor microenvironment enhances tumor angiogenesis in a tumor cell–specific manner. *Blood* 2008 Sep 15; 123(6):1311-7

Zhao Q, Egashira K, Hiasa KI, Ishibashi M, Inoue S, Ohtani K, Tan C, Shibuya M, Takeshita A, Sunagawa K. Essential role of vascular endothelial growth factor and Flt-1 signals in neointimal formation after periadventitial injury. Arterioscler Thromb. Vasc. Biol. 2004;24:2284-2289.

Zweers MC, Davidson JM, Pozzi A, Hallinger R, Janz K, Quondamatteo F, et al. Integrin alpha2beta1 is required for regulation of murine wound angiogenesis but is dispensable for reepithelialization. *J Invest Dermatol* 2007;127:467–78

.6 Abbreviations

%	percentage
℃	degree Celsius
Akt	„proteinkinase B“
Amp	Ampicillin
Ang	„Angiopoeitin“
BCA	bicinchroninic acid
Birc2	„baculoviral IAP repeat-containing 2“
BMP1	„bone morphogenetic protein” 1
BSA	bovine serum albumin
CD31	„Cluster of Differentiation“ 31
CRIB	„Cdc42-/Rac1-interactive binding-motive”
Crk	„tyrosine –protein kinase Crk“
C-terminal	carboxyl-terminal
CUB	„complement binding factors C1s/C1r, Uegf, BMP1”
CV	column volume
d	dermis
Da	dalton
DAPI	4,6-diamidino-2-phenylindol
db/db mouse	diabetic mouse
Dcn	decorin
ddH2O	double destilled water
Dll4	„Delta-like4”
DMEM	„Dulbeccos Modified Eagle Medium“
DNA	desoxyribonucleic acid
e	epidermis
E	embryonic day
dNTP	desoxyribonucleotide triphosphat
ECL	„enhanced chemiluminescence“
EDTA	Ethylenediaminetetraacetic acid
EGF/EGFR	„Epidermal Growth Factor“/„Epidermal Growth Factor“-Receptor
ELISA	Enzyme-Linked Immuno-Sorbent Assay
ERK	„extracellular-signal regulated kinase“
Ets2	„E26 avian leukemia oncogene 2“
FAK	„focal adhesion kinase”
FCS	fetal calf serum
FGF	„Fibroblast Growth Factor“
Flt1	„Fms-like-tyrosine-kinase-receptor”-1 (VEGFR-1)

Abbreviations

Fst	„Follistatin”
g	gram
GAG	glycosaminoglycan
Grb-2	„growth-factor-receptor-bound”-2
gt	granulation tissue
GTP	guanosintriphosphate
h	hour
H&E	Haematoxylin & Eosin
HEK	„human embryonic kidney"
HGF	„Hepatocyte Growth Factor”
HIF	„Hypoxia Inducible Factor”
HRP	„horse radish peroxidase“
HSPG	heparan sulphate proteoglycans
HUVE	„Human Umbilical Vein Endothelial” cells
Ig	immunoglobulin
IGF	„Insulin-like Growth Factor“
IgG	Immunglobulin G
Jak2	„Janus kinase 2“
K14 promoter	keratin-14 promoter
k_a	association rate constant
kb	kilo basepair
k_d	dissociation constant
kDa	kilodalton
KGF	Keratinocyte Growth Factor
L	liter
LC-MS/MS	Liquid chromatography tandem mass spectroscopy
LLC	„Lewis lung carcinoma” cells
M	mol/liter (molar)
MAM	„meprin, A5 antigen, receptor tyrosine phosphatase μ“
MAPK	„mitogen-activated proteinkinase“
MCP	„monocyte chemoattractant protein“
MES	2-(*N*-morpholino)ethanesulfonic acid
mg	milligram
MIP	„Macrophage inflammatory protein“
mL	milliliter
min	minute
MMP	„Matrixmetalloproteinase”
MW	molecular weight
ng	nanogram

NIP1	„neuropilin interacting protein-1"
nm	nanometer
Nrp-1	„Neuropilin"-1
N-terminal	amino-terminal
$p130^{Cas}$	„p130 Crk/associated substrate"
PAE	„porcine aortic endothelial" cells
PAGE	polyacrylamide-gelelectrophoresis
PAK	„p21-activated kinase"
PBS	phosphate-buffered saline
p.c.	„panniculus carnosus"
PCR	polymerase chain reaction
PDGFR	„Platelet Derived Growth Factor Receptor"
pg	picogram
pH	p(otential of) h(ydrogen)
PI3K	„Phosphatidylinositol-3-kinase"
PLC-γ	„Phospholipase C-γ"
PlGF	„Placenta Growth Factor"
PlGFStop	mutant „Placenta Growth Factor (1-118) "
PMSF	phenylmethylsulfonylfluoride
PMN	polymorphonuclear neutrophils
PVDF	polyvinylidene fluoride
Rac	„Ras-likeC3"
rh	recombinant human
rpm	rounds per minute
RTK	receptor tyrosine kinase
RU	response units
SDS	sodiumdodecylsulphate
sec	second
SEM	standard error of mean
Sft	subcutaneous fat tissue
SH-2	„Src-homology-2-domain"
SHP-2	„Src-homology-2-domain-containing PTP2"
SPR	Surface Plasmon Resonance
Src	„tyrosine-protein kinase Src"
Taq	*Thermus aquaticus* DNA polymerase
TBST	Tris-buffered saline + Tween 20
TGF	„Transforming Growth Factor"
Tie-2	„Angiopoietin-1 receptor"
TIMP	„Tissue inhibitor of metalloproteinase"

Abbreviations

Tris	Tris(hydroxymethyl)aminoethan
TSP	„Thrombospondin“
Tween	Polyoxyethylen-(20)-sorbitanmonolaurat
U	units
uPA	„urokinase-type plasminogen activator“
VEGFR	„Vascular Endothelial Growth Factor receptor“
VSMC	„vascular smooth muscle cell
w/v	weight per volume
µg	microgram
µl	microliter
µm	micrometer

Danksagung

Besonders danken möchte ich Frau Prof. Dr. Sabine Eming für die Überlassung des interessanten Themas und die Betreuung während meiner Zeit in ihrer Arbeitsgruppe. Außerdem möchte ich ihr für die konstruktive Betreuung meiner Doktorarbeit danken. Mit ihrem fundierten Fachwissen und vielen Anregungen hat sie maßgeblich zu dem Gelingen meiner wissenschaftlichen Arbeit beigetragen.

Herrn Prof. Dr. Thomas Krieg danke ich für die Bereitstellung des Arbeitsplatzes an der Klinik und Poliklinik für Dermatologie und Venerologie der Universität zu Köln.

Herrn Prof. Dr. Mats Paulsson möchte ich nicht nur für die Übernahme des Erstgutachtens, sondern in besonderem Maße auch für sein stetes Interesse und stimulierende Diskussion meiner Arbeit während der gesamten Doktorandenzeit danken. Herrn Prof. Dr. Matthias Hammerschmidt danke ich für die Übernahme des Zweitgutachtens.

In besonderem Maße möchte ich mich Herrn Prof. Dr. Manuel Koch und Frau Dr. Daniela Zwolanek für die Durchführung der SPR-Messungen, deren Auswertung und die konstruktiven Gespräche bedanken

Des Weiteren möchte ich mich bei allen Kolleginnen und Kollegen aus den Forschungslaboren der Dermatologie für die außerordentlich gute Zusammenarbeit bedanken. Die durchgehend freundliche, konstruktive und hilfsbereite Arbeitsatmosphäre hat maßgeblich zum Gelingen dieser Arbeit beigetragen. Besonders hervorheben möchte ich Stephanie Traub, Sebastian Lanvermann, Yvonne Meyer, Tina Lucas, Anna Riese, Rajeev Ranjan, Michael Piekarek, Sebastian Willenborg, Johanna Knipper und Christian Michels, die nicht nur auf fachlicher, sondern auch auf sozialer und freundschaftlicher Ebene dazu beigetragen haben, dass ich mich in den letzten Jahren während meiner Arbeit immer sehr wohl gefühlt habe.

Ganz herzlicher Dank gilt auch meiner Familie, auf die ich mich in allen Lebenslagen verlassen konnte und kann.

Mein größter Dank gilt jedoch Judith Helpenstein, deren bedingungsloser Rückhalt und Verständnis während meiner gesamten Promotion, in besonderem Maße aber während meiner Prüfungsphase, maßgeblich zum Gelingen dieser Arbeit beigetragen hat.

Erklärung

Ich versichere, dass ich die von mir vorgelegte Dissertation selbstständig angefertigt, die benutzten Quellen und Hilfsmittel vollständig angegeben und die Stellen der Arbeit - einschließlich Tabellen, Karten, Abbildungen -, die anderen Werken im Wortlaut oder dem Sinn nach entnommen sind, in jedem Einzelfall als Entlehnung kenntlich gemacht habe; dass diese Dissertation noch keiner anderen Fakultät oder Universität zur Prüfung vorgelegen hat; dass sie - abgesehen von unten angegebenen Teilpublikationen - noch nicht veröffentlicht worden ist sowie, dass ich eine solche Veröffentlichung vor Abschluss des Promotionsverfahrens nicht vornehmen werde. Die Bestimmungen dieser Promotionsordnung sind mir bekannt. Die von mir vorgelegte Dissertation ist von Frau Prof. Dr. med. Sabine Eming betreut worden.

Köln den 10.02.2011

Daniel Hoffmann